
Actin Regulatory Proteins in Dendritic Arborisation Neurons of *Drosophila*

Dissertation

zur Erlangung des

Doktorgrades (Dr. rer. nat.)

der Mathematisch-Naturwissenschaftlichen Fakultät

der Rheinischen Friedrich-Wilhelms-Universität Bonn

vorgelegt von

Tomke Stürner

aus Göttingen

BONN 2019

Angefertigt mit Genehmigung der Mathematisch-Naturwissenschaftlichen Fakultät der Rheinischen Friedrich-Wilhelms-Universität Bonn.

1. Gutachter: Prof. Dr. Gaia Tavosanis

2. Gutachter: Prof. Dr. Walter Witke

Tag der Promotion: 11.10.2019

Erscheinungsjahr: 2019

Erklärung

Hiermit erkläre ich, Tomke Stürner, an Eides statt, dass ich die vorliegende Doktorarbeit mit dem Titel “Actin Regulatory Proteins in the Dendritic Arborisation Neurons of *Drosophila*” selbständig verfasst habe, dass ich sie zuvor an keiner anderen Hochschule und in keinem anderen Studiengang eingereicht habe und keine anderen als die angegebenen Quellen und Hilfsmittel benutzt habe. Die Stellen der Arbeit, die dem Wortlaut oder dem Sinne nach anderen Werken entnommen wurden, sind unter Angabe der Quelle kenntlich gemacht. Teile der in dieser Doktorarbeit präsentierten Ergebnisse sind bereits in Stürner und Tatarnikova et al. [2019] veröffentlicht worden. Dies wird an den entsprechenden Stellen vermerkt.

UNTERSCHRIFT: DATUM:

Erklärung

Zusammenfassung

Dendriten sind die verzweigten Zellfortsätze von Nervenzellen, die zur Reizweiterleitung dienen. Dendriten vergrößern die rezeptive Oberfläche der Neurone. Die spezifische Morphologie der Dendriten definiert, welche Signale, mit welcher Intensität weitergeleitet werden und sagt somit viel über die Funktion von einem Neuron aus. Die Struktur und die Dynamik eines Dendriten-Baums werden durch das Cytoskelett definiert, welches seinerseits von einer Reihe spezifischer Proteinen reguliert wird.

In dieser Arbeit untersuche ich Dendriten anhand eines Modellsystems des peripheren Nervensystems (PNS) von *Drosophila*, die "dendritic arborisation"-Neurone (da-Neurone). Ich zeige, dass "WASP-family verprolin homologous protein" (WAVE) durch Rekrutierung des Aktin Nucleator Komplex Arp2/3 verzweigte Aktin-Strukturen an der Basis eines neu gebildeten Dendriten formt. Initiiert durch die GTPase Rac1 ist der Arp2/3 Komplex essenziell für die Entstehung von neuen Dendriten in allen da-Neuronen. Um zu verstehen, wie Aktinfilamente die weitere Bildung eines Dendriten koordinieren, habe ich mich gefragt, welche weiteren Aktin regulierenden Proteine (ARP) die Struktur und Dynamik von Dendriten beeinflussen. Hierfür habe ich mich auf einen Typ der da-Neurone konzentriert: die Klasse III der da-Neurone (c3da). Ich beschreibe hier ihre charakteristische Dendriten-Morphologie, mit kleinen aktinangereicherten terminalen Dendriten. Ich gehe besonders auf die Auswirkung von ARPs auf diese Dendriten-Morphologie ein. Es stehen ARPs im Fokus, die bereits bekannte Funktionen in c3da-Neurone haben oder bei denen die Annahme nahe lag, dass sie eine solche Funktion haben. Ein neuer Ansatz für eine gegenüberstellende *in vivo* Mutanten-Analyse ermöglicht es mir, die Dendriten-Phänotypen genau zu untersuchen und mit ihrer biochemischen Funktion zu korrelieren, um sie im Kontext von Dendriten-Bewegungen zu beschreiben. Dabei habe ich mich auf folgende ARPs konzentriert: die Aktin Nucleatoren Arp2/3, Spire und Capu/Formin2, den Aktin Bündelfaktor Singed/Fascin, das Aktin Bindungsprotein Ena/VASP und den Aktin Trenn- und Depolymerisationsfaktor Twinstar/Cofilin. Die Dendriten-Bäume der sechs ARP-Mutanten weisen alle weniger Dendriten in den c3da-Neuronen auf als in den wildtypischen Kontrollen, die für *singed*-, *ena*- und *twinstar*-Mutanten bereits beschrieben sind. Ich zeige in dieser Arbeit jedoch, dass die Dendriten-Bäume dieser ARP-Mutanten sehr unterschiedliche Morphologien aufweisen, die auf ihre jeweilige

Zusammenfassung

Funktion zurückzuführen sind. Ich habe außerdem neue Quantifizierungsmethoden in der „Trees Toolbox“ (<http://www.treestoolbox.org/>) in Matlab entwickelt und 28 verschiedene Dendriten-Parameter untersucht. Auf diese Weise löse ich in dieser Arbeit die modifizierten Dendriten-Morphologien quantitativ auf und untersuche neue mechanistische Aspekte der ARPs in Dendriten untersuchen. Indem ich dies mit der *in vivo* Zeitaufnahme kombiniere, kann ich zusätzlich das Zusammenspiel der verschiedenen ARPs beschreiben und untersuchen. Insbesondere gehe ich darauf ein, wie diese erwähnten ARPs verschiedene Aspekte der Dendriten-Dynamik der c3da-Neurone regulieren.

Zusammenfassung

Abstract

Dendrites are highly branched extensions of nerve cells, along which signals are received and propagated to the cell body. The correct morphology of dendrites is essential for the function of the nervous system. The underlying cytoskeleton defining the shape and dynamic rearrangement of dendritic branches is under the control of complex protein networks. The aim of this study is to elucidate how these regulators of the actin cytoskeleton define the diverse characteristic shapes and dynamics of dendritic trees.

Investigating the differentiation of *Drosophila* larva dendritic arborisation (da) neurons, I demonstrated that the WASP-family verprolin homologous protein (WAVE) through the recruitment of the Arp2/3 complex promotes the formation of a branched actin patch at the base of a newly forming branchlet. Initiated by the GTPase Rac1, the Arp2/3 complex is essential for branch formation in all classes of da neurons. To elucidate the mechanisms of actin organization following this initial step, I questioned whether additional actin cytoskeletal proteins are required for branching in these neurons. For this I concentrated on the class III da (c3da) neurons and characterised their dendrite morphology focusing on the actin enriched small terminal branchlets (TB). These actin enriched branches stay dynamic throughout larval stages making them a good model system to study actin dependent dendrite dynamics. I investigated the role of several actin regulatory proteins (ARP) that had published functions in c3da neurons and ones that I had previous indications that they might play a role in c3da neurons. A new comparative computational approach to *in vivo* mutant analysis allowed me to analyse the dendritic phenotypes further and correlate them with the biochemical function. This enabled me to position them in the context of branch dynamics. In addition, this approach uncovered which parameter alterations the different ARP mutants influence, specifically in the dendritic trees of c3da neurons.

I focus on the actin nucleators Arp2/3, Spire and Capu/Formin2, the bundling factor Singed/Fascin the actin binding protein Ena/VASP and the severing and depolymerisation factor Twinstar/Cofilin. Mutants of the different actin regulators all show reduced number of branches in c3da neurons which was previously described for *singed*, *ena*, *twinstar*. Furthermore, I demonstrate here that they all have diverse dendritic tree morphologies. I developed new quantification methods in the “Trees Toolbox” (<http://www.treestoolbox.org/>) in Matlab and probed 28 different dendrite parameters and

Abstract

thus was able to quantitatively resolve the modified dendrite morphologies and thus revealed new mechanistic aspects of these ARPs during dendrite branching. Moreover, by combining this with *in vivo* time-lapse imaging I described the interplay of ARPs and uncovered how these ARPs regulate different aspects of branch dynamics in these c3da neurons.

Abstract

Table of Contents

Erklärung.....	i
Zusammenfassung.....	iii
Abstract.....	vii
Table of Contents.....	1
List of Tables.....	3
List of Figures.....	3
1 General Introduction.....	5
1.1 Dendrites.....	5
1.1.1 Dendritic Arborisation Neurons of <i>Drosophila</i>	6
1.1.1.1 Transcriptional Regulation.....	9
1.1.1.2 Dendritic Organisation and Growth.....	10
1.1.1.3 Extrinsic Factors.....	11
1.1.2 Neural Computation of Dendritic Shape.....	13
1.1.3 Dendrite Dynamics.....	14
1.2 The Dendrite Actin Cytoskeleton.....	15
1.2.1 The Actin Cytoskeleton.....	16
1.2.2 Actin in Protrusions.....	18
1.2.3 Regulation by Actin Regulatory Proteins.....	19
1.2.4 Actin Regulatory Proteins in Dendrites.....	26
1.3 Aims of the Thesis.....	27
2. Transient localization of the Arp2/3 complex initiates neuronal dendrite branching <i>in vivo</i>	29
2.1. Introduction.....	29
2.1.1. Statement of Contribution.....	30

Table of Contents

List of Tables

2.2 Publication	31
2.3 Summary	58
3 Comparative computation analysis of actin-binding proteins <i>in vivo</i> unravels the single elements of dendrite dynamics.....	59
3.1 Introduction.....	59
3.1.1 Statement of Contribution.....	60
3.2 Manuscript	61
3.3 Summary	117
4 Conclusion	119
Acronyms.....	122
Copyright and Licensing.....	125
Curriculum Vitae	126
References.....	128
Acknowledgement	140

List of Tables

Table 1: Statement of Contribution for Stürner and Tatarnikova et al. 2019	30
Table 2: Statement of Contribution for Manuscript Stürner et al.	60

List of Figures

Figure 1: Dendritic Arborisation Neurons of <i>Drosophila</i>	9
Figure 2: Actin Structure in Dendrites.....	16
Figure 3: Treadmilling of Actin.....	18
Figure 4: Actin Dynamics.....	20
Figure 5: Actin Regulatory Proteins	26

List of Figures

1 General Introduction

1.1 Dendrites

What are dendrites and what is their function? Why are they so diverse in shape? How do they establish this complex morphology? Camillo Golgi developed a silver staining protocol that visualised neurons with all their parts (dendrites, cell body, axon) and in great detail for the first time and examined many regions of the nervous system Golgi (1873). Wilhelm His termed the collection of appendices in nerve cells as dendrites. They are highly branched extensions of nerve cells, along which signals are received and propagated to the cell body. The work by His on the development of nerve fibres eventually suggested that nerve cells were individual units (His, 1889). Nonetheless, it was not until the work of Ramón y Cajal that these questions started being addressed (Ramón y Cajal, 1899-1904). He established that the complexity of dendrites is a way to make room for a large number of connections while trying to keep the cell volume small, an energy and space saving alternative to increasing the cell body volume. Analogous to a root system of a plant, which is optimised for extraction of water and nutrients from the soil, a dendritic tree extracts information from its surrounding (Bejan, 2001). Over the years we have learned that depending on what information the dendritic tree should sample it exhibits various shapes. Many brain areas for instance are organised into layers such as the cortex, hippocampus or the retina, with dendrites connected to presynaptic partners in specific layers (Sanes & Zipursky, 2010). Thus, leaving the last question, on how complex dendrites are established, unanswered. Understanding the structural diversity of dendritic trees is essential for comprehending the function and contribution dendrites make to cognitive processes.

A variety of *in vitro* and *ex vivo* methods have been used to understand the cell biology of dendrites. However, the knowledge derived from these studies does not always reflect the natural dynamics of the system. Rather than the steady state growth suspected from fixed tissues, real-time imaging has demonstrated a dynamic extension and retraction of dendrites during differentiation (Dailey & Smith, 1996). Dendrites are shaped not only by their intrinsic properties but also by their extracellular environment (H. T. Kim, Lee, Kim, & Hwang, 2013; Kupferman et al., 2014; Lom & Cohen-Cory, 1999; W. K. Yang & Chien, 2019). Therefore, it is important to develop imaging approaches to follow dendrite differentiation *in vivo* (Pittet & Weissleder, 2011). The dendritic arborisation (da) neurons

of *Drosophila melanogaster* and the PVD neurons of *Caenorhabditis elegans* have provided effective model systems for *in vivo* imaging of dendrites with the additional advantage of being able to exploit the well-studied genetics of these two systems (Albeg et al., 2011). *Drosophila* da neurons have uniquely identifiable dendritic trees with reproducible dendrite morphologies, thought to be homologous to those of vertebrate neurons (Grueber, Yang, Ye, & Jan, 2005; Sanchez-Soriano et al., 2005).

1.1.1 Dendritic Arborisation Neurons of *Drosophila*

The highly stereotypical organisation of the dendritic trees of multidendritic dendritic arborisation (da) neurons of the *Drosophila* peripheral nervous system (PNS) makes them an ideal model system to study dendrite morphogenesis. Neurogenesis and cell fate determination in the *Drosophila* PNS have been studied extensively (Y. N. Jan & Jan, 1993). The availability of neuronal specific markers and a technique for expression of markers in a single neuron (MARCM) and subsets of neurons (Gal4/UAS), have allowed the analysis of dendritic morphogenesis in wild-type and mutant animals (Brand & Perrimon, 1993; Goodman et al., 1984; L. Y. Jan & Jan, 1982; Lee & Luo, 1999; Zipursky, Venkatesh, Teplow, & Benzer, 1984). The variety in dendritic tree complexity between classes of da neurons have made it possible to conduct genetic screens to identify genes involved in different dendritic morphologies. Unlike the mammalian peripheral sensory neurons which have mostly axon-like endings, the *Drosophila* da neurons are dendritic-like (Bodmer & Jan, 1987). They do not receive synaptic inputs but display mechanosensation such as proprioception, mechanical nociception and gentle-touch sensation (Cheng, Song, Looger, Jan, & Jan, 2010; Song, Onishi, Jan, & Jan, 2007; Tracey, Wilson, Laurent, & Benzer, 2003; Yan et al., 2013; Zhong, Hwang, & Tracey, 2010).

The da neurons grow almost two-dimensional dendrites between the epidermis and the extracellular matrix (ECM) wall of the larva, making them accessible to *in vivo* imaging. Each hemisegment A2-A6 of the larva contains 15 da neurons positioned in a ventral, lateral or dorsal cluster. In accordance with their increasing dendrite complexity these 15 neurons are categorised into four classes (Grueber, Jan, & Jan, 2002). The Class I da (c1da) neurons have the simplest dendritic trees and are essential for the sensory feedback loop that reports the sequential contraction of the larval muscles for peristaltic crawling movement (Hughes & Thomas, 2007; Song et al., 2007). Class II da (c2da) neurons have

long dendrites that extend to distant targets and together with Class III da (c3da) neurons mediate gentle touch responses (Tsubouchi, Caldwell, & Tracey, 2012; Yan et al., 2013). The dendritic trees of c3da neurons are additionally decorated with numerous small branchlets and are also required for cold sensation (Turner et al., 2016). The Class IV da (c4da) neurons have the most complex dendritic tree and play a role in the nocifensive escape behaviour to light, mechanical, chemical and thermal stimuli as well as to the attack of parasitic wasps (Hwang et al., 2007; Y. N. Jan & Jan, 2010; Xiang et al., 2010). In response to noxious thermal ($> 45^{\circ}\text{C}$) or mechanical stimulation the L3 larvae rotate around the anteroposterior axis (Tracey et al., 2003).

1 General Introduction

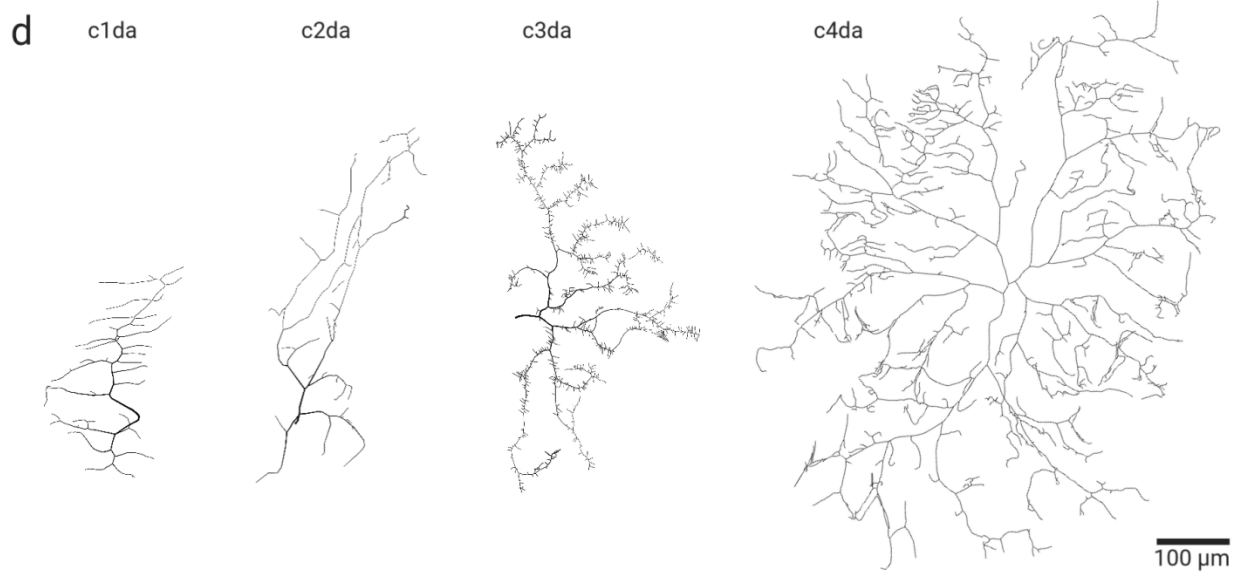
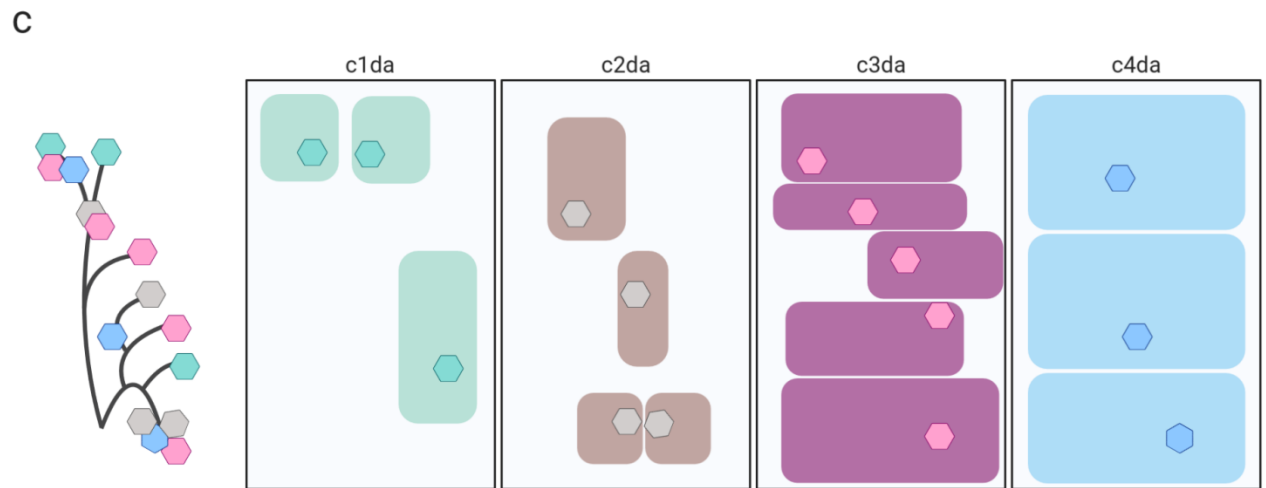
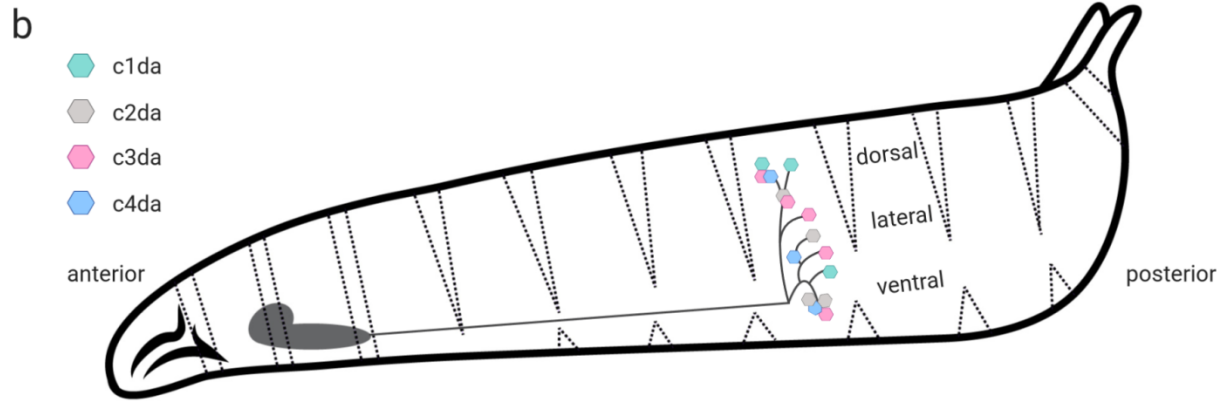
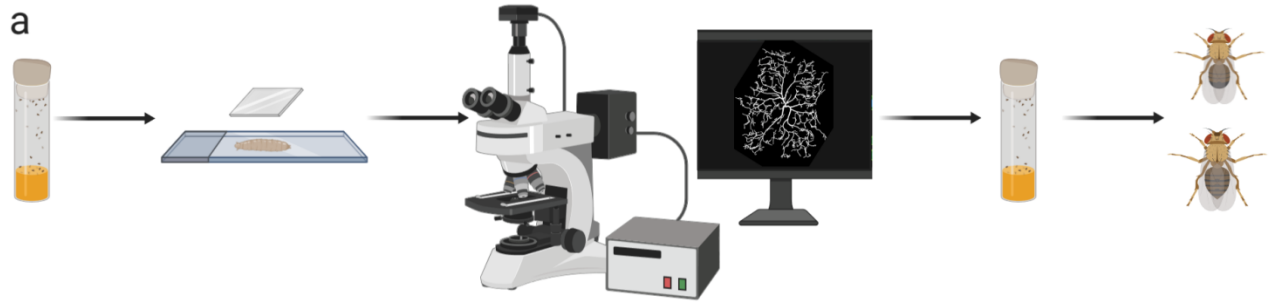


Figure 1: Dendritic Arborisation Neurons of *Drosophila*

a) *Drosophila* are kept and crossed in fly tubes containing food (yellow) and sealed with cellulose acetate plugs for air exchange. For imaging, *Drosophila* larva of the correct genotype are taken from such a tube and immobilised between the coverslip and the glass slide. After imaging of one neuron (example class IV ddaC neuron) the larva is placed back into a new fly tube and images are only kept if the larva develops into an adult *Drosophila*. b) Schematic illustration of a *Drosophila* larva with the mouthhooks (black) and larval brain (grey) anterior (to the left) and abdominal spiracles posterior (to the right). The soma of the 15 da neurons of one hemisegment are visualised as colored hexagons of the four different classes of da neurons and their axons project into the ventral nerve cord of the central nervous system (grey line). This pattern is repeated in each abdominal hemisegment. c) Schematic representation of the dendritic fields of the different classes of da neurons within one hemisegment. d) Computer tracings of one example of a dendritic tree of each class of da neurons (c1da: ventral vpda, c2da: lateral ldaC, c3da: lateral ldaB, c4da: dorsal ddaC). Neurons and larva in this figure are oriented with anterior to the left, posterior to the right, dorsal up and ventral down. Created with BioRender.

1.1.1.1 Transcriptional Regulation

The distinctive dendritic morphologies of the different classes of da neurons are controlled by different levels of single transcription factors (TF) and distinct combinations of TFs. The simple c1da neurons are the only da neurons containing the TF Abrupt and its ectopic expression in a different class of da neurons displaying complex dendrites, leads to a strong reduction in dendritic tree complexity (Li, Wang, Menut, & Gao, 2004; Sugimura, Satoh, Estes, Crews, & Uemura, 2004). The TF Spineless is expressed in all da neurons and harder to interpret as mutants of spineless result in an increase of c1da and c2da neurons but decrease of c3da and c4da dendrite complexity (M. D. Kim, Jan, & Jan, 2006). The molecular mechanisms by which Spineless acts are not known for da neurons but it is conceived that it might counteract class-specific programs (M. D. Kim et al., 2006). The TF Cut is also expressed in several da neuron classes. Highest levels of Cut can be detected in c3da neurons, followed by c4da and very low levels in c2da neurons (Grueber, Jan, & Jan, 2003). The loss of Cut in c3da neurons leads to a reduction in the dendritic tree complexity and ectopic over expression in c1da, c2da or c4da neurons leads to the formation of small terminal branchlets characteristic of c3da neurons (Grueber, Jan, et al., 2003). Cut expression is modulated by further

developmentally controlled TFs. The Longitudinal lacking (Lola) TF promotes Cut expression while the TEAD/TEF-1 transcription factor Scalloped (Sd) and Vestigial (Vg) repress Cut expression (Corty, Tam, & Grueber, 2016; Ferreira, Ou, Li, Giniger, & van Meyel, 2014). Cut in turn represses the expression of the TFs POU domain proteins (Pdm1/2) (Corty et al., 2016). The c4da neurons specifically express the TF Collier/Knot that promotes branching but suppresses the CUT-induced small terminal branchlets typical of c3da neurons, contributing to defining the differences in dendrite morphology between the two classes (Hattori, Sugimura, & Uemura, 2007; Jinushi-Nakao et al., 2007). Additionally, to mutant loss-of-function screens also RNA interference (RNAi) has been used to carry out large screens to identify transcriptional regulators that control dendritic tree shape. For the c1da neurons this has led to the identification of over 70 TFs that play an essential role in their stereotyped morphology (Parrish, Kim, Jan, & Jan, 2006). While only few of those have been further explored in detail, this result suggests a high level of complexity in transcriptional regulation of each neuronal type.

1.1.1.2 Dendritic Organisation and Growth

There are three main cellular mechanisms in da neurons that define the spreading and coverage of the respective receptive field of each neuron: self-avoidance, coexistence and tiling. Dendrites exhibit self-avoidance, which refers to the tendency of branches of the same cell to minimise crossing or overlap (Kramer & Stent, 1985). This ensures that dendrites cover a territory in a non-redundant manner. In the da neurons, this self-avoidance (isoneuronal avoidance) is mediated by the Down syndrome cell adhesion molecule (Dscam1), a member of the immunoglobulin superfamily (Matthews et al., 2007). Alternative splicing of the complex gene locus can potentially generate 19008 different isoforms that can interact via highly specific homophilic binding (Schmucker et al., 2000; Wojtowicz, Flanagan, Millard, Zipursky, & Clemens, 2004). Subsets of such isoforms are expressed in each neuron and homophilic binding initiates repulsion between dendritic branches of the same neuron. Neighbouring neurons are unlikely to express the same set of Dscam isoforms, allowing them to coexist in the same receptive fields, also described for mushroom body neurons and projection neurons of the antennal lobe (Soba et al., 2007; J. Wang, Zugates, Liang, Lee, & Lee, 2002; Zhu et al., 2006). Dendrites of dscam mutants collapse into tangled bundles (Matthews et al., 2007). In mammals the homologues of Dscam cannot undergo this alternative splicing and the self-avoidance in

certain types of neurons is mediated by the clustered Procadherins (Pcdhs) (Kohmura et al., 1998; Q. Wu & Maniatis, 1999; Zipursky & Sanes, 2010). Thus, although the specific molecule used is different, the logic of the mechanism supporting self-avoidance appears conserved across species. In addition to this self-avoidance, the dendrites of different neurons belonging to the same functional group often avoid displaying overlapping dendritic fields to guarantee a unique and non-overlapping representation of a receptive field. This principle is referred to as tiling (heteroneuronal avoidance) and is particularly relevant in sensory systems. Tiling behaviour often involves dendrite-dendrite repulsion between neurons, as also observed in the mammalian retina (Perry & Linden, 1982) and among the dendrites of sensory da neurons that tile the body wall of the fly larva (Grueber et al., 2002). In the case of da neurons, severing experiments have elucidated that neighbouring isoneuronal branches can grow into the wounded area to compensate the loss of dendritic branches, revealing a competitive interaction (Sugimura et al., 2003). While all da neurons coexist, only the c3da and c4da neurons show repulsive interactions between isoneuronal and heteroneuronal dendrites (Grueber, Ye, Moore, Jan, & Jan, 2003). The molecular pathway regulating the recognition and repulsion of heteroneuronal dendrites required for tiling remains unknown. Finally, once the dendrites have extensively covered their appropriate receptive field they need to be actively maintained (Parrish, Emoto, Jan, & Jan, 2007). In the c4da neurons the Polycomb group (PcG) genes and the Hippo pathway, through the NDR kinase Warts (WTS) and the WTS adaptor protein Salvador (SAV), promote dendrite maintenance (Parrish et al., 2007). Maintenance of dendritic fields even as the territory changes is essential for example as the animal grows in size. Additionally, the mechanisms to maintain dendritic trees have been scrutinised in a variety of investigations as defects in this mechanism are strongly correlated with mental retardation and precede cell death in neurodegeneration (Kaufmann & Moser, 2000).

1.1.1.3 Extrinsic Factors

Additionally, to intrinsic programs, extrinsic cues and substrate interactions direct dendrite morphology. The dendrites of da neurons grow on an epidermal layer in a largely two-dimensional manner and are intermittently enwrapped by epidermal cells; with different classes displaying varying degrees of enclosure (Tenenbaum, Misra, Alizzi, & Gavis, 2017). Loss of dendrite-ECM interactions result in uncharacteristic dendrite

crossings between and within c4da neuron dendritic trees as they are no longer retrained into the same layer thus do not interact to produce repulsion and tiling. There are several mechanisms that regulate the adhesion of the c4da neuron dendrites to the ECM. For one, the Tricornered (TRC) kinase and its regulatory activator Furry (FRY), targets of rapamycin, Sin1 and Ricor, and Turtle mediate the interaction of c4da neurons with the ECM (Emoto et al., 2004; Han et al., 2012; M. E. Kim, Shrestha, Blazeski, Mason, & Grueber, 2012; Koike-Kumagai, Yasunaga, Morikawa, Kanamori, & Emoto, 2009; Long, Ou, Rao, & van Meyel, 2009). Additionally, the semaphorins, extracellular signalling proteins that predominantly function through Plexin receptors regulate this interaction upstream of the TRC-FRY pathway (Perala, Sariola, & Immonen, 2012). Mutations in *sema-2b* cause detachment of dendrites from the ECM leading to increased crossing of dendrites (Meltzer et al., 2016). Moreover, loss of integrin function in c4da neurons or block of epidermal laminin production leads to defects of the dendrite adhesion to the ECM and loss of two-dimensional growth necessary for self-avoidance and space filling (Han et al., 2012; M. E. Kim et al., 2012; Meltzer et al., 2016). Loss of the re-arranged during transfection (Ret) kinase that physically interacts with integrins leads to dendrite adhesion defects and recent work has identified the upstream mediator of Ret, TGF- β ligand maverick (Mav) (Hoyer et al., 2018). Ret is required for the uptake of Mav, whose local levels determine dendrite growth preference (Hoyer et al., 2018). Moreover, the Robo receptor and its ligand Slit that have been extensively analysed in repulsion of axonal growth cones at the midline and axonal branching, play a role in dendrite morphology (Dickson & Gilestro, 2006; Ma & Tessier-Lavigne, 2007; K. H. Wang et al., 1999). In c4da neurons loss of Roundabout (Robo) or Slit results in faster elongation and less branching of dendrites, these two interactors are therefore thought to coordinate appropriate branching to space-fill the receptive field (Dimitrova, Reissaus, & Tavosanis, 2008). Furthermore, dendrites of the c3da and c4da neurons cover the body wall quickly during mid embryogenesis before growing into precise proportions with the constantly growing body wall of the larva; this scaling growth requires the microRNA bantam in epithelial cells (Parrish, Xu, Kim, Jan, & Jan, 2009). Therefore, in face of these developmental programs, interactions with the local environment and sensing of the environmental cues are essential for shaping the dendrite morphology.

1.1.2 Neural Computation of Dendritic Shape

Dendrite complexity characterising distinct neuron-subtypes is thus formed through a combination of extrinsic and intrinsic factors. This interaction finally establishes a robust structure that remains plastic to adapt to changes in the environment and modification by activity (Dong, Shen, & Bulow, 2015; Grueber, Jan, et al., 2003; Lefebvre, Sanes, & Kay, 2015; Puram & Bonni, 2013; Valnegri, Puram, & Bonni, 2015). For a variety of electrophysiological, pharmacological and histological studies dendritic trees are accurately traced into digital files in a labour-intensive manner. This allows a quantitative morphological and stereological characterisation of the dendritic trees. Web-accessible archives such as NeuroMorpho.Org store these digital reconstructions, which can be used for comparative geometric investigations, statistical assessments of synaptic contacts or computational models of biophysics. These studies can elucidate general questions of dendrite morphology: Is there a common branching rule for all neurons? What are the general features of a dendritic tree? Is there a basic principle of optimising synaptic efficacy?

The specific shape of dendrites has been observed from a mathematical point of view for several decades. The first steps towards this were taken by Hillman, who proposed that the dendritic morphology of any neuron could be described completely with fundamental parameters (Hillman, 1979, 1988). Additionally, to describing the dendritic tree with parameters Hillman was able to produce an algorithm that replicated the dendritic morphology. The theory behind an algorithm is that if it is able to mimic the accurate structure of a neuron, it must contain all the required information and thus be able to completely describe the morphology. Early versions of algorithms did not suit to capture many of the constraints and features of a dendritic tree. The branches in the algorithm of Hillman were, for example, based on single straight cylinders between bifurcations and consequently did not consider the tortuosity of the segments and thus the actual dendritic path length. It was, however, a first step to understanding the general principles underlying dendritic morphology. Computational constructs are useful to determine the influence of single geometry features on the system neuroanatomy or the interaction between parameters and for example electrophysiological activity (Rall, 1962). Computational techniques can simulate the physical and biological constraint of a dendritic tree and construct synthetic dendritic trees (G. A. Ascoli, 1999; Stiefel &

Sejnowski, 2007). A detailed data-driven computational model can be used to validate, predict and carry out new experiments within a biological process (G. A. Ascoli, 2002). Rule-based stochastic models from real dendritic trees can uncover new constraints or uncover the role of wiring constraints (G. A. K. Ascoli, J. L., 2000; Bird & Cuntz, 2019; Burke, Marks, & Ulfhake, 1992; Uemura, Carriquiry, Kliemann, & Goodwin, 1995). Balancing metabolic cost and the necessity to cover a receptive field is thought to determine the size and shape of dendritic trees (Shepherd, Stepanyants, Bureau, Chklovskii, & Svoboda, 2005; Wen & Chklovskii, 2008). It has been shown that optimisation to reduce wiring is implemented by dendritic trees and this can be shown mathematically. A so called balancing factor, that weighs the costs of material and conduction time, can describe this effect for a variety of dendritic trees (Cuntz, Forstner, Borst, & Hausser, 2010; Klyachko & Stevens, 2003; Wen, Stepanyants, Elston, Grosberg, & Chklovskii, 2009).

Understanding the role of dendrites in neuronal computation requires theories that can reveal the basic principles and benefits of a neuron having certain dendrite morphologies. Replicating single dendrite morphologies with algorithms have validated fundamental constraints of dendritic organisation and revealed general branching principles. These models are essential to simulate conditions that are very difficult to test experimentally but also for the ultimate step of building artificial neural networks that incorporate such single neuron models.

1.1.3 Dendrite Dynamics

Cellular and transcriptional mechanisms specify a general shape and size but are unlikely to determine the number and position of all dendritic branches in any mature dendritic tree, as this would completely forestall the plasticity of the nervous system. The formation of a dendritic branch is a very dynamic process in which short branchlets are constantly formed and retracted until they get stabilised and extended further (H. T. Cline, 2001; Q. Wu & Maniatis, 1999). The remodelling of branching patterns has been studied in the scale of minutes to hours (Jontes, Buchanan, & Smith, 2000; Kaethner & Stuermer, 1997; G. Y. Wu, Zou, Rajan, & Cline, 1999). Already the work of Dailey and Smith in developing pyramidal neurons of rat hippocampal slices showed new branches arise and disappear on primary dendrites (Dailey & Smith, 1996). *In vivo* imaging of optical tectal neurons in *Xenopus* or zebrafish larva has demonstrated that stabilisation of dendritic

branches occurs when new synapses are formed (Haas, Li, & Cline, 2006; Niell, Meyer, & Smith, 2004; Sin, Haas, Ruthazer, & Cline, 2002). Thus, one hypothesis to explain this dynamic behaviour of dendrites is that they sample the local environment for appropriate contact sites (Fiala, Feinberg, Popov, & Harris, 1998; Portera-Cailliau, Pan, & Yuste, 2003; Vaughn, 1989). Generally, whether a dynamic branch will survive to become part of the mature dendritic tree depends on several factors, including the formation of synapses but also cell-extrinsic cues, contact with a permissive substrate, and the activity of those synapses (H. Cline & Haas, 2008; Yuste & Bonhoeffer, 2004). Thus, a dendritic tree is not formed in a predetermined intrinsic manner but rather is shaped by its intrinsic signalling in interaction with the environment. Plastic dendritic branches and spines allow the neuron to change shape and turn over as the circuits refine (Holtmaat, Wilbrecht, Knott, Welker, & Svoboda, 2006; Majewska, Newton, & Sur, 2006; Vaillant et al., 2002).

As the information-receiving unit of a neuron, these dynamic processes are tightly regulated. The cytoskeleton is the underlying structure that defines the dendritic tree and is in turn influenced and rearranged by associated proteins.

1.2 The Dendrite Actin Cytoskeleton

The cytoskeleton is a network of interlinked protein filaments that not only stabilises eukaryotic cells but also regulates dynamic processes. It consists of three major filament types: microtubules, intermediate filaments and actin filaments. In the context of dendrites, microtubules and actin filaments play the pivotal role during dendrite development, shape maintenance, transport and dynamics (Pollard & Cooper, 2009). The cytoskeleton is capable of prompt assembly and disassembly to respond to the cell's necessities. The organisation and dynamics of microtubules and actin structures are controlled by microtubule associated proteins (MTs) and numerous actin regulatory proteins (ARPs), which extensively interact and feed back to each other (Coles & Bradke, 2015; Dominguez & Holmes, 2011; Georges, Hadzimichalis, Sweet, & Firestein, 2008).

Most studies on actin arrangement in dendrites have focused on dendritic spines (Izeddin et al., 2011; Korobova & Svitkina, 2010; Urban, Willig, Hell, & Nagerl, 2011); however, recently several new actin-based structures of dendrites have been discovered. The fine structure of the actin network has made it hard to visualise complex and dynamic actin structures. Preparations for electron microscopy are challenging on the fine actin network

that becomes rapidly destabilised and the resolution of optical microscopy is limited. Super resolution fluorescence microscopy has revealed actin patches, longitudinal actin fibres and periodic actin rings in the dendrites (Bar, Kobler, van Bommel, & Mikhaylova, 2016; D'Este, Kamin, Gottfert, El-Hady, & Hell, 2015; He et al., 2016; Willig et al., 2014). These structures are thought to support dendrite shape, help the organization of proteins along the membrane and in the case of actin patches serve as outgrowth points for filopodia in axons and dendrites (Korobova & Svitkina, 2010; Xu, Zhong, & Zhuang, 2013).

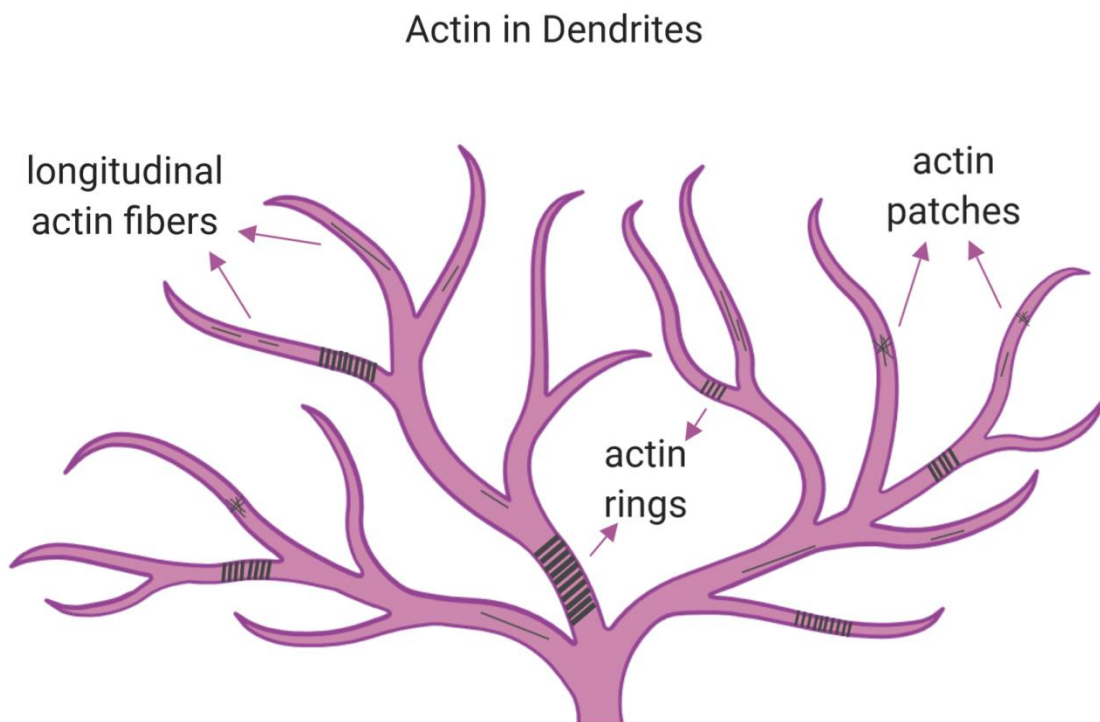


Figure 2: Actin Structure in Dendrites

Overview of different F-actin structures present in dendrites. Actin patches, longitudinal actin fibers and cortical periodic actin/spectrin lattice referred to as actin rings. Created with BioRender.

1.2.1 The Actin Cytoskeleton

Actin is a highly conserved protein, present in two states in eukaryotic cells; free monomers, referred to as globular actin (G-actin), which polymerise into helical filamentous actin (F-actin) (Figure 3a) (Fujii, Iwane, Yanagida, & Namba, 2010; Holmes,

Popp, Gebhard, & Kabsch, 1990; Reisler, 1993). Multicellular organisms have several isoforms of monomeric actin proteins with partially tissue specific distributions and functions (Perrin & Ervasti, 2010; Wagner, Mahowald, & Miller, 2002). Actin hydrolyses ATP within the filament to produce ADP and a phosphate group. However, the ADP-bound actin monomers can remain within the filament and the actin filament can contain ATP-actin, ADP-actin and actin bound to ADP and the phosphate group (Vavylonis, Yang, & O'Shaughnessy, 2005). All actin subunits (around 42 kDa) in a filament are facing with the ATP binding site to the 'pointed' end, making the filament polar (Verkhovskiy, Svitkina, & Borisy, 1997). Actin filaments can extend by adding actin monomers both from the 'pointed' (-) end and the 'barbed' (+) end, but the latter incorporates monomeric actin around ten times faster (Pollard, 1986; Vavylonis et al., 2005). Although differences in critical concentration of divalent cation availability, ionic strength and nucleotide state of the actin monomers can vary the polymerisation rate, it has been shown that the pointed end always has a lower critical concentration than the barbed end (*in vitro*: 0.8 μM and 0.1 μM) (Carlier, Pantaloni, & Korn, 1987; Fujiwara, Vavylonis, & Pollard, 2007; Gordon, Boyer, & Korn, 1977; Kuhn & Pollard, 2005; Pollard, 1986). A balance of association of actin monomers to the barbed end and dissociation of filaments subunits at the pointed end is referred to as treadmilling and can be observed in single actin filaments *in vitro* (Figure 3a) (Pollard, 1986) as well as in intracellular lamellipodial actin arrays (Watanabe & Mitchison, 2002).

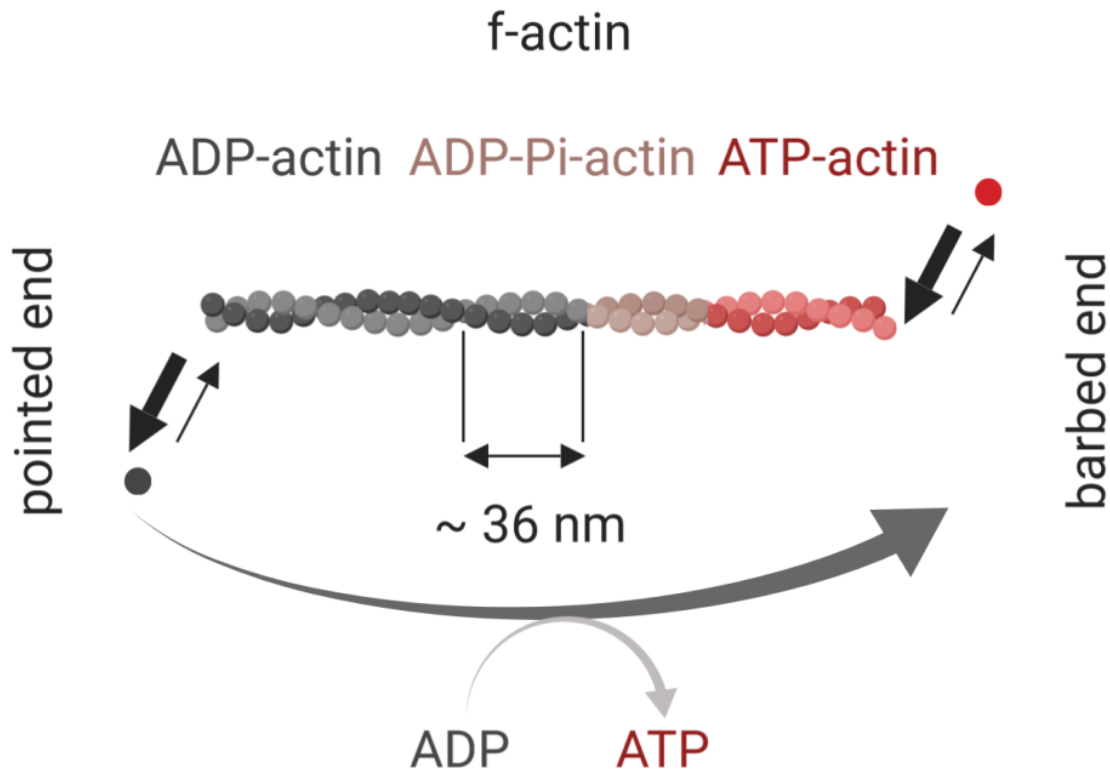


Figure 3: Treadmilling of Actin

Actin filaments (F-actin) are linear polymers of globular actin (G-actin) with a helical repeat every ~ 26 nm. Actin filaments are polar structures, with different ends, termed pointed end and barbed end. Free ATP-actin proteins are added to the barbed end of the filament. After some time, ATP will hydrolyse and subsequently release free inorganic phosphate (Pi) molecules to yield ADP-actin. In the presence of ATP actin filaments and actin monomers exist in a balance, with the barbed end of actin filaments growing and the pointed end shrinking is a process referred to as treadmilling. Created with BioRender.

1.2.2 Actin in Protrusions

Actin filaments can assemble at the leading edge of a cell with the fast growing ‘barbed’ ends, providing the cell with pushing forces required to form protrusions (Kovar & Pollard, 2004). The structural polarity of the actin filament, with one end growing faster than the other, and treadmilling, to free new monomers to be recycled, enables actin to push with the barbed end toward for example the plasma membrane (Borisy & Svitkina, 2000; Elson, Felder, Jay, Kolodney, & Pasternak, 1999; Woodrum, Rich, & Pollard, 1975). Membrane protrusions in cells are supported by parallel actin bundles for filopodia

or a branched actin network for lamellipodia. Filopodia are fine protrusions especially important for the cells to probe their environment, characteristically containing bundling and crosslinking proteins as well as anti-capping factors (Svitkina et al., 2003; Vignjevic et al., 2006). In the growth cone, a highly dynamic actin-supported extension of the axon, the filopodia guide the neurites in the preferred direction (O'Connor, Duerr, & Bentley, 1990; Robles, Huttenlocher, & Gomez, 2003). Lamellipodia can create even stronger pushing forces in the cell, to for instance propel the leading edge forward (Abercrombie, Heaysman, & Pegrum, 1970; Small, Isenberg, & Celis, 1978).

1.2.3 Regulation by Actin Regulatory Proteins

The organisation and dynamics of the actin cytoskeleton are regulated by over 100 different ARPs that are grouped according to their function (Dent, Gupton, & Gertler, 2011; Lappalainen, 2016; Letourneau, 2009; Pollard & Cooper, 2009). The assembly of F-actin has to be very dynamic to achieve the different actin functions (Blanchoin, Boujemaa-Paterski, Sykes, & Plastino, 2014). It is though that to control space and time of F-actin polymerisation the spontaneous polymerisation of G-actin to F-actin has to be prevented. This is achieved on one hand by the instability of the actin dimer, trimer and even tetramer, on the other hand by sequestering proteins like Profilin and β -Thymosin (Figure a, b) (Pantaloni & Carlier, 1993; Sept & McCammon, 2001). This kinetic barrier is overcome by so called actin nucleators or nucleation complexes (Pollard & Cooper, 2009; Quinlan & Kerkhoff, 2008). Currently there are three main actin nucleator classes: Formins, actin related protein 2/3 (Arp2/3) and the tandem actin binding domain (TBM) nucleators.

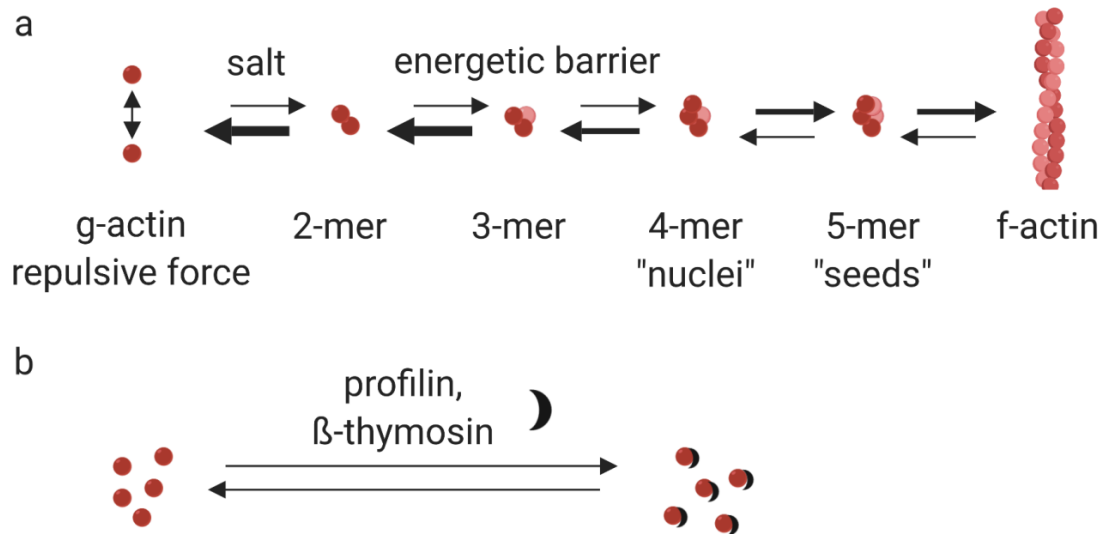


Figure 4: Actin Dynamics

a) G-actin molecules electrostatically repulse each other. Activation of the monomer via salt binding is thought to increase the availability of G-actin (Cooper, Buhle, Walker, Tsong, & Pollard, 1983; Frieden & Patane, 1985; Gershman, Newman, Selden, & Estes, 1984). The trimers and tetramers are sequentially formed, however, these are energetically highly unfavourable reactions (Oda, Aihara, & Wakabayashi, 2016). Once the tetramer is formed the reaction to a filament proceeds fast until the concentration of monomers comes to a critical concentration (Oda et al., 2016). b) Formation and stabilisation of F-actin is regulated by proteins that bind free monomers. Thymosin binding inhibits its association with F-actin. Profilin binding inhibits the association with the pointed end but enhances its association to the barbed end of F-actin. Created with BioRender.

Formins

The formin family proteins assemble in a donut shaped dimer and stabilize actin dimers and trimers to actin nuclei by encircling them with their Formin homology 2 (FH2) domains (Figure 5a) (Higgs & Peterson, 2005; Otomo & Rosen, 2005). The Formin homology 1 (FH1) domain is proline-rich and can recruit and bind Profilin-bound actin. Additionally, to their function as actin nucleators, Formins can elongate filaments by binding to the barbed end and continuously adding actin monomers to the growing filament in a coordinated action of multiple domains (Breitsprecher et al., 2012; Kovar, 2006; Paul & Pollard, 2009; Pring, Evangelista, Boone, Yang, & Zigmond, 2003; Pruyne et al., 2002). There are Formins that can bind along the length of actin filaments and

microtubules promoting cytoskeletal network bundling and coordination (Chhabra & Higgs, 2006; Gurel et al., 2014). The binding of Formins to microtubules inhibits actin filament nucleation fully but has no effect on the rate of actin elongation (Gaillard et al., 2011; Rosales-Nieves et al., 2006).

Arp2/3 Complex

The Arp2/3 complex comprises multiple isoforms of seven subunits. The Arp2-Arp3 component mimics an actin dimer that is thought to elongate towards the barbed end while the remaining subunits (ArpC1-5) make contact with the mother filament (Figure 5b) (Dominguez & Holmes, 2011; Pollard & Beltzner, 2002). By binding to existing actin filaments, it can nucleate the growth of new filaments from their sides. Arp2/3 is the only nucleator known to induce branched actin (Pollard, Blanchoin, & Mullins, 2000; Welch & Mullins, 2002). Activation of the Arp2/3 complex requires ATP hydrolysis and binding of so called nucleation-promoting factors (NPFs) that induce a conformational change within the complex (Goley et al., 2006). There are two classes of NPFs. The Class I NPFs have a conserved C-terminal Wiskott-Aldrich homology 2 (WH2), Cofilin-homology and acidic region (WCA) domain that interacts with G-actin and the Arp2/3 complex (Chereau et al., 2005). The Class II NPFs activate the Arp2/3 complex to a much weaker extent as they cannot recruit G-actin to the complex; the best studied example of this group is cortactin (Urano et al., 2001; Weaver et al., 2001).

TBM Nucleators

The TBM nucleators contain multiple WH2 domains that appear in tandem repeats of up to four domains. Each domain can bind an actin monomer; thereby the TBM nucleator brings several actin monomers in close proximity (Figure 5c). Some TBM nucleators like Spire, Vibrio parahaemolyticus and Vibrio cholera factors (VopL/VopF) or adenomatous polyposis coli (APC) have been suggested to form dimers and to detach shortly after actin nucleus formation for the filament to be formed in the right conformation (Namgoong et al., 2011; Okada et al., 2010; Quinlan, Heuser, Kerkhoff, & Mullins, 2005). In the case of Spire the dimerization is dependent on its kinase non-catalytic C-lobe domain (KIND) domain, that has been suggested to autoinhibit Spire by binding to its FYVE-type domain, but can also bind to the Formin Capu/Formin2, thereby inhibiting the nucleation activity of the Formin and accelerating the activity of Spire (Cicarelli, Bork, & Kerkhoff, 2003; Quinlan, Hilgert, Bedrossian, Mullins, & Kerkhoff, 2007; Zeth et al., 2011). The TBM

nucleators have a lower nucleation activity than the Arp2/3 complex or Formins, with a suggested switch from actin nucleation to actin sequestering at low nucleator:actin ratios for Spire, Cordon Bleu (Cobl) and VopF (Ahuja et al., 2007; Avvaru, Pernier, & Carlier, 2015; Bosch et al., 2007).

Ena/VASP

Enabled (Ena)/Vasodilator-stimulated phosphoprotein (VASP) proteins encompass an N-terminal Ena/VASP homology 1 (EVH1) domain that can bind to specific proline-rich motifs, which are found in a variety of proteins, including Formins, the receptor Robo, and a number of Class I NPFs (Bashaw, Kidd, Murray, Pawson, & Goodman, 2000; Castellano, Le Clainche, Patin, Carlier, & Chavrier, 2001; Chen et al., 2014). A proline-rich domain binds Profilin-actin complexes and the EVH2 domain mediates tetramerization and interacts with G- and F-actin (Figure 5d) (Bachmann, Fischer, Walter, & Reinhard, 1999; Breitsprecher et al., 2008; Huttelmaier et al., 1999). Although the EVH domains have a high similarity to WH2 domains, the ability of Ena/VASP proteins in nucleating actin filaments in pyrene actin polymerization assays has not been confirmed *in vivo* (Huttelmaier et al., 1999; Lambrechts et al., 2000). There are several possible functions described for Ena/VASP ranging from elongation and anti-capping to anti-branching and bundling. The anti-capping hypothesis is based on work in fibroblast, in which genetic depletion of Ena/VASP leads to shorter and more highly branched actin filaments in the lamellipodium. This is supported by total internal reflection fluorescence microscopy (TIRF) assays, which demonstrate increased filament elongation when purified Capping protein (CP) and VASP were present (Bear et al., 2002; Pasic, Kotova, & Schafer, 2008). The strongest evidence for an anti-branching effect is in a visual assay from Skoble and colleagues in which VASP reduces branching induced by the Arp2/3 complex (Skoble, Auerbuch, Goley, Welch, & Portnoy, 2001). Bundling by Ena/VASP oligomers has been observed in the distal tips of actin bundles in filopodia (Applewhite et al., 2007; Lanier et al., 1999).

Bundling Factors

The actin filaments that Ena/VASP preferably binds to are bundled by different cross-linking proteins (Faix & Rottner, 2006; Gupton & Gertler, 2007; Harker et al., 2019). The cross-linker α -actinin can bundle parallel and antiparallel fibres and is best studied in focal adhesions and stress fibers in which it bundles with wide spacing (Sjoblom,

Salmazo, & Djinovic-Carugo, 2008). There are even cross linkers that can bundle mixed polarity filaments, such as Fimbrin in the lamellipodium (Hanein et al., 1998). The filaments in filopodia are mostly bundled by Fascin, which bundles parallel filaments with very narrow spacing (Figure 5d) (Cant, Knowles, Mooseker, & Cooley, 1994; S. Yang et al., 2013). It is thought to provide the uniform thickness and stability required for the bundle to push the membrane outwards (Svitkina et al., 2003; Vignjevic et al., 2006). Stabilisation can also be provided to the single filaments through the binding of for example tropomyosin. In the cell, it not only stabilises but also regulates access of other actin regulatory proteins (Blanchoin, Pollard, & Hitchcock-DeGregori, 2001; Ono & Ono, 2002).

Capping Proteins

Once an actin filament is formed highly conserved capping proteins can bind to the barbed end and inhibit further extension (Figure 5e) (Caldwell, Heiss, Mermall, & Cooper, 1989; Cooper & Pollard, 1985). The most abundant capper is the Capping protein (CP), important for example in dendritic spine formation of hippocampal neurons and the uniform alignment of barbed ends in striated muscle (Fan, Tang, Vitriol, Chen, & Zheng, 2011; Pappas, Bhattacharya, Cooper, & Gregorio, 2008). A number of other proteins, such as Gelsolin-family members, Adducins and Eps8, have been described to have barbed-end capping activity (Fowler, 2013; Higgs, 2004; Nag, Larsson, Robinson, & Burtnick, 2013).

Depolymerisation Factors

Depolymerisation and severing of actin filaments is crucial for the rapid reorganisation required for dynamic cellular processes. The actin-depolymerisation factor (ADF)/Cofilin, Gelsolin and other actin severing and depolymerising proteins promote rapid actin filament disassembly (Bamburg, 1999; Lappalainen & Drubin, 1997; Ydenberg et al., 2015). Binding of ADF/Cofilin, preferably to ADP-actin, leads to a change in the conformation and mechanical properties of the actin filament (McGough, Pope, Chiu, & Weeds, 1997; Prochniewicz, Janson, Thomas, & De la Cruz, 2005). ADF/Cofilin saturated filaments are stable but if the filament is only partially decorated ADF/Cofilin leads to severing of the filament (Figure 5f) (Carlier et al., 1997; De La Cruz, 2009). Bulk solution assays have demonstrated that ADF/Cofilin increases the concentration of G-actin and accelerates filament treadmilling (Carlier et al., 1997).

Single filament assays report slow pointed-end depolymerisation in the presence of ADF/Cofilin and fast depolymerisation at the barbed-end of ADF/Cofilin decorated filaments (Andrianantoandro & Pollard, 2006; Wioland et al., 2017). Thus, suggesting a shift in the depolymerisation instead or additionally to a general increase in the dissociation rate of actin subunits (Hild, Kalmar, Kardos, Nyitrai, & Bugyi, 2014). Most vertebrates express three ADF/Cofilin isoforms, non-muscle Cofilin, muscle Cofilin and ADF (Abe, Ohshima, & Obinata, 1989; Bamburg, 1999; Morgan, Lockerbie, Minamide, Browning, & Bamburg, 1993; Nishida, Maekawa, & Sakai, 1984). LIM-kinases and Slingshot phosphatases phosphorylate and dephosphorylate all ADF/Cofilin proteins, respectively, and are critical for the regulation of actin cytoskeleton dynamics (Kiuchi, Nagai, Ohashi, & Mizuno, 2011; Mizuno, 2013; Morgan et al., 1993; Van Troys et al., 2008). There are, however, fundamental differences in actin dynamics of the different isoforms described for example in macrophage and dendritic cells and further supported by different phenotypes in mouse mutants (Bellenchi et al., 2007; Gurniak, Perlas, & Witke, 2005; Jonsson, Gurniak, Fleischer, Kirfel, & Witke, 2012). Invertebrates often only express one ADF/Cofilin gene; *Drosophila* for example has *twinstar* (Gunsalus et al., 1995).

These actin regulatory proteins are most notably regulated by the Rho family GTPases that respond to a variety of extracellular signals. Cdc42, Rac1 and RhoA are recognised as the most relevant members of this family, responsible for the regulation of actin in filopodia, lamellipodia and stress fibre formation (Etienne-Manneville & Hall, 2002).

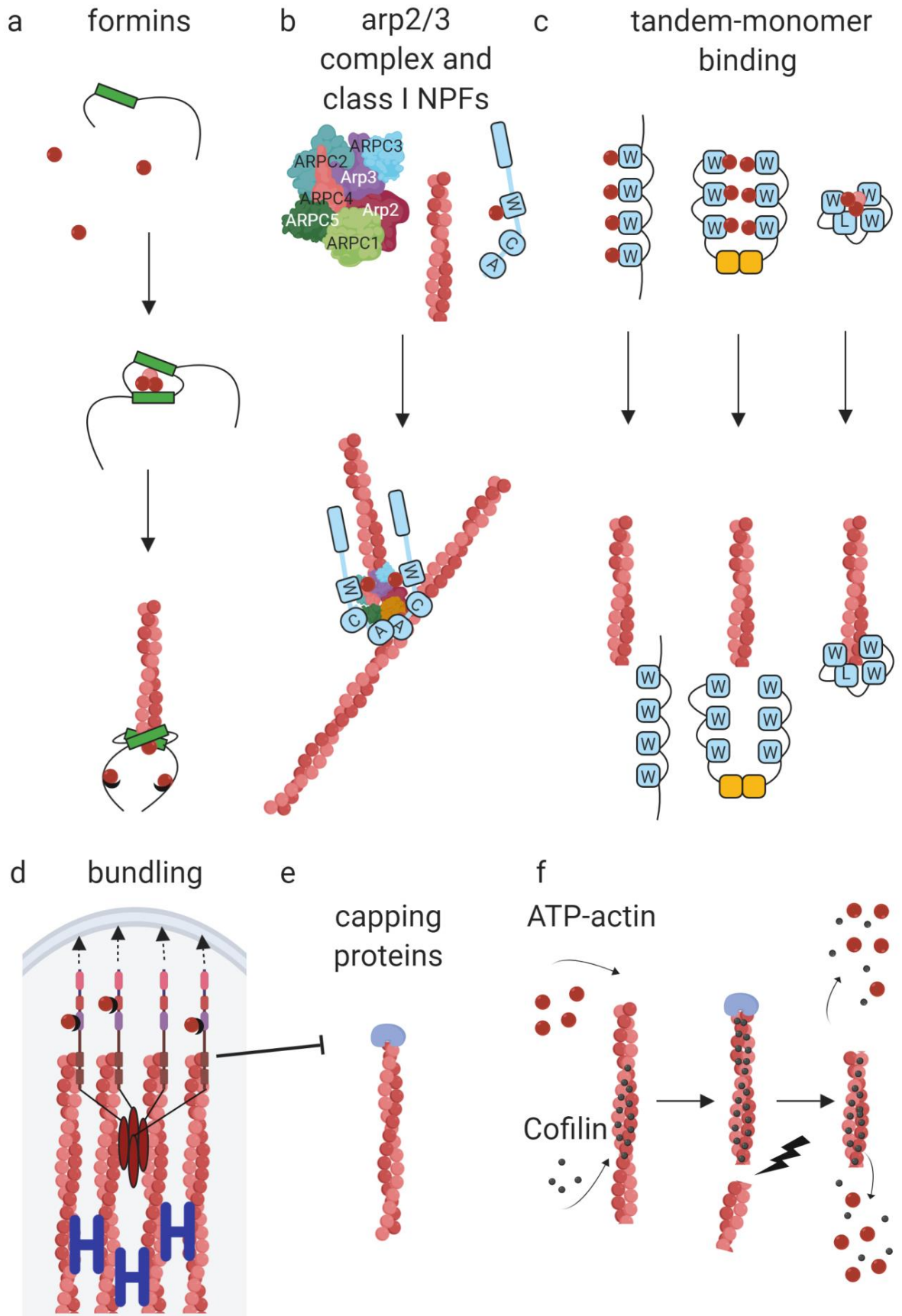


Figure 5: Actin Regulatory Proteins

a) Nucleation factors can overcome the energetic initial polymerisation steps. Formin dimers can bind two G-actin with their FH2domains (green) and recruit Profilin-bound actin with its FH1domain. They can also associate to the barbed end with the FH2domains and elongate by adding Profilin-bound actin with the FH1domains. The Arp2/3 complex once activated by for example an NPF type I can nucleate actin from the side of an existing filament. The TBM nucleators, as dimers or single molecules, bring together actin monomers and form an actin nucleus. Some dissociate from the end after nucleation and others remain associated to the end. b) Ena (red) can bind to F-actin, Profilin-bound G-actin and to various proteins in membranes with its EVH1domain. Ena is thought to form tetramers thereby bundling F-actin. Bundling of actin can also occur through cross-linking proteins (blue) that can bundle parallel, antiparallel or both orientations of F-actin. c) Capping proteins can bind to the ends of F-actin and inhibit assembly and disassembly. Capping protein (CP, light blue) can bind to the barbed end and thereby stabilize it. d) Cofilin can only bind to the ADP-actin region of F-actin and therefore has a preference for pointed end of F-actin. Cofilin binding at the pointed end leads to faster depolymerisation. The presence of capping proteins allows the growing of Cofilin domains to also reach the barbed end. When a filament is partially decorated with Cofilin it is likely to sever at the domain boundaries. Created with BioRender.

1.2.4 Actin Regulatory Proteins in Dendrites

The Rho GTPase proteins are the main regulators of ARPs in the context of dendrite development, Rac1 and Cdc42 promoting and RhoA inhibiting branch formation (Lee, Winter, Marticke, Lee, & Luo, 2000; Ng et al., 2002; Scott, Reuter, & Luo, 2003). New dendritic branches arise from the main branch in filopodia-like actin-rich microstructures. Blocking of F-actin polymerisation with cytochalasin D in early developing hippocampal neurons in culture diminishes this formation (Dent et al., 2011). Local accumulation of actin at branching sites in the c3da neurons in *Drosophila* was observed to precede new branch formation (Andersen, Li, Resseguie, & Brenman, 2005). Recently improved *in vivo* imaging in another class of da neurons have characterised how the actin severing protein Twinstar/Cofilin regulates so called actin blobs that propagate along actin branches and precede branch formation in c4da neurons (Nithianandam & Chien, 2018).

Loss of the actin nucleation factor Cobl in hippocampal neurons, under the regulation of Rho GTPases, leads to a loss of dendritic branches and Cobl localises at the site before

dendrite branching occurs (Ahuja et al., 2007; Hou et al., 2015). In dorsal habenular neurons a similar effect was seen with the actin nucleator Daam1a (Colombo et al., 2013). Loss of the actin anti-capping factor Ena/VASP in *Drosophila* neurons also leads to a simplification of the dendritic tree (Gao, Brenman, Jan, & Jan, 1999). Overexpression of N-WASP in cultured hippocampal neurons increases the number of dendritic branches and blocking reduces distal branches and is thought to function through the activation of the Arp2/3 complex (Nakamura et al., 2011). A study on the actin nucleator Spire, has shown that it is suppressed by the transcription factor Lola in specific classes of neurons in *Drosophila* and its disinhibition caused formation of small dendritic branches uncharacteristic for this neuron (Ferreira et al., 2014; Gates, Kannan, & Giniger, 2011). Importantly, the loss of the actin bundling protein Singed/Fascin is only relevant in c3da neurons and responsible for their characteristic small terminal branches (Nagel et al., 2012). Thus, indicating that different types of dendrite branches of neurons might rely on specific sets of ARPs.

In spite of the progress on individual biochemical activities of all these regulatory proteins and our understanding on fundamental principles governing dendritic trees, the question of how actin regulatory proteins together form a dendritic tree can only be answered to a minor extent. As individual neuron classes require unique branching architecture they also require a class specific repertoire of actin regulatory proteins.

1.3 Aims of the Thesis

In this work, we want to understand how actin regulatory proteins regulate the actin cytoskeleton of dendritic branches *in vivo*. In order to devise how different constellations of actin regulatory proteins collectively form diverse dendritic trees and dynamics, it would be profoundly helpful to know how these proteins affect the different aspects of dendrite elaboration. The individual actin regulatory proteins have been well characterised biochemically; however, understanding the function of these proteins *in vivo* is an ongoing challenge that I am contributing to with this work. The primary goal of this thesis is to understand how different actin regulatory proteins might work together to establish the characteristics of a specific dendritic tree and its branch dynamics. The resulting graphical and mathematical models represent a framework for further investigation of the dendritic trees of c3da neurons and the actin regulatory proteins involved in forming them.

1 General Introduction

2. Transient localization of the Arp2/3 complex initiates neuronal dendrite branching *in vivo*

This chapter of the thesis represents a paper that was published 4th of April 2019 by The Company of Biologists Ltd <http://www.biologists.com/user-licence-1-1>.

2.1 Introduction

Dendrites can be highly branched and account for over 90% of the postsynaptic surface of some neurons (Sholl, 1956). The branching of the dendritic tree directly determines the size of the receptive field and the input signals, influencing the intrinsic firing pattern of the neuron (Dong et al., 2015; van Elburg & van Ooyen, 2010). Positioning of new dendritic branches along the main dendrite and stabilisation or disappearing of these branches generates stereotypical architectures that are cell type specific (Lefebvre et al., 2015). How is such a new branch formed? What are the general principles that place a new dendritic branch? When does a branch stabilise or disappear?

It is unlikely that the exact number and positions of branches of a mature dendritic tree is completely predetermined by cellular and transcriptional mechanisms, however, it specifies the general shape and size. Live imaging studies in *Drosophila* da neurons have demonstrated that a focal actin accumulation precedes new dendritic branch formation (Andersen et al., 2005; Nithianandam & Chien, 2018). In dendrites, the actin cytoskeleton undergoes continual turnover and actin nucleation is the limiting step, owing to the instability of small actin oligomers (Cooper et al., 1983; Frieden, 1983; Sept & McCammon, 2001). The Arp2/3 complex, is one of the nucleation-promoting factors that help to overcome this energy consuming step in actin filament formation (Pollard, 2007). It initiates actin polymerisation along or at the barbed ends of a pre-existing actin filament at a 70° angle, which results in the formation of a branched actin network (Mullins, Heuser, & Pollard, 1998; Pantaloni, Boujemaa, Didry, Gounon, & Carlier, 2000; Svitkina & Borisy, 1999). The assembly of a branched actin filament network is thought to produce the force needed to protrude the membrane (Pollard & Borisy, 2003). The Arp2/3

complex, is the only actin nucleator able to form such network, triggering the question whether the Arp2/3 complex and its regulatory mechanism is the factor controlling new dendritic branch formation.

This publication provides essential knowledge on how a new branch is formed and the role of the Arp2/3 complex in new dendritic branch formation *in vivo*. Additionally, to delineating Arp2/3 function and transient localisation this paper reveals the regulation through the Class I NPF WAVE (WASP-family verprolin homologous protein) and the Rho GTPase Rac1.

2.1.1 Statement of Contribution

Table 1: Statement of Contribution for Stürner and Tatarnikova et al. 2019

Task	Author
Conceptualisation	T.S., A.T., H.C., G.T.
Methodology	T.S., A.T., J.M., B.S., H.C., M.N., V.S.
Software	B.S., H.C.
Formal analysis	T.S., A.T., J.M., B.S., H.C., G.T.
Investigation	T.S., A.T., J.M., B.S., Y.Z., M.N.
Resources	G.T., H.C., S.B., V.S.
Writing - original draft	G.T.
Writing - review & editing	T.S., G.T.
Supervision, project administration and funding acquisition	G.T.

2.2 Publication

Transient localization of the Arp2/3 complex initiates neuronal dendrite branching *in vivo*

Tomke Stürner*, Anastasia Tatarnikova*, Jan Mueller, Barbara Schaffran, Hermann Cuntz, Yun Zhang, Maria Nemethova, Sven Bogdan, Vic Small, Gaia Tavosanis

Development 2019 146: dev171397 doi: 10.1242/dev.171397

* = equal contribution

RESEARCH REPORT

Transient localization of the Arp2/3 complex initiates neuronal dendrite branching *in vivo*

Tomke Stürner^{1,§}, Anastasia Tatarnikova^{1,2,§,¶}, Jan Mueller^{3,*}, Barbara Schaffran¹, Hermann Cuntz^{4,5}, Yun Zhang^{1,‡}, Maria Nemethova^{3,*}, Sven Bogdan⁶, Vic Small³ and Gaia Tavosanis^{1,**}

ABSTRACT

The formation of neuronal dendrite branches is fundamental for the wiring and function of the nervous system. Indeed, dendrite branching enhances the coverage of the neuron's receptive field and modulates the initial processing of incoming stimuli. Complex dendrite patterns are achieved *in vivo* through a dynamic process of *de novo* branch formation, branch extension and retraction. The first step towards branch formation is the generation of a dynamic filopodium-like branchlet. The mechanisms underlying the initiation of dendrite branchlets are therefore crucial to the shaping of dendrites. Through *in vivo* time-lapse imaging of the subcellular localization of actin during the process of branching of *Drosophila* larva sensory neurons, combined with genetic analysis and electron tomography, we have identified the Actin-related protein (Arp) 2/3 complex as the major actin nucleator involved in the initiation of dendrite branchlet formation, under the control of the activator WAVE and of the small GTPase Rac1. Transient recruitment of an Arp2/3 component marks the site of branchlet initiation *in vivo*. These data position the activation of Arp2/3 as an early hub for the initiation of branchlet formation.

KEY WORDS: Neuron, Dendrite, Actin, Arp2/3, WAVE, Time-lapse imaging

INTRODUCTION

Neurons extend branched dendrites to establish appropriate connections within a circuit. Dendrite branching enhances the coverage of the receptive field of a neuron and modulates the initial processing of incoming stimuli. Complex dendrite patterns are achieved *in vivo* through a dynamic process of branch extension and retraction that initiates with the formation of a filopodium-like dendrite branchlet (Jontes et al., 2000; Kaethner and Stuermer, 1997; Sugimura et al., 2003; Wu et al., 1999). Branchlets are generally short processes of less than 30 µm in length, but their appearance and distinct dynamics vary among different types of

neuron (Nagel et al., 2012). Only a subset of these dynamic branchlets is stabilized and can elongate into bona fide branches that remain for extended periods of time with the potential of branching further, while most disappear within a range of minutes to hours (Dailey and Smith, 1996; Heiman and Shaham, 2010; Niell et al., 2004). The initial step that allows the initiation of a dendrite branchlet is thus key to elaborating dendrite morphologies.

Actin is expected to play a central role in the formation of dynamic dendrite branchlets. Super-resolution microscopy recently revealed details of the organization of the actin cytoskeleton in dendrites, including periodical actin rings (D'Este et al., 2015). Additionally, patches of actin were observed in dendrites in electron microscopy preparations of primary hippocampal neuron cultures, as well as in pyramidal cells of the adult mouse cortex imaged *in vivo* with stimulated emission depletion (STED) nanoscopy (Korobova and Svitkina, 2010; Willig et al., 2014). These actin patches contain the actin nucleator complex Actin-Related Protein 2/3 (Arp2/3) and give rise to dendrite spines (Korobova and Svitkina, 2010; Saarikangas et al., 2015). However, the dynamic structure of actin supporting the process of bona fide dendrite branch formation has not been clarified. In *Drosophila* sensory class III dendritic arborisation (cIII_{da}) neurons, the formation of dendrite branchlets is predicted by the accumulation of a marker for dynamic F-actin: GMA (Andersen et al., 2005). GMA is a genetically encoded GFP-tagged actin-binding domain of moesin (Edwards et al., 1997) and its accumulation suggests a rapid remodelling or nucleation of actin at the site of branch formation. Additionally, GMA and LifeAct, an alternative F-actin marker, localize in dynamic puncta in *Drosophila* sensory class IV_{da} (cIV_{da}) neurons, at sites of new branch formation (Nithianandam and Chien, 2018). The Arp2/3 complex is a strong candidate for reshaping actin at the site of branch formation, as it promotes dendrite branching in cultured hippocampal neurons (Dharmalingam et al., 2009; Zhang et al., 2017) and is a major target of the small GTPase Rac1, a conserved key regulator of dendrite morphology (Govek et al., 2005).


Combining *in vivo* time-lapse analysis of fluorescently tagged actin regulators in *da* neurons, genetic analysis and electron tomography, we demonstrate that the Arp2/3 complex is the major actin nucleator involved in the initiation of dendrite branchlet formation, under the control of the suppressor of cAMP receptor/WASP family verprolin homology protein (SCAR/WAVE). Our data reveal a fundamental mechanism for dendrite branch formation via actin remodelling.

RESULTS AND DISCUSSION

To address the specific regulatory events at the core of the process of initial dendrite branch formation, we concentrated on the *Drosophila* larval sensory *da* neurons (Gao et al., 1999; Jan and Jan, 2010; Singhania and Grueber, 2014). These fall into four morphologically and functionally distinct neuronal subclasses, which range from the

¹Deutsches Zentrum für Neurodegenerative Erkrankungen e.V./German Center for Neurodegenerative Diseases (DZNE), 53127 Bonn, Germany. ²MPI for Neurobiology, 82152 Munich-Martinsried, Germany. ³Institute of Molecular biotechnology (IMBA), 1030 Wien, Austria. ⁴Ernst Strüngmann Institute (ESI) for Neuroscience in Cooperation with Max Planck Society, 60528 Frankfurt, Germany. ⁵Frankfurt Institute for Advanced Studies, 60438 Frankfurt, Germany. ⁶Institut für Physiologie und Pathophysiologie, Abteilung Molekulare Zellphysiologie, Phillips-Universität Marburg, 35037 Marburg, Germany. *Present address: IST Austria, 3400 Klosterneuburg, Austria. †Present Address: School of Life Science, Sun Yat-Sen University, 510275 Guangzhou, PR China. ‡These authors contributed equally to this work. §Deceased

**Author for correspondence (gaia.tavosanis@dzne.de)

 G.T., 0000-0002-8679-5515

Received 7 September 2018; Accepted 8 March 2019

2. Transient localization of the Arp2/3 complex initiates neuronal dendrite branching in vivo

simple cIIda to the complex cIIIda and space-filling cIVda neurons (Grueber et al., 2002). We first investigated the dynamics of actin enrichment within differentiating cIVda neuron dendrites in live second instar larvae. Dynamic actin, highlighted by GMA (Edwards et al., 1997), was enriched within the distal dendrite branches, which exhibit a higher rate of *de novo* branchlet formation (Fig. 1A). It displayed a highly dynamic localization with GMA puncta, as well as longer stretches of GMA enrichment forming and disappearing within minutes (Fig. 1C,D; Movie 1). Although transient GMA enrichment did not per se predict a site of *de novo* branch formation, the appearance of a novel branchlet was preceded by a persistent punctum of GMA enrichment. Indeed, 90% of all analysed *de novo* branch formation events showed actin accumulation of more than 30% relative to the basal level ($n=85$) (Fig. 1B). These data indicate that polymerization of actin is highly dynamic during dendrite differentiation in cIVda neurons. Moreover, they suggest that actin polymerization is a required step but does not suffice for the formation of a novel branch.

The initial assembly of an actin filament requires actin nucleators that stabilize the first seed of G-actin molecules (Firat-Karalar and Welch, 2011; Rottner et al., 2017). Therefore, to reveal the molecular

machinery underlying branch formation, we performed a late cell-autonomous knockdown in cIIda, cIIIda and cIVda neurons of actin nucleators, including the formins Capu, dDAAM, Dia, Fhos, FMNL and Formin3, the WH2 domain protein Spire, and components of the Arp2/3 complex (Dietzl et al., 2007). This approach allowed bypassing the initial phase of neuronal polarity establishment and primary neurite elongation to observe specific effects during terminal dendritic branching. The knock down of subunits of the Arp2/3 complex, including Arp2, Arp3 or Arpc1, strongly reduced the number of dendrite branches in cIVda (Fig. S1A,D) and cIIIda neurons (Fig. S1B,E). Although the primary branches (Fig. S1D-F) were not modified, other branch orders were reduced in number in cIVda and cIIIda neurons (Fig. S1D,E).

We thus addressed the *in vivo* role of Arp2/3 in dendrite branchlet formation. Using mosaic analysis with a repressible cell marker (MARCM) (Lee and Luo, 1999), we generated single cIVda neuron clones carrying null mutations of the Arp2/3 subunit *Arpc1* (*Arpc1^{Q25sd}* or *Arpc1^{R337st}*) (Hudson and Cooley, 2002; Zallen et al., 2002). These two alleles led to a strong reduction in overall branch density in cIVda neurons, validating the RNAi phenotype (Fig. 2A-C,E). In addition, in *Arpc1^{Q25sd}* mutant clones, high order

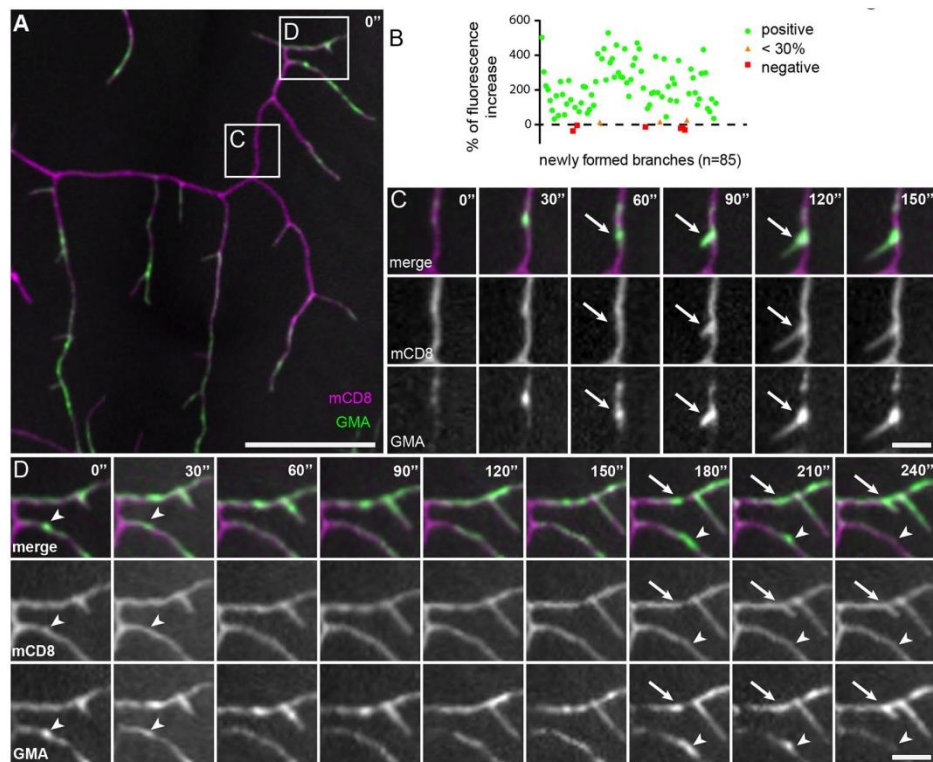


Fig. 1. Actin localization is highly dynamic in dendrite branches of differentiating cIVda neurons. (A) Localization of dynamic actin (GMA, green) within dendrite branches of differentiating cIVda neurons of second instar larvae. Dendrites dynamics are visualized using mCD8-cherry (magenta; genotype *Gal4^{109(2)80j} +; UAS-mCD8-Cherry/UAS-GMA*). The initial image of a time-lapse series is shown here (see Movie 1). Scale bar: 50 μ m. (B) Distribution of the percentage of increase in signal above background at the site of new branch formation for 85 recorded events. Green dots indicate events in which more than 30% increase in signal above background was recorded 30 s before branch initiation (89.4% of events). In three instances, the increase was lower than 30% (3.5% of events, orange triangles) and in six instances there was no increase (7% of events, red squares). (C,D) Magnification of the two boxed regions in A. 2.5 min (C) and 4 min (D) of this time-lapse series are shown, with arrows indicating the sites of new branch formation. Arrowheads in D indicate a site of actin accumulation that is not followed by the formation of a branch within the imaging time. Scale bar: 10 μ m. $n=10$ movies.

2. Transient localization of the Arp2/3 complex initiates neuronal dendrite branching in vivo

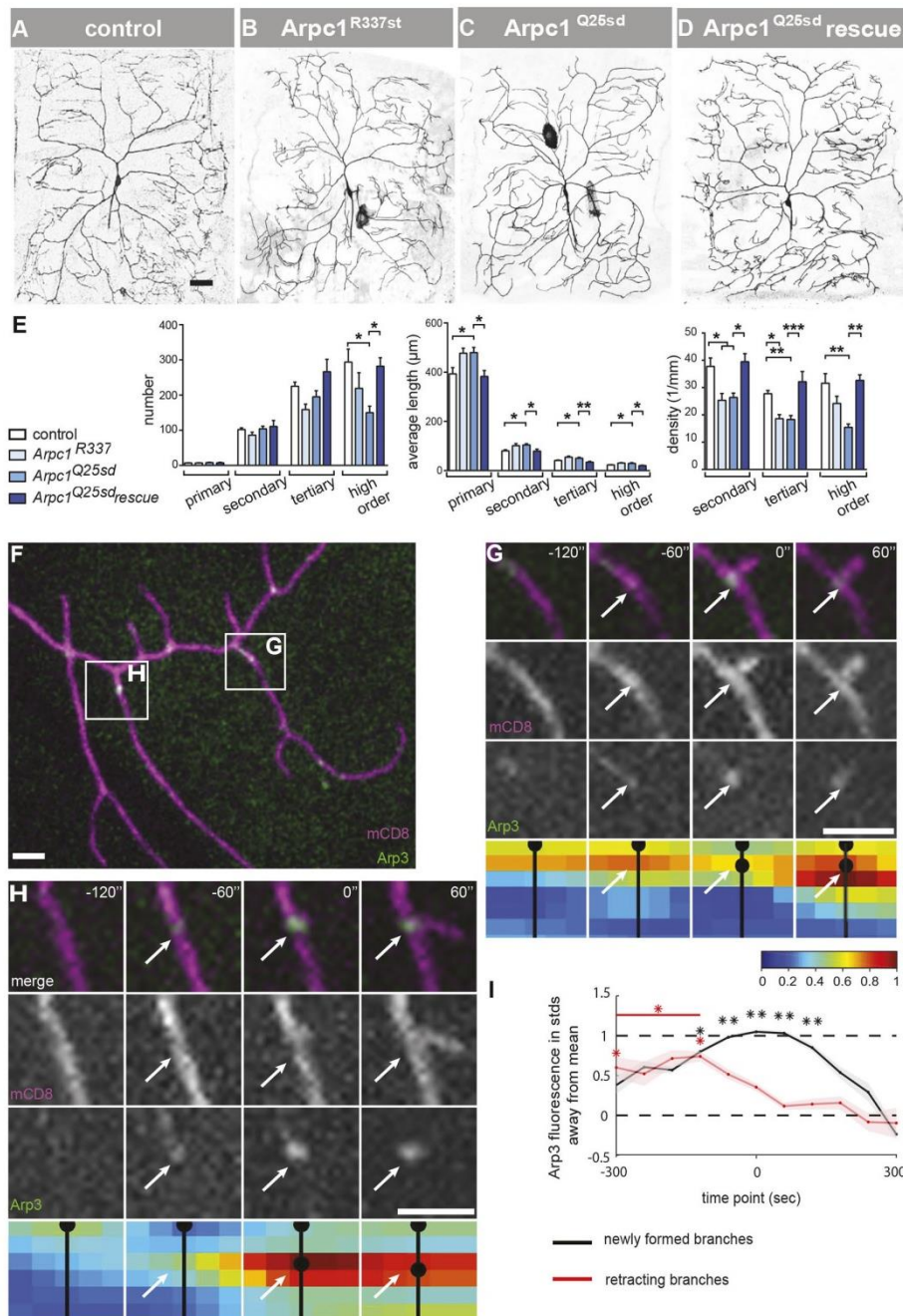


Fig. 2. See next page for legend.

branch number was reduced and average branch length increased (Fig. 2E). The *cIVda* neuron phenotype was rescued by expressing *Arpc1-GFP* in the mutant neurons (Hudson and Cooley, 2002), demonstrating that the dendrite branching phenotype derives from

the loss of *Arpc1* function and that *Arpc1* is required cell-autonomously (Fig. 2D,E).

To distinguish whether the reduction in the number of branches observed upon loss of *Arp2/3* function is due to a defect in branch

Fig. 2. The Arp2/3 complex supports cIVda dendrite branching and transiently localizes at branching points. (A–D) A single ddaC neuron clone obtained by MARCM of control neurons (A), of neurons mutant for *Arpc1* (*Arpc1^{R337st}* allele) (B) or for *Arpc1* (*Arpc1^{Q25sd}*) (C) alleles, or of neurons mutant for *Arpc1^{Q25sd}* but expressing GFP-tagged full-length *Arpc1* (D). Scale bar: 50 μ m. *n*=5. (E) Average number of dendrite branches, average length of dendrite branches and branch density in the analysed genotypes [$*P \leq 0.05$; $**P \leq 0.01$; $***P \leq 0.001$]. (F) Time-lapse imaging of differentiating class IV ddaC neurons of second instar larvae expressing Arp3-GFP (green) and mCD8cherry (magenta) imaged every 60 s. (G,H) Three-minute time lapse of the regions boxed in F. Arrows indicate the sites where new branchlets will form. The panel series below represents, using a heat map, the enrichment of Arp3-GFP observed in the time-lapse at the various time points (dots are branching sites; see supplementary Materials and Methods). Scale bars: 10 μ m. *n*=18. (I) Summary of Arp3-GFP fluorescence at appearing (black line) and disappearing (red line) branch points relative to the standard deviation of fluorescence on the remaining part of the branch (74 dendritic paths analysed). The straight lines indicate the mean fluorescence; shaded areas indicate the standard deviations around the mean.

formation or to an increased rate of branch retraction, we studied dendrite branching dynamics using time-lapse imaging of class IV ddaC neurons of second instar larvae expressing control or *Arp2* RNAi constructs. ddaC neurons in which *Arp2* was knocked down had a much lower rate of *de novo* dendrite branch formation (0.28 ± 0.26 in comparison with 2.37 ± 0.70 newly formed branchlets per 100 μ m, *n*=5), whereas the rates of extension and partial or complete retraction were not affected (Fig. S2A,B,D; Movie 2). Hence, Arp2/3 complex promotes branching in cIVda neurons primarily by initiating *de novo* formation of dendrite branches.

To investigate the localization of the Arp2/3 complex during dendrite differentiation, we expressed GFP-tagged Arp3 (Arp3-GFP) in cIVda neurons of second instar larvae, under the control of *Gal4^{ppk}*, a condition that does not alter the morphology of cIVda neurons (data not shown). Arp3-GFP was enriched at discrete puncta (Fig. 2F; Movie 3). Newly forming branches were almost invariably marked by the presence of Arp3-GFP at the branching point (Fig. 2I, black line). Furthermore, Arp3-GFP localization marked the site of subsequent branch formation 60 s in advance (Fig. 2G–I). Thus, Arp3 localization strongly correlated with the formation of a new branchlet and predicted the site of branchlet formation. The localization was transient and the signal decreased rapidly again after the initiation of branchlet elongation (Fig. 2I). Consistently, we observed a decrease of Arp3-GFP fluorescence when branchlets disappeared (Fig. 2I). Taken together, the phenotypic characterization of Arp2/3 complex loss of function, together with the Arp3-GFP localization observed in live-cell imaging, suggest that the local recruitment of the Arp2/3 complex is an early step towards dendrite branch formation.

The nucleating activity of the Arp2/3 complex is intrinsically low and requires activation via interaction with the VCA (verprolin-homology, central, acidic) domain of Wiskott-Aldrich syndrome protein (WASP) family of proteins (Campellone and Welch, 2010). Using RNAi we knocked down the WASP family proteins characterized in fly in da neurons and found that only a reduction of the SCAR/WAVE function resulted in a similar phenotype to the one observed upon loss of Arp2/3 function (Fig. S3). Cell type-specific knockdown of WAVE resulted in a reduction of branch number and density in cIIIda and cIVda neurons, and a reduction of branches in cIda (Fig. S3A–F). To validate the knockdown data, we generated single *wave^{Δ37}* mutant cell clones by MARCM (Zallen et al., 2002). The densities of secondary, tertiary and higher-order branches in *wave^{Δ37}* mutant class IV ddaC neurons were clearly reduced (Fig. 3B,C). Interestingly, a membrane-tagged WAVE construct lacking the VCA domain for Arp2/3 activation and acting

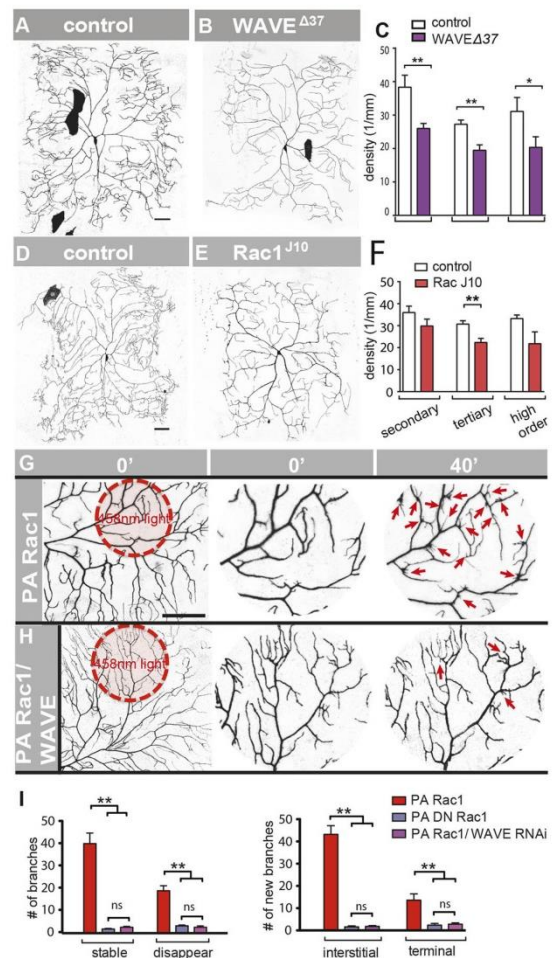


Fig. 3. WAVE and Rac1 control cIVda dendrite branch number. (A,B,D,E) Single ddaC cell clones obtained by MARCM of either control neurons (A,D) or neurons mutant for *wave* (*wave^{Δ37}*) (*n*=6) (B) or for *Rac1^{J10}* (*n*=4) (E). Scale bars: 50 μ m. (C) The density of branches is reduced in *wave^{Δ37}* clones. (F) The density of tertiary dendrite branches is reduced in *Rac1^{J10}* mutant clones. (G,H) Images from time-lapse recordings of ddaC neurons expressing membrane-tagged red fluorescent *mCherry* and (G) photoactivatable constitutively active Rac1 (*PA Rac1*; Movie 4) or (H) *PA Rac1* and *Wave* RNAi-inducing constructs (*PA Rac1/WAVE RNAi*; Movie 6) under the control of *ppk-Gal4*. The red circle represents the ROI illuminated with 458 nm light. Scale bar: 50 μ m (left). *n*=5. The central and right panels show a magnification of the highlighted ROI circle prior to and after 40 min of photoactivation, respectively. The arrows indicate some of the newly formed single branchlets or groups of branchlets. (I) Quantification of the number of newly formed branches in the 40 min of imaging. $*P \leq 0.05$; $**P \leq 0.01$; ns, not significant ($P > 0.05$).

as a dominant-negative (*WAVE^{ΔVCAmyr}*) (Stephan et al., 2011) reproduced the *wave* mutant phenotype that displayed a reduction in the number and density of secondary, tertiary and higher-order branches (Fig. S4C,D). RNAi-mediated *wave* knockdown in ddaC neurons produced a strong reduction of *de novo* branch formation. The remaining dendritic branches appeared to be more stable and

less dynamic than the control (Fig. S2C,D; Movie 2). Thus, WAVE, like Arp2/3, is primarily required for *de novo* formation of dendrite branchlets. The activation and membrane recruitment of WAVE is in turn under tight regulation by the conserved multiprotein WAVE regulatory complex (WRC) (Chen et al., 2010). Within the WRC, the Sra-1 and Nap-1 dimer is essential for both Rac1-mediated regulation of the WRC and its recruitment to the membrane (Chen et al., 2010). *Sra-1* knockdown by RNAi yielded a similar effect to the loss of Arp2/3 or loss of WAVE, namely a clear reduction in the density of secondary and high-order branches of c1Vda neurons (Fig. S4F,G). Together, these data suggest that WAVE is a major activator of Arp2/3 during dendrite branch formation in c1Vda neurons.

The small GTPase Rac1 is a central determinant of cytoskeleton organization through the regulation of multiple proteins, including the WRC (Steffen et al., 2004; Tahirovic et al., 2010). Furthermore, da neurons overexpressing Rac1 display an increased number of terminal dendrite branchlets (Andersen et al., 2005; Emoto et al., 2004; Lee et al., 2003; Nagel et al., 2012). We therefore asked whether Rac1 drives the activation of WAVE and Arp2/3, and promotes dendrite branchlet formation. Single c1Vda neuron MARCM clones mutant for Rac1 (*Rac1¹¹⁰*) (Hakeda-Suzuki et al., 2002) displayed a reduction in the number of tertiary branches (Fig. 3D-F), indicating that appropriate branching of c1Vda neurons requires Rac1 (Lee et al., 2003; Nagel et al., 2012; Soba et al., 2015). Next, we used a photoactivatable form of a constitutively active mutated Rac1 protein (PA-Rac1CA) (Wang et al., 2010; Wu et al., 2009). When applying localized photoactivation in a restricted region of interest (ROI) of c1Vda neurons, this construct was de-suppressed and produced strong and rapid formation of single branchlets and of groups of branchlets (Fig. 3G,I; Movie 4). Such an effect was not elicited in unilluminated ROIs upon overexpression of a dominant-negative PA-Rac1DN or of a light-insensitive LI PA-Rac1CA (Fig. S4H-J; Movie 5). A large fraction of the branchlets formed after illumination appeared along the length of existing dendrites, rather than at dendrite tips, and remained stable (Fig. 3J). Importantly, the dendrite overbranching locally induced by PA-Rac1CA was largely suppressed in the background of cell-autonomous *wave* RNAi (Fig. 3H,I; Movie 6). Thus, Rac1-induced branchlet formation requires WAVE in da neurons.

The Arp 2/3 complex binds to already existing actin filaments and is the only actin nucleator generating characteristic branched F-actin networks (Mullins et al., 1998). We thus attempted to locate the activity of the Arp2/3 complex in a structural context and carried out electron microscopy of dendrite branching points in primary neuronal cultures (Small et al., 2008). We obtained striking images of branching points of dendrites of larval brain neuron primary cultures (Fig. 4). In dendrite branches, we observed a few microtubules and long actin filaments extending parallel to the cortical membrane (Fig. 4B), similar to what has been reported for cultured rat hippocampal neurons (Xu et al., 2013). In contrast, the branchlets were filled by a tight bundle of actin filaments (Fig. 4F). However, we did not observe regions of branched actin filaments within the dendrite branchlets, as reported for the filopodia that give rise to dendrite spines (Korobova and Svitkina, 2010). At branching points, actin filaments appeared more dispersed and less bundled than along the main dendrites (Fig. 4B). Splayed microtubule filaments were present at branching points (Fig. 4B). In all analysed tomograms of branching points in dendrites ($n=5$ fully traced tomograms out of 12 sets), we observed several patches of short highly branched actin filaments (Fig. 4C-E,G). To follow the actin filaments in 3D and to unambiguously trace actin branching points, we performed EM tomography of dendrite branching points and reconstructed actin and microtubules (Fig. 4H; Movie 7). In the

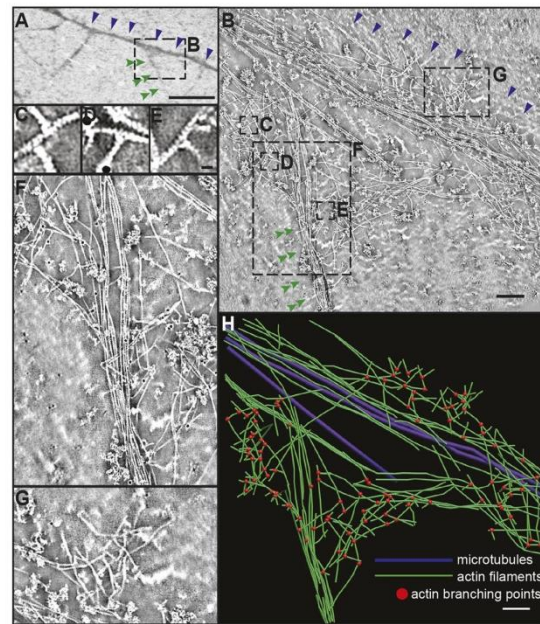


Fig. 4. Electron tomography reveals patches of branched actin at the base of dendrite branchlets. (A) Low-magnification image of a dendrite branch of a cultured larval brain neuron. Blue arrowheads indicate the dendrite branch. Green double arrowheads indicate a branchlet. Scale bar: 5 μm. (B) Electron tomogram image of the dendrite branching point boxed in A. Blue arrowheads indicate the dendrite branch shown in A. Green double arrowheads indicate the same branchlet as in A. Scale bar: 1 μm. The patches boxed in B are magnified in C-G. Scale bar in E: 100 nm. (F) Single filaments converge from the actin patches into the dendrite branchlet. (H) Still image from a 3D reconstruction of the tomogram shown in A. See also Movie 7. The red dots indicate the actin branching points. Scale bar: 1 μm.

tilted images we could define unequivocally sites of actin branching (Movie 7), a clear indication of Arp2/3 activity. Single filaments derived from a patch of branched actin converged into actin bundles forming the core of a branchlet (Fig. 4F). Thus, patches of branched F-actin were specifically present at the base of dendritic branching points, supporting a role for Arp2/3 in dendrite branching.

The data presented here delineate a model of the mechanism underlying dendritic branching. This involves the initial activation of Rac1, leading to recruitment and local activation of the WRC. The subsequent transient recruitment of the Arp2/3 complex promotes the nucleation of branched actin filaments close to the plasma membrane that can thus be pushed forward to form an initial process.

One major trait of neuronal morphology is the density of dendrite branches (Stuart et al., 2007), which is likely produced by a combination of frequency of *de novo* branch formation and incidence of stabilization of the produced branchlets (Ziv and Smith, 1996). Our data indicate that the distribution of sites of Arp2/3 complex activation plays a major role in the control of branch formation frequency. Rac1 activity promotes actin recruitment at sites of dendrite spine formation and of dendrite filopodium initiation (Cheadle and Biederer, 2012; Galic et al., 2014; Korobova and Svitkina, 2010). Furthermore, Rac1 is responsible for the localization of WAVE at the growth cone

plasma membrane of mouse cerebellar granule neurons (Tahirovic et al., 2010). We thus hypothesize that activated Rac1 might recruit WRC at various locations along the length of a dendrite, but once a crucial concentration of active WAVE is reached, Arp2/3 can locally remodel the actin cytoskeleton to promote the formation of an actin patch. This cascade closely resembles the initiation of axonal branch formation (Armijo-Weingart and Gallo, 2017). In addition, the localization of WRC can be supported by a large family of molecules containing a short WRC interacting receptor sequence (WIRS) (Chen et al., 2014). In fact, molecular complexes including WIRS-containing proteins were recently shown to contribute to the localization of axon or dendrite branching sites in *C. elegans* HSN and PVD neurons, respectively, in part by binding to the WRC (Chia et al., 2014; Zou et al., 2018). The transmembrane receptor Robo, which promotes branching in cIVda neurons, contains a WIRS domain and might represent a potential candidate for the localization of WRC in these neurons to support branch formation (Chen et al., 2014; Dimitrova et al., 2008). How the localization of WIRS-containing activators might in turn become spatially restricted to initiate branch formation at discrete locations along the dendrite is not clear.

Taken together, we have revealed the details of the initial step into the formation of a dendrite branchlet *in vivo* with high temporal and spatial resolution. We suggest that, given the potential pathways of activation of WRC, in different neurons a concentration of active Arp2/3 that is sufficient for initiating branchlet formation might be achieved by stochastic enrichment of the activators or by the tethered localization of activator complexes at specific sites.

MATERIALS AND METHODS

Fly lines and genetics

All flies were kept at 25°C unless otherwise noted. The fly strains used are listed in the supplementary Materials and Methods. MARCM was performed as described by Nagel et al. (2012) (see supplementary Materials and Methods). For all RNAi experiments, animals carried a da neuron class-specific driver (*Gal4^{ppk}*, *Gal4^{IG11}* or *Gal4^{C161}*), *UAS-mCD8GFP*, *UAS-Dcr2*, and a target or control RNAi. Embryos were allowed to develop at 25°C until examined as third instar larvae.

Microscopy

Live late third instar larvae expressing *UAS-mCD8GFP* in subsets of da neurons were mounted in 70% glycerol and immobilized with a cover slip for visualization with a Leica TCS SP2 confocal microscope. For time-lapse imaging, second instar live larvae expressing *UAS-mCD8GFP* in subsets of da neurons were immobilized in an imaging chamber (Dimitrova et al., 2008) filled with halocarbon oil to allow oxygen exchange, and confocal z-stacks (six images spaced by 1 µm) were obtained using a Carl Zeiss LSM7 confocal microscope every 5 min over a period of 30 min. Two-colour imaging of *Gal4^{109/230/+}; UAS-mCD8-Cherry/UAS-GMA* or *Gal4^{109/230/+}; UAS-mCD8-Cherry/UAS-Arp3-GFP* larvae was performed as previously described (Nagel et al., 2012) with several modifications. Briefly, for GMA, imaging stacks spaced by 1 µm were obtained every 30 s over a period of 10 min with a dual camera system; for Arp3 GFP, images were obtained every min over a period of 10–15 min with a single camera. In both cases, a Yokogawa Spinning-Disc on a Nikon stand (Andor) with two back-illuminated EM-CCD cameras (Andor iXON DU-897) was used. Two colour images of dual camera recordings were aligned automatically using Huygens essentials (Scientific Volume Imaging). Abdominal segment A6 was imaged for GMA and segments A1–2 for Arp3 GFP. Larvae expressing Arp3 GFP were kept at 29°C until imaging. To determine a point of new branch formation, newly forming branches were observed during the time-lapse images and their first appearance was set as the time-point 0 s. Accumulation of GMA was measured at the time point –30 s as the maximum intensity of a round region of interest (ROI) of 7 pixels diameter. A threshold for background GMA signal was set by averaging 20 randomly set ROIs along

dendrite branches for each video ($n=11$). The spatiotemporal analysis of the Arp3-GFP signal along individual branches is described in detail in the supplementary Materials and Methods.

Photoactivation

All flies expressing photoactivatable constructs were raised under standard conditions but in full darkness. They carried: *ppk-Gal4 UAS-mCherry* and *UAS-PA Rac1 CA*, *UAS-PA DN Rac1*, *UAS-LI Rac1* or *UAS-PA Rac1 CA* and *UAS Wave* RNAi. Living late third instar larvae were prepared for live confocal imaging under a dimmed red light. Photoactivation of PA-Rac1 and live-cell imaging were performed using a Carl Zeiss LSM5 confocal microscope. To photoactivate the Rac1 constructs (CA, LI or DN), the indicated region of interest (ROI) of the dendritic tree of a ddaC neuron in living L3 larvae was repeatedly illuminated using a 5 mW 445 nm laser at 0.2% power for 20 s in a photobleaching mode and the membrane marker mCherry was imaged in the red channel every minute (Kato et al., 2014; Wu et al., 2009).

Image analysis and statistics

Quantification of a dendritic tree complexity was performed by manual tracing of dendritic branches from maximum projections of original image stacks in ImageJ using the NeuronJ plug-in and FIJI. Dendrites were separated in specific clusters (Figs S1, S3) according to their morphology and distance from the cell soma. Density was measured as number of branches of a given order divided by total length of lower order branches. Bar graphs and tables express the data of dendritic length and number as mean±s.e.m. Unless otherwise noted, data were analysed for statistical significance using two-tailed unpaired Student *t*-test for comparing two groups or one-way ANOVA for more than two groups at $P<0.05$. If normal distribution of the dataset was confirmed using the Shapiro-Wilk normality test, the ANOVA Bonferroni's post test was used for multiple comparison, otherwise the Kruskal-Wallis test with a Dunn's post test was used. Asterisks in graphs and tables represent the significance of *P*-values comparing indicated groups with control (* $P<0.05$; ** $P<0.01$; *** $P<0.001$; **** $P<0.0001$). For time-lapse analysis, every time point was analysed separately. At least five animals per genotype were used for quantification.

Electron microscopy and cell-culture

Electron microscopy experiments were obtained with primary neuronal culture of larval mushroom body neurons. Dissociated neuronal cultures from *Drosophila* brain tissue were prepared as described previously (Kraft et al., 2006) and cultured on formvar-coated gold finder EM grids for 48 h at 25°C. The cells were examined and preselected on an inverted Zeiss Observer epifluorescence microscope and extracted at room temperature with cytoskeleton buffer [10 mM MES buffer, 150 mM NaCl, 5 mM EGTA, 5 mM glucose, 5 mM MgCl₂ (pH 6.8)] containing 0.25% glutaraldehyde and 0.5% Triton for 40 s. For electron tomography, neurons were fixed with 2% glutaraldehyde in the same buffer for 15 min and grids were stained with 6–8% sodium silicotungstate (SST), including 1 mg/ml phalloidin. Electron tomography was obtained using an FEI Tecnai F30 Helium (Polaris) microscope, and actin filaments were manually tracked using IMOD, as previously described (Mueller et al., 2014; Vinzenz et al., 2012).

Acknowledgements

We dedicate this manuscript to the family of our dear colleague Anastasia Tatarnikova, whom we prematurely lost during the course of this work. We are grateful to Dr Fikret-Gürkan Agircan for his great experimental support during revision. We thank J. Zallen for sharing fly lines and the Bloomington Stock Center for providing reagents. We are grateful to Rüdiger Klein (MPI of Neurobiology) for hosting A.T., to Michael Sixt (IST Austria) for his support, and to Frank Bradke and Peter Soba for helpful discussions and comments on the manuscript. Members of the Tavasani lab provided many helpful comments.

Competing interests

The authors declare no competing or financial interests.

Author contributions

Conceptualization: T.S., A.T., H.C., G.T.; Methodology: T.S., A.T., J.M., B.S., H.C., M.N., V.S.; Software: B.S., H.C.; Formal analysis: T.S., A.T., J.M., B.S., H.C., G.T.;

Investigation: T.S., A.T., J.M., B.S., Y.Z., M.N.; Resources: H.C., S.B., V.S.; Writing - original draft: G.T.; Writing - review & editing: T.S., G.T.; Supervision: G.T.; Project administration: G.T.; Funding acquisition: G.T.

Funding

This work was supported by a Deutsche Forschungsgemeinschaft grant to G.T. (SPP 1464 TA 265/4), and by a Bundesministerium für Bildung und Forschung grant (01GQ1406-Bernstein Award 2013) and a Deutsche Forschungsgemeinschaft grant (CU 217/2-1) to H.C.

Supplementary information

Supplementary information available online at <http://dev.biologists.org/lookup/doi/10.1242/dev.171397.supplemental>

References

- Andersen, R., Li, Y., Resseguie, M. and Brenman, J. E. (2005). Calcium/calmodulin-dependent protein kinase II alters structural plasticity and cytoskeletal dynamics in *Drosophila*. *J. Neurosci.* **25**, 8878-8888. doi:10.1523/JNEUROSCI.2005-05.2005
- Armijo-Weingart, L. and Gallo, G. (2017). It takes a village to raise a branch: cellular mechanisms of the initiation of axon collateral branches. *Mol. Cell Neurosci.* **84**, 36-47. doi:10.1016/j.mcn.2017.03.007
- Campellone, K. G. and Welch, M. D. (2010). A nucleator arms race: cellular control of actin assembly. *Nat. Rev. Mol. Cell Biol.* **11**, 237-251. doi:10.1038/nrm2867
- Cheadle, L. and Biederer, T. (2012). The novel synaptogenic protein Farp1 links postsynaptic cytoskeletal dynamics and transsynaptic organization. *J. Cell Biol.* **199**, 985-1001. doi:10.1083/jcb.201205041
- Chen, Z., Borek, D., Padrick, S. B., Gomez, T. S., Metlagel, Z., Ismail, A. M., Umetani, J., Billadeau, D. D., Otwinowski, Z. and Rosen, M. K. (2010). Structure and control of the actin regulatory WAVE complex. *Nature* **468**, 533-538. doi:10.1038/nature09623
- Chen, B., Brinkmann, K., Chen, Z., Pak, C. W., Liao, Y., Shi, S., Henry, L., Grishin, N. V., Bogdan, S. and Rosen, M. K. (2014). The WAVE regulatory complex links diverse receptors to the actin cytoskeleton. *J. Cell Biol.* doi:10.1016/j.jcb.2013.11.048
- Chia, P. H., Chen, B., Li, P., Rosen, M. K. and Shen, K. (2014). Local F-actin network links synapse formation and axon branching. *Cell* **156**, 208-220. doi:10.1016/j.cell.2013.12.009
- Dailey, M. E. and Smith, S. J. (1996). The dynamics of dendritic structure in developing hippocampal slices. *J. Neurosci.* **16**, 2983-2994. doi:10.1523/JNEUROSCI.16-09-02983.1996
- Dharmalingam, E., Haecel, A., Pinyol, R., Schwintzer, L., Koch, D., Kessels, M. M. and Qualmann, B. (2009). F-BAR proteins of the syndapin family shape the plasma membrane and are crucial for neuromorphogenesis. *J. Neurosci.* **29**, 13315-13327. doi:10.1523/JNEUROSCI.3973-09.2009
- D'Este, E., Kamin, D., Göttfert, F., El-Hady, A. and Hell, S. W. (2015). STED nanoscopy reveals the ubiquity of subcortical cytoskeleton periodicity in living neurons. *Cel Rep.* **10**, 1246-1251. doi:10.1016/j.celrep.2015.02.007
- Dietzl, C., Chen, D., Schnorfer, F., Su, K.-C., Barinova, Y., Fellner, M., Gasser, B., Kinsey, K., Oettel, S., Scheibla, S. et al. (2007). A genome-wide transgenic RNAi library for conditional gene inactivation in *Drosophila*. *Nature* **448**, 151-156. doi:10.1038/nature05954
- Dimitrova, S., Reissaus, A. and Tavanian, G. (2008). Slit and Robo regulate dendrite branching and elongation of space-filling neurons in *Drosophila*. *Dev. Biol.* **324**, 18-30. doi:10.1016/j.ydbio.2008.08.028
- Edwards, K. A., Demsky, M., Montague, R. A., Weymouth, N. and Kiehart, D. P. (1997). GFP-moesin illuminates actin cytoskeleton dynamics in living tissue and demonstrates cell shape changes during morphogenesis in *Drosophila*. *Dev. Biol.* **191**, 103-117. doi:10.1006/dbio.1997.8707
- Emoto, K., He, Y., Ye, B., Grueber, W. B., Adler, P. N., Jan, L. Y. and Jan, Y.-N. (2004). Control of dendritic branching and tiling by the Tricornered-kinase/Fury signaling pathway in *Drosophila* sensory neurons. *Cell* **119**, 245-256. doi:10.1016/j.cell.2004.09.036
- Firat-Karalar, E. N. and Welch, M. D. (2011). New mechanisms and functions of actin nucleation. *Curr. Opin. Cell Biol.* **23**, 4-13. doi:10.1016/j.cob.2010.10.007
- Galic, M., Tsai, F.-C., Collins, S. R., Mats, M., Bandara, S. and Meyer, T. (2014). Dynamic recruitment of the curvature-sensitive protein ArhGAP44 to nanoscale membrane deformations limits exploratory filopodia initiation in neurons. *Elife* **3**, e03116. doi:10.7554/eLife.03116
- Gao, F.-B., Brenman, J. E., Jan, L. Y. and Jan, Y. N. (1999). Genes regulating dendritic outgrowth, branching, and routing in *Drosophila*. *Genes Dev.* **13**, 2549-2561. doi:10.1101/gad.13.19.2549
- Govek, E.-E., Newey, S. E. and Van Aelst, L. (2005). The role of the Rho GTPases in neuronal development. *Genes Dev.* **19**, 1-49. doi:10.1101/gad.1256405
- Grueber, W. B., Jan, L. Y. and Jan, Y. N. (2002). Tiling of the *Drosophila* epidemium by multidendritic sensory neurons. *Development* **129**, 2867-2878.
- Hakeda-Suzuki, S., Ng, J., Tzu, J., Dietzl, C., Sun, Y., Harms, M., Nardine, T., Luo, L. and Dickson, B. J. (2002). Rac function and regulation during *Drosophila* development. *Nature* **416**, 438-442. doi:10.1038/416438a
- Halachmi, N., Nachman, A. and Salzberg, A. (2012). Visualization of proprioceptors in *Drosophila* larvae and pupae. *J. Vis. Exp.* **64**, e3846. doi:10.3791/3846
- Heiman, M. G. and Shaham, S. (2010). Twigs into branches: how a filopodium becomes a dendrite. *Curr. Opin. Neurobiol.* **20**, 86-91. doi:10.1016/j.conb.2009.10.016
- Hudson, A. M. and Cooley, L. (2002). A subset of dynamic actin rearrangements in *Drosophila* requires the Arp2/3 complex. *J. Cell Biol.* **156**, 677-687. doi:10.1083/jcb.200109065
- Jan, Y.-N. and Jan, L. Y. (2010). Branching out: mechanisms of dendritic arborization. *Nat. Rev. Neurosci.* **11**, 316-328. doi:10.1038/nrn2836
- Jontes, J. D., Buchanan, J. and Smith, S. J. (2000). Growth cone and dendrite dynamics in zebrafish embryos: early events in synaptogenesis imaged in vivo. *Nat. Neurosci.* **3**, 231-237. doi:10.1038/72936
- Kaethner, R. J. and Stuermer, C. A. (1997). Dynamics of process formation during differentiation of tectal neurons in embryonic zebrafish. *J. Neurobiol.* **32**, 627-639. doi:10.1002/(SICI)1097-4695(19970605)32:6<627::AID-NEU7>3.0.CO;2-1
- Kato, T., Kawai, K., Egami, Y., Kakehi, Y. and Araki, N. (2014). Rac1-dependent lamellipodial motility in prostate cancer PC-3 cells revealed by optogenetic control of Rac1 activity. *PLoS ONE* **9**, e97749. doi:10.1371/journal.pone.0097749
- Korobova, F. and Svitkina, T. (2010). Molecular architecture of synaptic actin cytoskeleton in hippocampal neurons reveals a mechanism of dendritic spine morphogenesis. *Mol. Biol. Cell* **21**, 165-176. doi:10.1091/mbc.e09-07-0596
- Kraft, R., Escobar, M. M., Narro, M. L., Kurtis, J. L., Efrat, A., Barnard, K. and Restifo, L. L. (2006). Phenotypes of *Drosophila* brain neurons in primary culture reveal a role for fascin in neurite shape and trajectory. *J. Neurosci.* **26**, 8734-8747. doi:10.1523/JNEUROSCI.2106-06.2006
- Lee, T. and Luo, L. (1999). Mosaic analysis with a repressible cell marker for studies of gene function in neuronal morphogenesis. *Neuron* **22**, 451-461. doi:10.1016/S0896-6273(00)80701-1
- Lee, A., Li, W., Xu, K., Bogert, B. A., Su, K. and Gao, F. B. (2003). Control of dendritic development by the *Drosophila* fragile X-related gene involves the small GTPase Rac1. *Development* **130**, 5543-5552. doi:10.1242/dev.00792
- Mueller, J., Pfanzelt, J., Winkler, C., Narita, A., Le Clairche, C., Nemethova, M., Carlier, M.-F., Maeda, Y., Welch, M. D., Ohkawa, T. et al. (2014). Electron tomography and simulation of baculovirus actin comet tails support a tethered filament model of pathogen propulsion. *PLoS Biol.* **12**, e1001765. doi:10.1371/journal.pbio.1001765
- Mullins, R. D., Heuser, J. A. and Pollard, T. D. (1998). The interaction of Arp2/3 complex with actin: nucleation, high affinity pointed end capping, and formation of branching networks of filaments. *Proc. Natl. Acad. Sci. USA* **95**, 6181-6186. doi:10.1073/pnas.95.11.6181
- Nagel, J., Delandre, C., Zhang, Y., Forstner, F., Moore, A. W. and Tavanian, G. (2012). Fascin controls neuronal class-specific dendrite arbor morphology. *Development* **139**, 2999-3009. doi:10.1242/dev.077800
- Niell, C. M., Meyer, M. P. and Smith, S. J. (2004). In vivo imaging of synapse formation on a growing dendritic arbor. *Nat. Neurosci.* **7**, 254-260. doi:10.1038/nn1191
- Nithianandam, V. and Chien, C.-T. (2018). Actin blobs prefigure dendrite branching sites. *J. Cell Biol.* **217**, 3731-3746. doi:10.1083/jcb.201711136
- Rottner, K., Faix, J., Bogdan, S., Linder, S. and Kerkhoff, E. (2017). Actin assembly mechanisms at a glance. *J. Cell Sci.* **130**, 3427-3435. doi:10.1242/jcs.206433
- Saarikangas, J., Kourdogli, N., Senju, Y., Chazal, G., Segerstrale, M., Minkeviciene, R., Kuurne, J., Matilla, P. K., Garrett, L., Höfner, S. M. et al. (2015). MIM-induced membrane bending promotes dendritic spine initiation. *Dev. Cell* **33**, 644-659. doi:10.1016/j.devcel.2015.04.014
- Singhania, A. and Grueber, W. B. (2014). Development of the embryonic and larval peripheral nervous system of *Drosophila*. *Wiley Interdiscip. Rev. Dev. Biol.* **3**, 193-210. doi:10.1002/wdev.135
- Small, J. V., Aulinger, S., Nemethova, M., Koestler, S., Goldie, K. N., Hoenger, A. and Resch, G. P. (2008). Unravelling the structure of the lamellipodium. *J. Microsc.* **231**, 479-485. doi:10.1111/j.1365-2818.2008.02060.x
- Soba, P., Han, C., Zheng, Y., Perea, D., Miguel-Aliaga, I., Jan, L. Y. and Jan, Y. N. (2015). The Ret receptor regulates sensory neuron dendrite growth and integrin mediated adhesion. *Elife* **4**, e05491. doi:10.7554/eLife.05491
- Steffen, A., Rottner, K., Ehinger, J., Innocenti, M., Scita, G., Wehland, J. and Stradal, T. E. B. (2004). Sra-1 and Nap1 link Rac to actin assembly driving lamellipodia formation. *EMBO J.* **23**, 749-759. doi:10.1038/sj.emboj.7600084
- Stephan, R., Gohl, C., Fleige, A., Klämbt, C. and Bogdan, S. (2011). Membrane-targeted WAVE mediates photoreceptor axon targeting in the absence of the WAVE complex in *Drosophila*. *Mol. Biol. Cell* **22**, 4079-4092. doi:10.1091/mbc.e11-02-0121
- Stuart, G., Spruston, N. and Häusser, M. (2007). *Dendrites*, 2nd edn. Oxford: New York: Oxford University Press.
- Sugimura, K., Yamamoto, M., Niwa, R., Satoh, D., Goto, S., Taniguchi, M., Hayashi, S. and Uemura, T. (2003). Distinct developmental modes and lesion-

2. Transient localization of the Arp2/3 complex initiates neuronal dendrite branching in vivo

RESEARCH REPORT

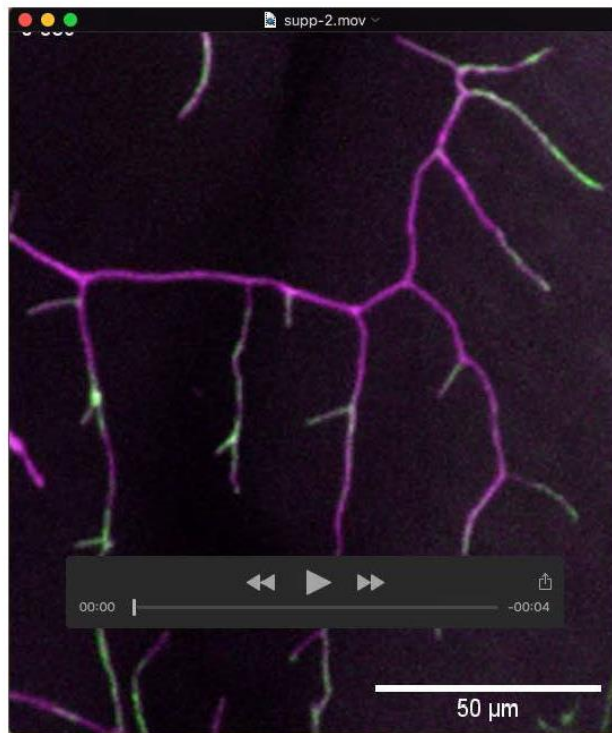
Development (2019) 146, dev171397. doi:10.1242/dev.171397

- induced reactions of dendrites of two classes of *Drosophila* sensory neurons. *J. Neurosci.* **23**, 3752-3760. doi:10.1523/JNEUROSCI.23-09-03752.2003
- Tahirovic, S., Hellal, F., Neukirchen, D., Hindges, R., Garvalov, B. K., Flynn, K. C., Stradal, T. E., Chrostek-Grashoff, A., Brakebusch, C. and Bradke, F. (2010). Rac1 regulates neuronal polarization through the WAVE complex. *J. Neurosci.* **30**, 6930-6943. doi:10.1523/JNEUROSCI.5395-09.2010
- Vinzenz, M., Nemethova, M., Schur, F., Mueller, J., Narita, A., Urban, E., Winkler, C., Schmeiser, C., Koestler, S. A., Rottner, K. et al. (2012). Actin branching in the initiation and maintenance of lamellipodia. *J. Cell Sci.* **125**, 2775-2785. doi:10.1242/jcs.107623
- Wang, X., He, L., Wu, Y. I., Hahn, K. M. and Montell, D. J. (2010). Light-mediated activation reveals a key role for Rac in collective guidance of cell movement in vivo. *Nat. Cell Biol.* **12**, 591-597. doi:10.1038/ncb2061
- Willig, K. I., Steffens, H., Gregor, C., Herholt, A., Rossner, M. J. and Hell, S. W. (2014). Nanoscopy of filamentous actin in cortical dendrites of a living mouse. *Biophys. J.* **106**, L01-L03. doi:10.1016/j.bpj.2013.11.1119
- Wu, G. Y., Zou, D. J., Rajan, I. and Cline, H. (1999). Dendritic dynamics in vivo change during neuronal maturation. *J. Neurosci.* **19**, 4472-4483. doi:10.1523/JNEUROSCI.19-11-04472.1999
- Wu, Y. I., Frey, D., Lungu, O. I., Jaehrig, A., Schlichting, I., Kuhlman, B. and Hahn, K. M. (2009). A genetically encoded photoactivatable Rac controls the motility of living cells. *Nature* **461**, 104-108. doi:10.1038/nature08241
- Xu, K., Zhong, G. and Zhuang, X. (2013). Actin, spectrin, and associated proteins form a periodic cytoskeletal structure in axons. *Science* **339**, 452-456. doi:10.1126/science.1232251
- Zallen, J. A., Cohen, Y., Hudson, A. M., Cooley, L., Wieschaus, E. and Schejter, E. D. (2002). SCAR is a primary regulator of Arp2/3-dependent morphological events in *Drosophila*. *J. Cell Biol.* **156**, 689-701. doi:10.1083/jcb.200109057
- Zhang, S.-X., Duan, L.-H., He, S.-J., Zhuang, G.-F. and Yu, X. (2017). Phosphatidylinositol 3,4-bisphosphate regulates neurite initiation and dendrite morphogenesis via actin aggregation. *Cell Res.* **27**, 253-273. doi:10.1038/cr.2017.13
- Ziv, N. E. and Smith, S. J. (1996). Evidence for a role of dendritic filopodia in synaptogenesis and spine formation. *Neuron* **17**, 91-102. doi:10.1016/S0896-6273(00)80283-4
- Zou, W., Dong, X., Broederdorf, T. R., Shen, A., Kramer, D. A., Shi, R., Liang, X., Miller, D. M., III, Xiang, Y. K., Yasuda, R. et al. (2018). A Dendritic guidance receptor complex brings together distinct actin regulators to drive efficient F-actin assembly and branching. *Dev. Cell* **45**, 362-375.e363. doi:10.1016/j.devcel.2018.04.008

2. Transient localization of the Arp2/3 complex initiates neuronal dendrite branching in vivo

Development: doi:10.1242/dev.171397: Supplementary information

Supplemental Information

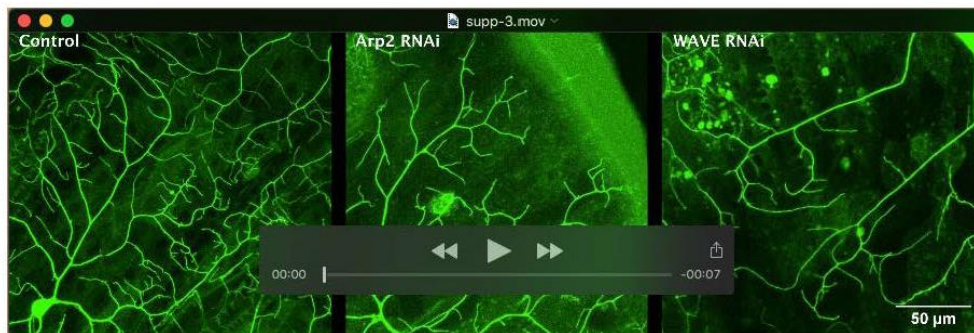


Movie 1. GMA dynamic localization in class IV neuron dendrites. (Related to Fig. 1)

Localization of dynamic actin within dendrite branches of differentiating class IV neurons of 2nd instar larvae, visualized with GMA (green). Dendrite dynamics are visualized with membrane-tagged red fluorescent cherry (magenta; *UAS-mCD8cherry*) [genotype *Gal4¹⁰⁹⁽²⁾⁸⁰/+; UAS-mCD8-Cherry/ UAS-GMA*]. Images for this time-lapse series were obtained by spinning disc confocal microscopy every 30 seconds over a period of 10 minutes. Arrows point to sites of *de novo* branch formation. Arrowheads indicate sites of GMA accumulation that do not result in *de novo* branch formation in the recording. Scale bar = 50 μ m.

2. Transient localization of the Arp2/3 complex initiates neuronal dendrite branching in vivo

Development: doi:10.1242/dev.171397: Supplementary information



Movie 2. Reduction of Arp2 or W ave function suppresses *de novo* branch formation.

(Related to Fig. 2, to Fig. 3 and to Fig. S2)

Time-lapse imaging of class IV ddaC neurons of 2nd instar larvae expressing control, *Arp2* or *wave* RNAi constructs and *UASmCD8GFP* to highlight dendrite morphology. Images were obtained every 5 minutes over a 30 minutes recording time. Arrows point to representative events of *de novo* terminal branch formation. *De novo* branch formation events are clearly reduced upon *Arp2* or *wave* RNAi. In addition the remaining branches are less dynamic. Scale bar = 50 μ m.

2. Transient localization of the Arp2/3 complex initiates neuronal dendrite branching in vivo

Development: doi:10.1242/dev.171397: Supplementary information

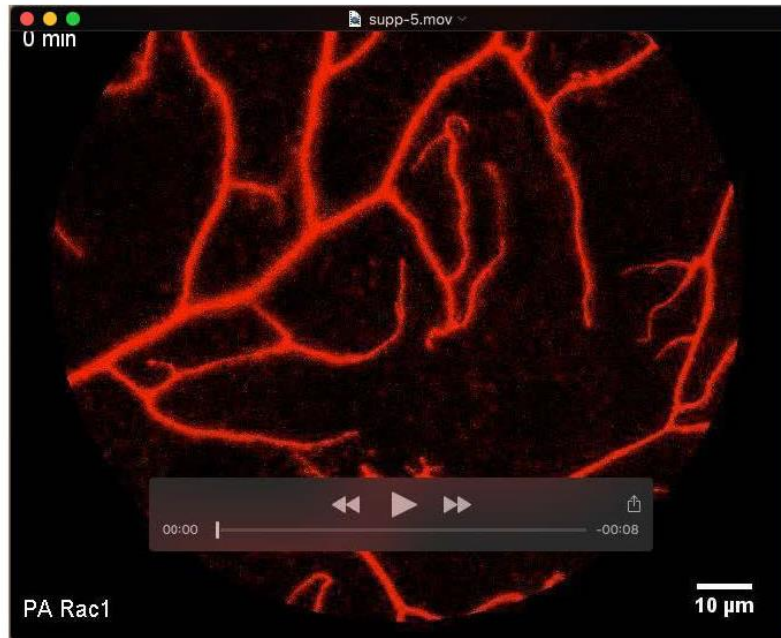


Movie 3. Dynamic Arp3GFP localization predicts *de novo* branchlet formation. (Related to Fig. 2)

Localization of GFP-tagged Arp3 under the control of *Gal4^{DNV}* within dendrite branches of differentiating c1Vda neurons of 2nd instar larvae (green). Dendrite dynamics were visualized with membrane-tagged red fluorescent cherry (magenta; *UAS-mCDB-cherry*) [genotype *Gal4^{103/2380}/+*; *UAS-mCDB-Cherry/UAS-Arp3-GFP*]. Images for this time-lapse series were obtained by spinning disc confocal microscopy every minute over a period of 10 minutes. Arrows point to sites of Arp-3-GFP accumulation, which precedes *de novo* branch formation. Scale bar = 10 μm.

2. Transient localization of the Arp2/3 complex initiates neuronal dendrite branching in vivo

Development. doi:10.1242/dev.171397. Supplementary information

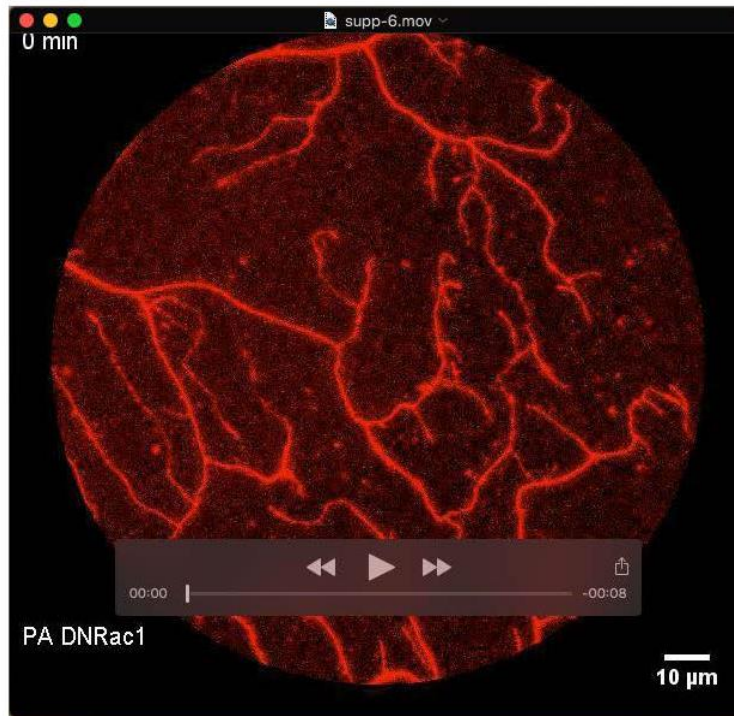


Movie 4. Local activation of PA -Rac1CA promotes branchlet formation. (Related to Fig. 3)

Time-lapse recording of a ROI of a *ddaC* class IV neuron of a third instar larva expressing the photoactivatable constitutive active Rac1 construct PA-Rac1CA [genotype *ppk-Gal4/ UAS-mCherry PA Rac1*]. Localized photoactivation within the shown region of interest was obtained with a 5 mW 458 nm laser. *UAS-mCherry* was imaged every minute over a 40 minutes period. After photoactivation single branchlets and groups of branchlets abundantly emerged from the existing dendrite branches (arrows). Scale bar = 10 μm .

2. Transient localization of the Arp2/3 complex initiates neuronal dendrite branching in vivo

Development: doi:10.1242/dev.171397: Supplementary information

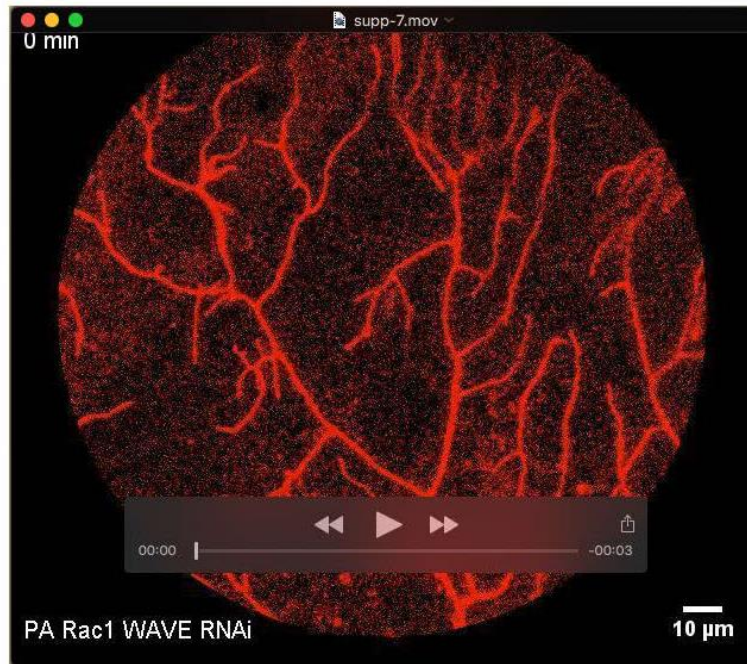


Movie 5. Local activation of PA -Rac1DN does not promote branchlet formation. (Related to Fig. 3)

Time-lapse recording of a ROI of a *ddaC* class IV neuron of a third instar larva expressing the photoactivatable dominant-negative Rac1 construct PA-Rac1DN [genotype *ppk-Gal4/UAS-mCherry PA Rac1DN*]. Localized photoactivation within the region of interest was obtained with a 5 mW 458 nm laser. *UAS-mCherry* was imaged every minute over a 40 minutes period. Minimal formation of filopodia was observed after photoactivation. Scale bar = 10 μm .

2. Transient localization of the Arp2/3 complex initiates neuronal dendrite branching in vivo

Development: doi:10.1242/dev.171397: Supplementary information



Movie 6. *wave* RNAi suppresses filopodium formation after local activation of PA-Rac1CA.

(Related to Fig. 3)

Time-lapse recording of a ROI of a *ddaC* class IV neuron of a third instar larva expressing the photoactivatable constitutive active Rac1 construct PA-Rac1CA in the background of cell-autonomous *wave* RNAi [genotype *wave* RNAi / *UAS-mCherry PA Rac1CA*; *ppk-Gal4*]. Localized photoactivation within the region of interest was obtained with a 5 mW 458 nm laser. *UAS-mCherry* was imaged every minute over a 40 minutes period. The abundant formation of filopodia by PA Rac1 CA is largely suppressed upon *wave* RNAi. Scale bar = 10 μm.

2. Transient localization of the Arp2/3 complex initiates neuronal dendrite branching in vivo

Development: doi:10.1242/dev.171397: Supplementary information



Movie 7. Patches of branched actin are present at the base of banchlets. (Related to Fig. 4)

Movie obtained from the 3D reconstruction of EM tomograms of the sample shown in Fig. 6. Points of branched actin filaments are highlighted with red circles. In the schematic, microtubules are highlighted in violet and actin filaments in green. Each identified point of branched actin is shown with a red dot. Patches of branched actin are clearly localized at the branching point.

2. Transient localization of the Arp2/3 complex initiates neuronal dendrite branching in vivo

Development: doi:10.1242/dev.171397: Supplementary information

Supplemental Experimental procedures

Fly lines

The following fly strains were obtained from Bloomington: *Arpc1*^{R337} *FRT40A/Cyo* [including a *nub*¹ allele, reported in Bloomington], *Arpc1*^{Q25sd} *FRT40A/Cyo*, *UAS Arpc1 GFP*, *UAS Arp3 GFP*, *UAS GMA*, *UAS mCherry PA Rac1 Q61L*; *MRKS/TM6B Tb*, *UAS mCherry C450M PA Rac1 Q61L*; *MRKS/TM6B Tb*, *UAS mCherry PA Rac1 T17N*; *MRKS/TM6B Tb*, *Gal4*¹⁰⁹⁽²⁸⁰⁾, *Gal4*^{bbk}, *Gal4*⁴⁷⁷, *Gal4*^{iG11}, *Gal4*^{C161}. The following lines were obtained from the Vienna Drosophila RNAi center: *v60100*^{control}, *v101999*^{Arp2}, *v29943*^{Arp2}, *v29944*^{Arp2}, *v108951*^{Arp3}, *v35258*^{Arp3}, *v352560*^{Arp3}, *v108951*^{Arp3}, *v100573*^{Arpc1}, *v42172*^{Arpc1}, *v101400*^{Capu}, *v34278*^{Capu}, *v24885*^{DAAM}, *v103921*^{DAAM}, *v103914*^{Dia}, *v20518*^{Dia}, *v45837*^{Fhos}, *v45838*^{Fhos}, *v34412*^{FMNL1}, *v34413*^{FMNL1}, *v28437*^{Formin3}, *v109380*^{Spire}, *v21908*^{wave}, *v108220*^{wasp}, *v39769*^{wash}. The following lines were previously generated in the Bogdan lab (Stephan et al., 2011): *Arp3*^{schwächling} */TM6 Tb*, *Wave*^{Δ37} *FRT40A/Cyo*, *UAS Sra1 RNAi*, *UAS Wave GFP/TM6B Tb*, *UAS Wave Cherry/TM6B Tb*. The line *Rac1*^{J10} *FRT80B/ TM6B Tb* was kindly provided by S. Hakeda-Suzuki (Hakeda-Suzuki et al., 2002).

Generation of MARCM clones

MARCM was performed as in (Nagel et al., 2012). Briefly, to produce clones, females of *Gal4*^{elavC155}, *UAS-mCD8-GFP*, *hs-FLP*, *w*; *tub-Gal80 FRT 40A /Cyo* or *Gal4*^{elavC155}, *UAS-mCD8-GFP*, *hs-FLP*, *w*; ; *tub-Gal80*, *FRT 80B /TM3* were mated with *yw*; *FRT40A/Cyo*, *yw*; *Arpc1*^{R337} *FRT40A/Cyo*, *yw*; *Arpc1*^{Q25sd} *FRT40A /Cyo*, *w*; *FRT40A WAVE*^{Δ37} */Cyo*, *yw*; *FRT80B/TM6 B* or *Rac1*^{J10} *FRT80B/ TM6B Tb*, respectively. The embryos were collected for 2 hours, incubated for 3 hours at 25°C, heat-shocked at 38 °C for 45min twice and raised at 25°C until examined as third instar larvae.

Spatiotemporal analysis of the Arp3-GFP signal along individual branches

2. Transient localization of the Arp2/3 complex initiates neuronal dendrite branching in vivo

Development: doi:10.1242/dev.171397: Supplementary information

In each time-lapse image stack all dendritic subtrees with appearing or disappearing branch points were reconstructed for each time step. The reconstructions were done semi-automatically in the TREES toolbox (Cuntz et al., 2010) starting at the origin of the subtree where the apparent change in topology took place. The reconstructed branched structures were in turn used to retrieve the GFP signal from the original image stacks. In order to not miss any GFP signal due to slight movement artifacts, the GFP images were treated in the following way: The maximum intensity projection over the z-dimension (10 frames with a z spacing of 5-10 μm) was used and the signal was convolved with a difference of Gaussian filter with space constants of 3 and 30 bins respectively corresponding to ca 0.4 and 4.0 μm . In this way the close vicinity was strengthened but the background was subtracted. The signal was then mapped on the tree structures reconstructed from the Cherry signal. Branch and termination points were cross-referenced between time-lapse reconstructions from the same branch at different time points. The referenced branch and termination points were used to identify appearing and disappearing branch points. Using custom made code in Matlab in combination with the TREES toolbox, the GFP signals were then separately computed for all individual paths along which such topological changes occurred. Along those paths the signals were interpolated in 6 seconds time steps and 1.33 μm steps in space. The signals at the appearing and disappearing branch points were then extracted from the paths along the time dimension and used for Figure 3D in the overall statistic.

2. Transient localization of the Arp2/3 complex initiates neuronal dendrite branching in vivo

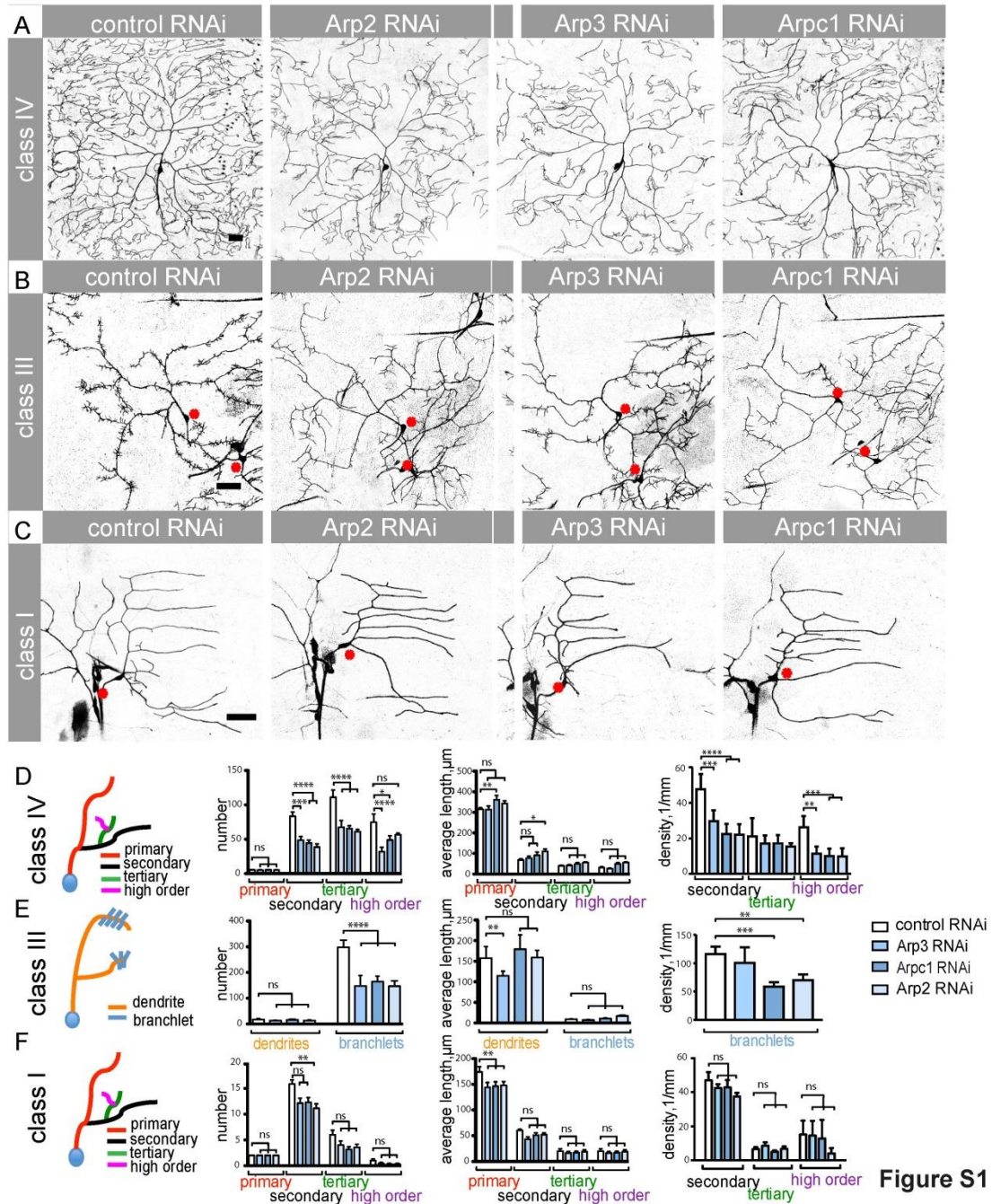
Development: doi:10.1242/dev.171397: Supplementary information

References

- Armijo-Weingart, L., and Gallo, G. (2017). It takes a village to raise a branch: Cellular mechanisms of the initiation of axon collateral branches. *Mol Cell Neurosci*.
- Cuntz, H., Forstner, F., Borst, A., and Hausser, M. (2010). One rule to grow them all: a general theory of neuronal branching and its practical application. *PLoS Comput Biol* 6.
- Hakeda-Suzuki, S., Ng, J., Tzu, J., Dietzl, G., Sun, Y., Harms, M., Nardine, T., Luo, L., and Dickson, B.J. (2002). Rac function and regulation during *Drosophila* development. *Nature* 416, 438-442.
- Nagel, J., Delandre, C., Zhang, Y., Forstner, F., Moore, A.W., and Tavosanis, G. (2012). Fascin controls neuronal class-specific dendrite arbor morphology. *Development* 139, 2999-3009.
- Stephan, R., Gohl, C., Fleige, A., Klambt, C., and Bogdan, S. (2011). Membrane-targeted WAVE mediates photoreceptor axon targeting in the absence of the WAVE complex in *Drosophila*. *Mol Biol Cell* 22, 4079-4092.

2. Transient localization of the Arp2/3 complex initiates neuronal dendrite branching in vivo

Development: doi:10.1242/dev.171397: Supplementary information



Development • Supplementary information

2. Transient localization of the Arp2/3 complex initiates neuronal dendrite branching in vivo

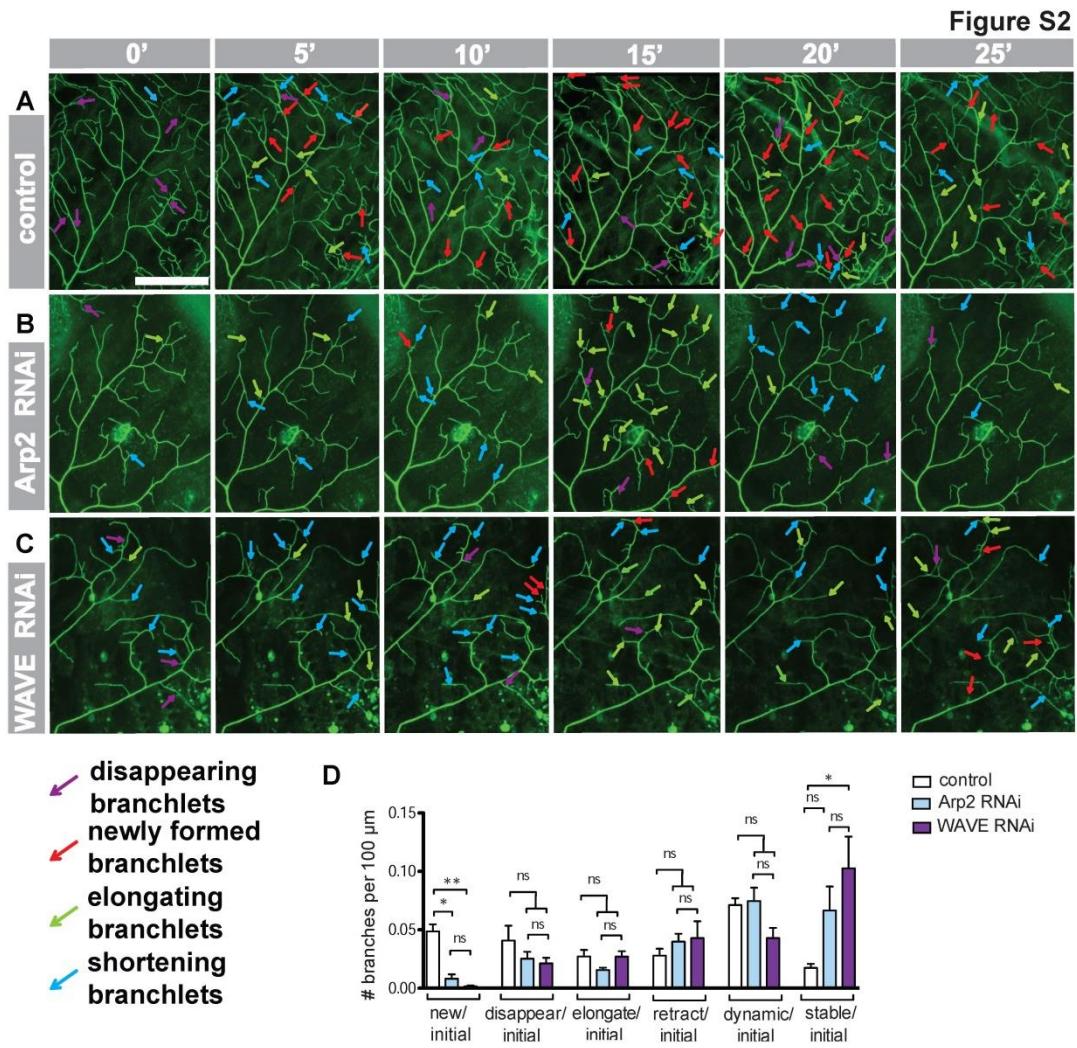
Development: doi:10.1242/dev.171397: Supplementary information

Figure S1. Depletion of Arp2/3 subunits leads to a reduction in arbor complexity in morphologically distinct classes of PNS neurons. (Related to Fig. 2)

(A-C) Class IV, III or I neurons in 3rd instar larvae expressing control RNAi or RNAi against Arp2/3 complex components under the control of type-specific drivers (*Gal4^{ppk}*, *Gal4^{C161}* and *Gal4^{G11}* for class IV, III and I da neurons, respectively). Asterisks indicate cell bodies. Scale bars: A-C: 50 μ m. (D-F) Quantification of the dendrite morphology after RNAi. Tracings and length measures of the images were obtained in ImageJ. The left panels represent the used definition of branching order. Suppression of Arp2/3 reduces the number and branch density in class IV and III neurons. Class IV and III: n=5; class I: n=10. Average \pm s.d.

2. Transient localization of the Arp2/3 complex initiates neuronal dendrite branching in vivo

Development: doi:10.1242/dev.171397: Supplementary information



2. Transient localization of the Arp2/3 complex initiates neuronal dendrite branching in vivo

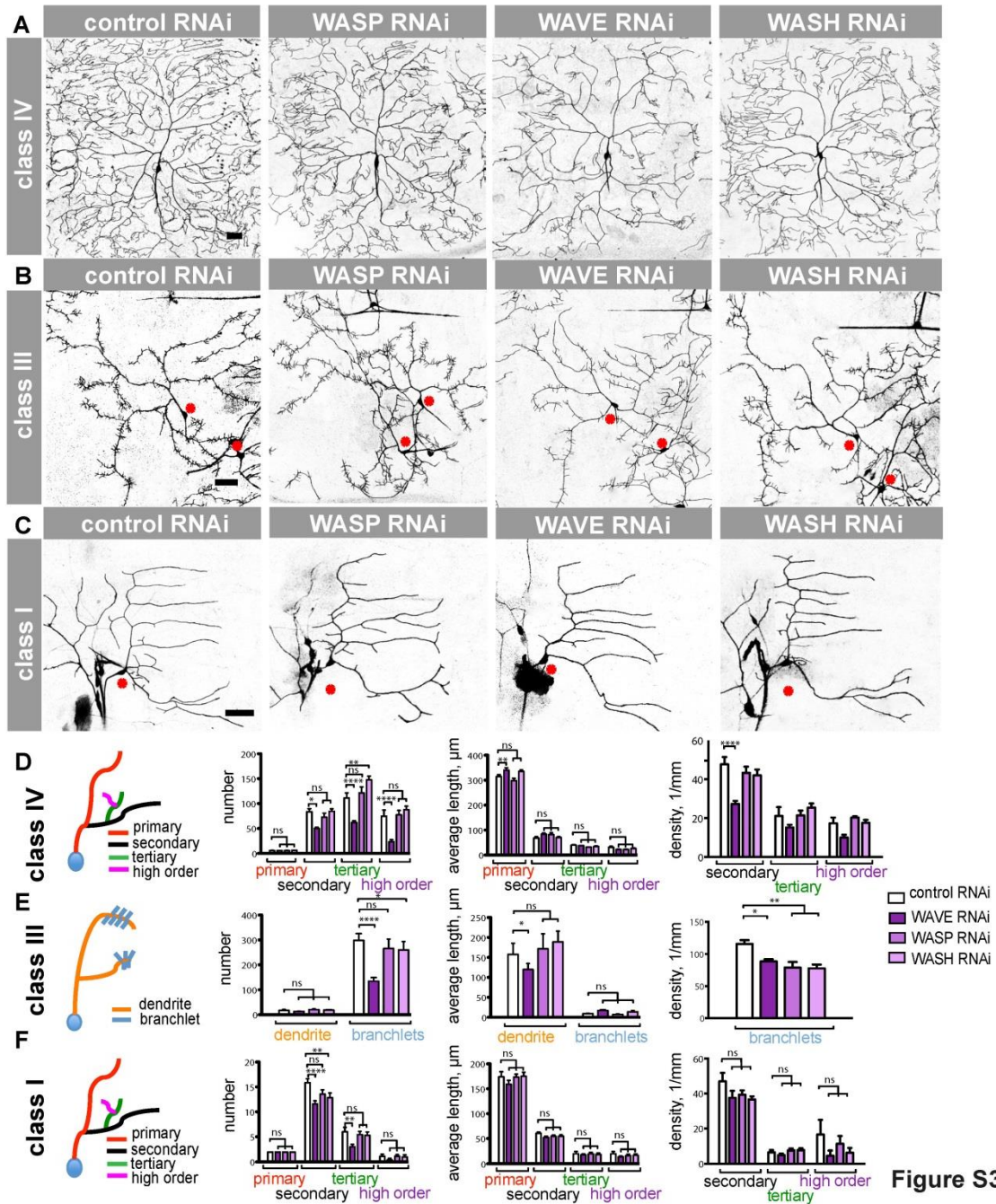
Development: doi:10.1242/dev.171397: Supplementary information

Figure S2. Arp2/3 and Wave are required for *de novo* formation of branches. (Related to Fig. 2 and to Fig. 4)

(A) Time-lapse imaging of differentiating class IV ddaC neurons of 2nd instar larvae cell-autonomously expressing control (A), *Arp2* (B) or *wave* (C) RNAi-inducing constructs. Stacks of optical sections were obtained by confocal microscopy every 5 minutes over a 25-minute period and maximal projections of the stacks at each time point are represented. Arrows indicate branchlets that disappear over the imaging period (purple), that are formed *de novo* (red), that elongate (green) or shorten (blue). See also Supplemental Movie S2. Scale bar = 50 μm , n=5. (D) Quantification of the branchlet dynamics of class IV neurons expressing control, *Arp2* or *wave* RNAi-inducing constructs. The number of newly formed or retracting branches was calculated as a ratio with respect to the initial branch numbers at the beginning of the time-lapse series. The number of newly formed branchlets was significantly reduced upon *Arp2* or *wave* knock-down, while the remaining branchlets were more stable upon *Wave* knock-down.

2. Transient localization of the Arp2/3 complex initiates neuronal dendrite branching in vivo

Development: doi:10.1242/dev.171397: Supplementary information



2. Transient localization of the Arp2/3 complex initiates neuronal dendrite branching in vivo

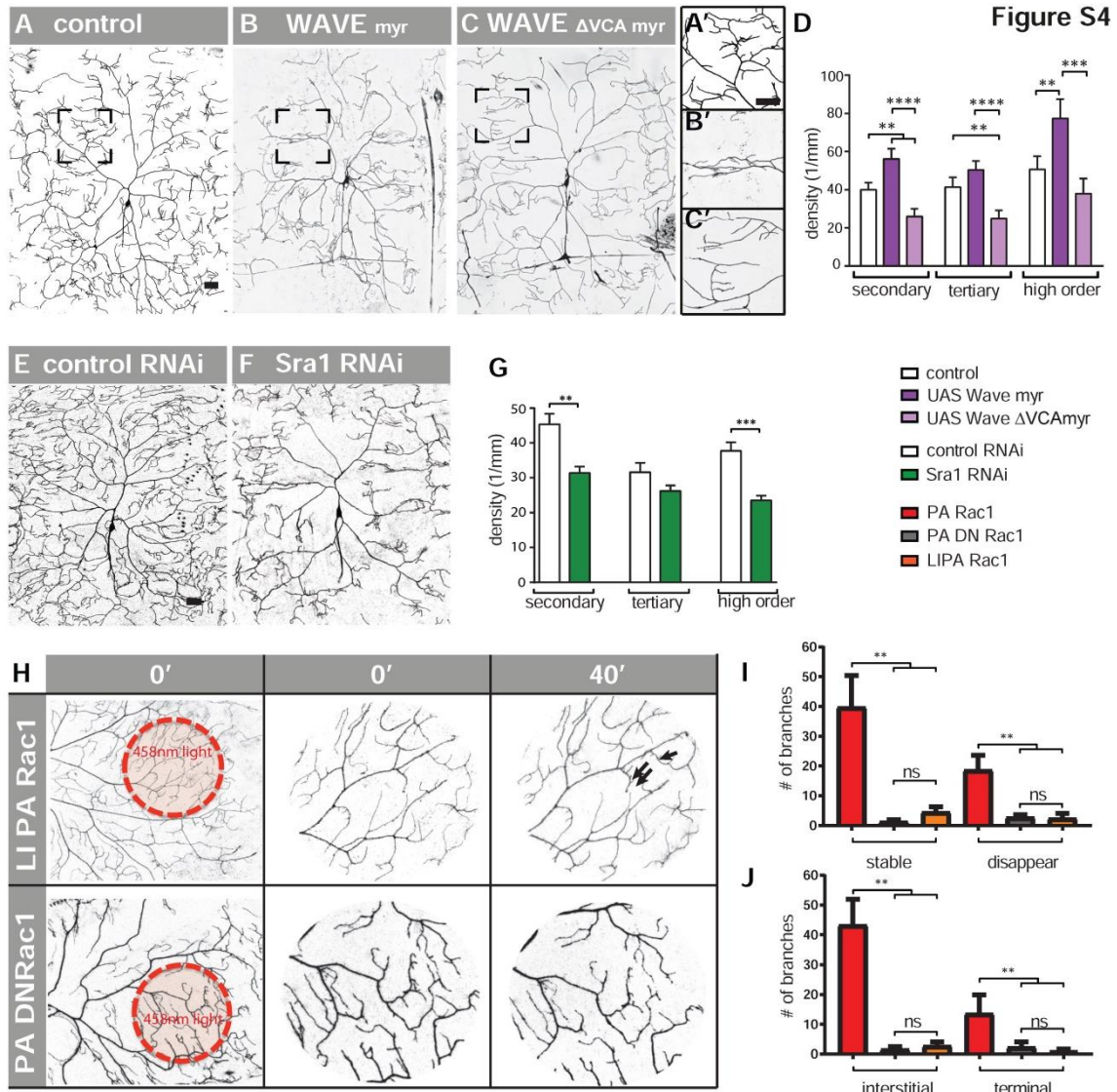
Development: doi:10.1242/dev.171397: Supplementary information

Figure S3. Depletion of WAVE phenocopies the loss of Arp2/3 function. (Related to Fig. 3)

(A-C) Class IV, III or I neurons in 3rd instar larvae expressing control RNAi or RNAi against WASP family proteins, namely WASP, WAVE and WASH under the control of type specific drivers (*Gal4^{ppk}*, *Gal4^{C161}* and *Gal4^{IG11}* for class IV, III and I da neurons, respectively). Asterisks indicate cell bodies. Scale bars (A- C)= 50 μ m. Class IV and III: n=5; class I: n=10. (D-F) Quantification of dendrite morphology after RNAi. Tracings and length measures of the images were obtained in ImageJ. The left panels represent the used definition of branching order. Suppression of WAVE reduces the number and branch density in class IV and III neurons and the number of branches in class I as well. Knock-down of WASP or WASH does not seem to affect dendrite number or density.

2. Transient localization of the Arp2/3 complex initiates neuronal dendrite branching in vivo

Development: doi:10.1242/dev.171397: Supplementary information



2. Transient localization of the Arp2/3 complex initiates neuronal dendrite branching in vivo

Development: doi:10.1242/dev.171397: Supplementary information

Figure S4. WAVE, Sra1 and Rac1 control dendrite complexity. (Related to Fig. 3)

(A-C) Class IV ddaC neurons expressing constitutively active *wave^{myr}* or dominant negative *wave^{ΔVCA myr}*, respectively. Scale bar= 50 μm, n=7. (A'-C') Increased magnification of the regions boxed in D-F. (D) Overexpression of constitutively active *wave^{myr}* with *ppk-Gal4* induces a disorganized tree and increased density of terminal branches. In contrast, the overexpression of *wave^{ΔVCA myr}* suppresses branch formation. (E, F) Single ddaC neurons expressing control or *Sra1* RNAi. (G) Shows the density of second order, tertiary order and higher order branches for control and *Sra1* RNAi. Scale bar= 50 μm, n=7. (H) Images from time-lapse recordings of class IV neurons expressing membrane-tagged red fluorescent *mCherry* and non-photoactivatable constitutive-active Rac1 (*LI PA Rac1*) or photoactivatable dominant-negative Rac1 (*PA DN Rac1*). The left panels show the dorsal arborization of a class IV ddaC neuron expressing the indicated construct. The red circle represents the ROI illuminated with 458nm light. Scale bar for the left panels = 50 μm. The central panels show a magnification of the highlighted ROI circle prior to photoactivation. The panels on the right show the same region after 40 minutes of activation. The arrows point to some of the newly formed single branchlets or groups of branchlets. (I, J) Quantification of the number of newly formed branches in the 40 minutes of imaging.

2.3 Summary

The Arp2/3 complex nucleates branched filament networks to push forward the leading edge of motile cells and for endocytosis (Pollard & Borisy, 2003). Electron microscopy images in this paper show for the first time that such a branched actin network is localised at the base of small dendritic branches, suggesting a similar force generation for the formation of a branch. We demonstrate that the Arp2/3 complex, the only actin nucleator thus far known to form branched actin, is essential for new branch formation in all classes of da neurons. Moreover, similarly to actin, the Arp2/3 complex localises transiently at the base before a new branch arises.

Activation of the Arp2/3 complex requires a significant conformational change (Robinson et al., 2001). Nucleation-promoting factor (NPF), such as the WCA (WASP-homology-2, cofilin-homology and acidic region) domain containing proteins, can activate the Arp2/3 complex. In *Drosophila*, there are three proteins known so far, WASP, WAVE, WASH and we demonstrate that WAVE is the NPF activating Arp2/3 in new branch formation. WAVE is probably acting in the WAVE regulatory complex (WRC), as another subunit of the complex, *Sra1* mutants, gave similar defects in the dendrite morphology. Through light induced activation of Rac1 in control or WAVE RNAi background we further demonstrate that Rac1 is one of the small GTPases upstream of this branch inducing mechanism.

Revealing for the first time how transient localisation of the Arp2/3 complex controls dendrite branching *in vivo* in this work, together with recent work on Twinstar/Cofilin and Singed/Fascin, set the stage for further *in vivo* characterisation of actin regulatory proteins in da neurons (Nagel et al., 2012; Nithianandam & Chien, 2018).

3 Comparative computation analysis of actin-binding proteins *in vivo* unravels the single elements of dendrite dynamics

This chapter of the thesis represents a manuscript that has been prepared for submission at eLife Sciences Publications, Ltd.

3.1 Introduction

What is the composition of the neuron-specific repertoire of actin regulatory molecules and how do they contribute to branch formation in space and time? Constantly improved imaging techniques and advantageous invertebrate model systems, such as the da neurons of *Drosophila*, have inspired us to trust we can answer this question even *in vivo* within the coming years.

Genetic and live imaging studies in invertebrate models have already shown how single cytoskeletal components regulate specific branch types (Andersen et al., 2005; Nagel et al., 2012; Zou et al., 2018). Previous publications suggest that neuron and even branch-specific sets of ARPs are required to form specific dendritic trees. Therefore, understanding the function of an ARP in dendritic branching requires focusing on one class of neuron and one type of dendritic branch in comparison. To understand the actin regulatory mechanisms that control the formation of a specific dendritic type, we combine genetics with high-resolution microscopy *in vivo*. The da neurons offer a variety of dendritic trees of different complexity and structure to choose from. The c3da neurons provide a high complexity and the advantage that there are two types of branches, long main branches and small actin enriched branches, that we decided to concentrate on. We investigated ARPs that were well characterised biochemically and that we knew or expected to play a role in these c3da neurons. This work elaborates a more comprehensive picture of the repertoire of actin regulatory proteins required for the unique dendritic architecture of c3da neurons.

3.1.1 Statement of Contribution

Table 2: Statement of Contribution for Manuscript Stürner et al.

Task	Author
Conceptualisation	T.S., H.C., G.T.
Methodology	T.S.
Software	M.P., A.C., H.C.
Formal analysis	T.S., A.C., H.C., G.T.
Investigation	T.S.
Resources	H.C., G.T.
Writing - original draft	T.S.
Writing - review & editing	T.S., G.T., H.C.
Supervision, project administration and funding acquisition	G.T.

3.2 Manuscript

Comparative computation analysis of actin-binding proteins *in vivo* unravels the single elements of dendrite dynamics

Tomke Stürner, André Castro, Maren Philipps, Hermann Cuntz*,
Gaia Tavosanis*

* = equal contribution

Comparative computation analysis of actin-binding proteins *in vivo* unravels the single elements of dendrite dynamics

T. Stürner¹, A. Castro², M. Philipps¹, *H. Cuntz^{2#}, *G. Tavosanis^{1#}

1: German Center for Neurodegenerative Diseases (DZNE), Bonn, Germany

2: Ernst Strüngmann Institute (ESI) for Neuroscience in Cooperation with Max Planck Society, Frankfurt am Main, Germany

#: Equal Contribution

*To whom correspondence should be addressed

The cytoskeleton defines the morphology of dendrites through a series of dynamic processes under the control of complex protein signalling networks. By performing *in vivo* time-lapse recordings and developing new quantification methods, we elucidate how six actin-regulatory proteins (ARP) coordinate different aspects of branch dynamics. For this we concentrate on the class III dendritic arborisation (c3da) neurons of *Drosophila* larva with their actin enriched terminal branchlets (TB). We find that remodelling of actin through Twinstar is a prerequisite, Arp2/3 not only initiates a branch but also constrains its retraction and disappearance, Spire and Capu function together in new branch formation but Spire also destabilises the branchlet, Singed gives the branchlet its characteristic form but restricts the overall dynamics and Ena limits the length of the branchlet and favours the retraction. In this work, we delineate specific functions of these different ARPs, reveal new mechanistic aspects of TB dynamics and derive a mathematical growth model for the c3da neurons.

Introduction

Regulated dendritic outgrowth and branching throughout development is essential to establish a dendritic tree that is optimised to perceive specific inputs (Jan and Jan 2010). Given its core role in the definition of morphology, it is not surprising that the convergence point of many signalling pathways is the regulation of the underlying cytoskeleton. The ensemble of numerous actin-regulatory proteins (ARP) drives the morphological changes that lead to dendritic branch formation (Lanoue and Cooper 2019). Analysis of the biochemical properties of ARPs performed in a series of *in vitro* studies with purified proteins has revealed their biochemical properties in isolation (Mullins, Heuser et al. 1998, Pruyne, Evangelista et al. 2002, Breitsprecher, Kieseewetter et al. 2008). Subsequently additional elegant studies have characterized ARPs *in vitro* (Gertler, Niebuhr et al. 1996, Kovar, Harris et al. 2006, Smith, Daugherty-Clarke et al. 2013). However, we still lack a clear understanding of how they work, either together or separately, to produce dendritic branches *in vivo*.

The dendritic arborisation (da) neurons of *Drosophila melanogaster* have proven to be a fruitful system for studying actin in dendrite morphogenesis *in vivo*. This system enables us to monitor transgenic expression of genetically encoded reporters through the transparent cuticle of the larva. A variety of green fluorescent actin fusion proteins that incorporate into the actin filaments have enabled visualisation and characterisation of actin in these neurons (Kiehart, Galbraith et al. 2000, Andersen, Li et al. 2005, Hatan, Shinder et al. 2011, Haralalka, Shelton et al. 2014, Nithianandam and Chien 2018). This has recently led to the description of a new actin structure, actin blobs, which accumulate before a new dendritic branchlet is formed (Nithianandam and Chien 2018). Moreover, genetic studies in these neurons have demonstrated the *in vivo* function in actin remodelling of several cytoskeletal regulators such as the severing protein Twinstar/Cofilin (Nithianandam and Chien 2018), the actin nucleators Arp2/3 (Sturner, Tatarnikova et al. 2019) and Spire (Ferreira, Ou et al. 2014), the actin barbed end binding protein Ena/VASP (Gao, Brenman et al. 1999) and the actin bundling protein Singed/Fascin (Nagel, Delandre et al. 2012). This *in vivo* analysis of single ARPs revealed class-specific functions in the dynamic formation, extension and retraction of a dendritic branch. An ARP may cause a dendritic alteration in one class of da neuron and have no function at all in another, such as Singed, which is specific to the c3da neurons TBs (Nagel, Delandre et al. 2012). This makes it considerably more difficult when trying

to understand the coordinated action of ARPs even in a relatively simple context such as branch formation.

In order to understand how these ARPs work in concert, we focused on one type of dendritic branch in just one class of da neuron and its dynamics. The c3da neurons sense gentle touch through the mechanosensitive ion channels NOMPC (Yan, Zhang et al. 2013) and Brv1 (Zhang, Li et al. 2018). They have long primary branches and characteristic short actin enriched terminal branches that stay dynamic (Grueber, Jan et al. 2002, Nagel, Delandre et al. 2012), making them the ideal model system to study actin dependent branch dynamics *in vivo*.

Previous studies exploring the functional role of these ARPs relied on single well described dendrite features or methods, such as the number of branches of Strahler order or Sholl analysis (Nagel, Delandre et al. 2012, Ferreira, Ou et al. 2014, Vormberg, Effenberger et al. 2017, Bird and Cuntz 2019). This is sufficient to state the requirement of a given protein for the system, but not enough to understand its actual molecular function on the dendritic tree architecture (Gillette and Ascoli 2015). More recently, several studies have demonstrated that combining quantitative morphometry or data driven models with genetic studies in da neuron is extremely beneficial to understanding the global rules of dendritic trees. Determining, for example, that complex dendritic trees are constrained by resource optimization, while smaller dendritic trees try to conserve their path distance to the soma (Nanda, Das et al. 2018) or establishing a mathematical model, the stretch-and-fill model, to describe the development of the class IV da neurons (c4da) and uncover the balance between space filling and optimal wiring (Baltruschat L. submitted 2018). Therefore, to address the question of how ARPs are involved in branch dynamics, we decided to extend this approach, comparing different mutants with a detailed computational analysis of morphology and dynamics of branches.

In this study, we imaged, traced and performed a thorough computational analysis of the morphology and dynamics of c3da neuron dendritic trees. We analysed the function of six different ARPs, two of which, *spire* and *capu*, have not been previously characterised in c3da neurons. Our data demonstrate how a variety of morphometrics and a time-lapse analysis can help to extrapolate the distinct function an ARP has in branch dynamics. This allows us, for the first time, to build a model for the role of ARPs in branch dynamics, based on comparable data from one specific neuron cell type *in vivo*. This

detailed analysis of the dendritic trees of c3da neurons allows us to derive a mathematical growth model for the c3da neurons that can replicate their characteristic morphology.

Results

C4da stretch-and-fill model does not apply to c3da neurons

The c3da neurons tile the body wall and scale with the growing larva similarly to the c4da neurons covering around 70% of the body wall (Grueber, Jan et al. 2002). Recent advances in modelling *in-vivo* dendritic tree of c4da neurons have led to a stretch-and-fill (saf) model that reproduces the morphology not only of c4da neurons but also other space filling dendritic trees, including the Purkinje cells and hippocampus pyramidal cells (Baltruschat L. submitted 2018). We therefore attempted to model the c3da neurons with this saf model.

To define the surface area of the computed neuron we imaged a control ldaB c3da neuron of the abdominal segment A5 of early larval instar 3 (L3) *in vivo* and traced it in the TREES toolbox (www.treestoolbox.org) (Cuntz, Forstner et al. 2010) (Fig. 1a). To start modelling c3da neurons, we utilized the surface area derived from tracing this particular neuron as target area. We then distributed target points randomly in this target area that the model should connect utilising a given total length, derived from the real dendritic tracing. By optimally wiring these randomly distributed points a synthetic dendritic tree was built according to the saf model (Fig.1b) (Baltruschat L. submitted 2018). It was evident that the synthetic dendritic tree differs from the original, especially in the characteristic morphology of the smaller branches. Branches below a length of 10 μ m made up 90% of the dendritic branches in c3da neurons which could not be replicated in the modelled dendritic trees (Fig. 1c). While the main branches, defined as longer than 10 μ m, had a comparable distribution of length as in control, the proportion of terminal branches, defined as smaller than 10 μ m, was shifted. Instead of over 90% of branches below a length of 10 μ m the synthetic neuron had 60% (Fig.1c, d, e).

The saf model that successfully reproduces c4da neurons cannot be applied to the c3da neurons because of the number, shape and distribution of the characteristic small dendritic branches, suggesting that the c3da neurons dendrites do not represent a classical space filling dendritic trees. The most prominent difference between the synthetic trees and the real dendritic trees are the number and distribution of the short TBs.

Figure 1

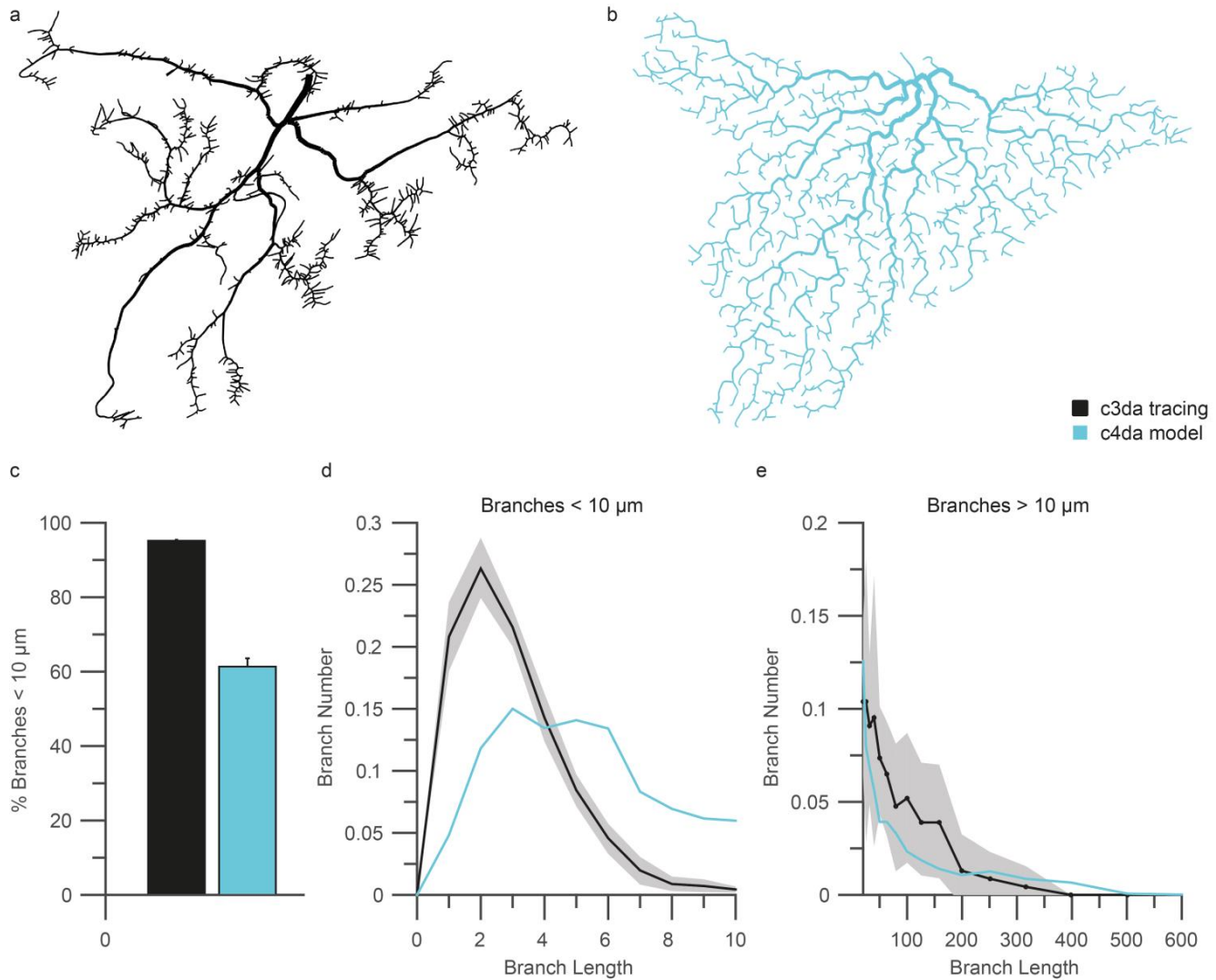


Fig. 1 Stretch-and-fill model in c3da neurons. a) Tracing of a c3da (IaB) neuron, genotype: *C161G4UASmCD8GFP/+*. b) Synthetic dendritic tree generated with the saf model from Bartruschat et al. (Bartruschat L. submitted 2018) and allowed to develop within the target area derived from the tracing in a). c) The percentage of branches that are up to 10 μm in length in the real c3da dendritic trees compared to synthetic dendritic trees (n=10 each). Error bars in SD. d and e) The fraction of branches (%) plotted against the length of branches (μm) up to 10 μm (d) or above 10 μm (e) for the real dendritic tree in black (n=10) and one synthetic dendritic tree in light blue.

The barbed ends of actin filaments are localised at the tip of small dendritic branchlets

These terminal branchlets (TB) below 10 μm are characteristic of the c3da neurons (Grueber, Jan et al. 2002). They are actin and Singed enriched straight branchlets that dynamically extend and retract throughout larval stages (Nagel, Delandre et al. 2012). To understand how these branches are formed and how their dynamics are coordinated by ARPs we first need to understand how the actin cytoskeleton is organised. We have recently shown the cytoskeletal structure at the base of dendritic branches through EM tomography. For the rest of the branchlet the EM data shows that straight actin filaments are organised in parallel (Sturner, Tatarnikova et al. 2019).

To address the dynamics of actin and the orientation of these filaments we performed a Fluorescence Recovery After Photo bleaching (FRAP) analysis of GFP labelled actin in the dendritic branchlets of *lidaB* c3da neurons. For an internal reference we also expressed a cherry-tagged membrane targeted chimera, to visualise the dendritic branchlet and to estimate general bleaching. Fluorescence recovery of actin GFP signal after photo bleaching reveal two important characteristics of actin: the velocity of actin turnover (half-time recovery = $t^{1/2}$) and the treadmilling of actin (retrograde movement = r) (Lai, Szczodrak et al. 2008). By only bleaching at the tips of growing dendritic branchlets we additionally wanted to examine where new actin monomers are added to the actin filaments (Fig. 2a).

We observed a sharp actin GFP signal merely 30 seconds after photo bleaching at the tip of the growing dendritic branch suggesting incorporation of actin at the front of the branchlet (Fig.2c, arrow). The membrane targeted chimera signal was unaffected by experimental bleaching. To calculate the actin turnover and possibly the treadmilling of actin we tracked the length and fluorescence intensity of the branchlet over time and measured the fluorescence within the bleached area (Fig.2b). The average half-time of recovery of the actin GFP signal was 2.5 minutes after photobleaching (Fig.2b, $t_{1/2}$). A kymograph of the GFP fluorescence over time and space visualised the treadmilling of actin within the growing branchlet (Fig.2d). The average retrograde movement of the bleached area was 0,13 $\mu\text{m}/\text{min}$.

F-actin structures have highly variable lifetimes, ranging from rapid changes at the leading edge of migrating cells (full recovery = 50 seconds) to stable actin bundles in

stress fibres (full recovery = 6 minutes) (Wang 1985, Hotulainen and Lappalainen 2006, Lai, Szczodrak et al. 2008). Actin recovery in these small terminal branches of c3da neurons took around 5 minutes, placing it close to the recovery time of the tightly bundled actin of stress fibres. New actin monomers added at the tip of the branchlet and the proximal disassembly resulted in the observed treadmilling of f-actin, similarly to what had been observed for filopodia at the leading edge (Abercrombie, Heaysman et al. 1971). The molecular mechanism that mediates this process is still highly controversial (Faix and Rottner 2006, Gupton and Gertler 2007). The velocity in retrograde movement of the bleached area in this study (0,13 $\mu\text{m}/\text{min}$) was very slow in comparison to what had been measured in the filopodia of primary hippocampal neurite-forming neuron in culture (4,46 $\mu\text{m}/\text{min}$) (Flynn, Hellal et al. 2012). However, it was comparable to the retrograde flow rates observed for example in ADF/Cofilin knockout mutant neurons in cell culture (0.14 $\mu\text{m}/\text{min}$) (Flynn, Hellal et al. 2012). This could mean that the dynamics of elongating c3da TBs are resistant to Twinstar, the Cofilin homologue in *Drosophila*.

3 Comparative computation analysis of actin-binding proteins in vivo unravels the single elements of dendrite dynamics

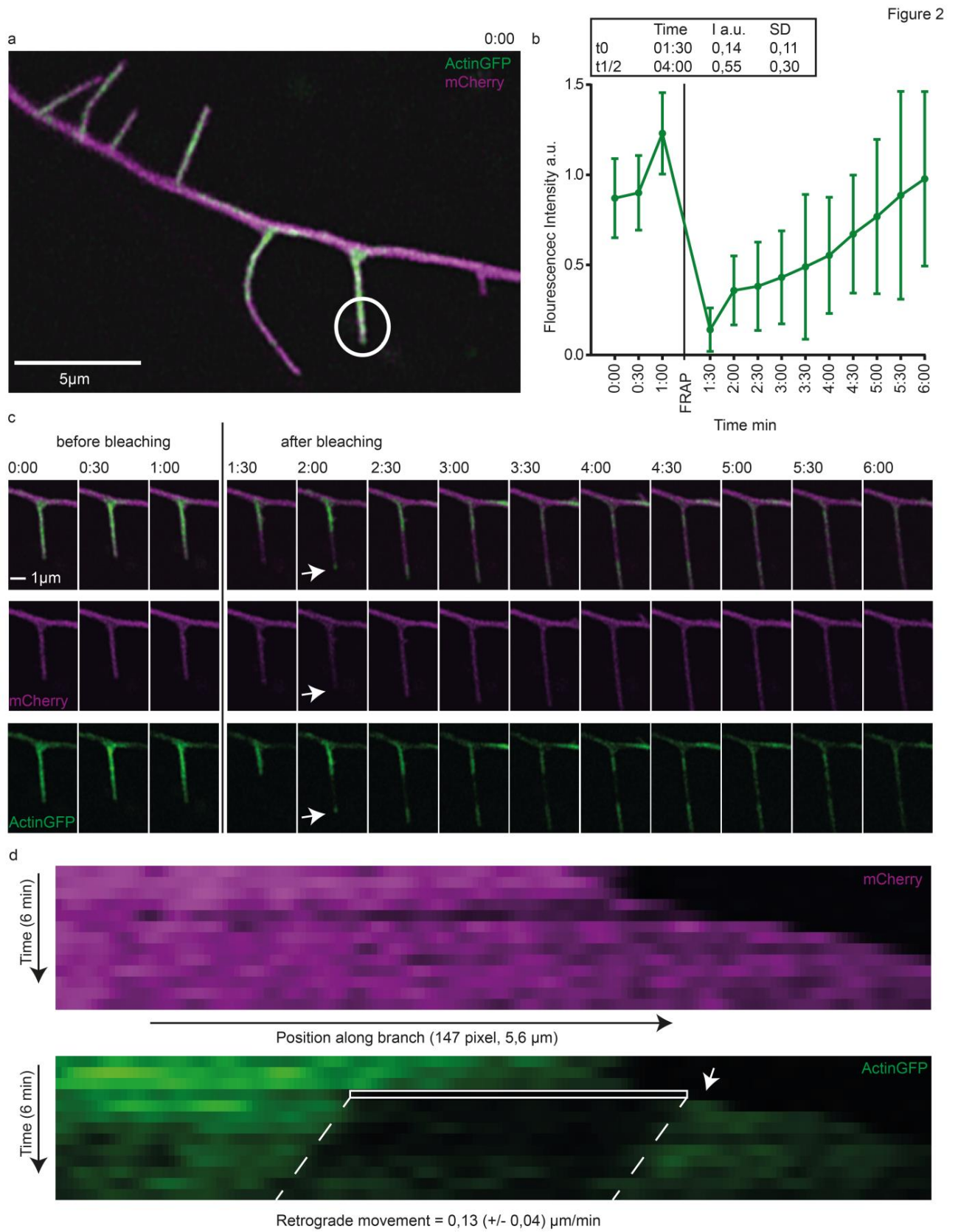


Fig. 2 FRAP analysis of actin in terminal branches. a) Representative overview image of a dendritic branch of a c3da (ldaB) neuron at time point 0:00 of the time-lapse series. The white circle indicates the area that will be photobleached with the 488nm laser after 1 minute (after 3 image series). b) FRAP curve for the average GFP Fluorescence intensity of 8 time series. A line analysis over time, space and the two channels was used to calculate the normalised intensity values per pixel. The fluorescent signal in the bleached area are normalised to the prebleaching mean and corrected for the background. Error bars represent the standard deviation. The average 50% recovery was calculated and the time point closest was assigned $t_{1/2}$. c) The terminal branchlet was imaged every 30 seconds for the time-lapse of 6 minutes. The white arrow is pointing to the bright GFP signal at the growing branchlet tip after photo bleaching. d) A representative kymograph of the same dendritic branchlet over time and space. The bleached area is highlighted with a white rectangle and dotted white lines indicate the retrograde movement of this area. The white arrow is pointing to the bright GFP signal after photo bleaching. Normalised intensity values under a threshold of 30% were used to plot the line and calculate the average retrograde movement. Magenta = *UASmCD8Cherry*, Green= *UASp-GFP.Act5C*, n=8 time series.

Six Actin-binding proteins all show reduced number of branches in c3da neurons

Through a thorough literature search and a targeted screen of actin nucleators, elongators, bundlers and depolymerisation factors we were able to derive six ARPs that play an important role for the branchlets of c3da neurons (Fig.3, see Supplementary Methods). The organisation and orientation of actin filaments (Figure 2) allowed us to speculate upon where these ARPs might be placed within the dendritic branchlet. The c3da neuron of early third instar larva of the six ARP mutants and corresponding controls were imaged *in vivo*. The neurons were traced and analysed in the TREES toolbox allowing a more accurate phenotypic description with an improved resolution.

The expression levels of the actin nucleator Spire are negatively regulated by the longitudinals lacking (Lola) transcription factor (Gates, Kannan et al. 2011). Loss of *lola* in c4da neurons leads to an increase in Spire levels that correlates with a smaller dendritic tree and inappropriate F-actin-rich small dendrites (Ferreira, Ou et al. 2014). In our hands *spire* mutants did not display a phenotype in c4da neurons. Nonetheless, loss of *spire* and the actin nucleator *capu* both reduced the total number of branches of c3da neurons by

roughly a third; a phenotype that we could rescue with the corresponding full length constructs (Fig. 3g, see Supplementary Fig. 1). This represents a specific role in c3da neurons that had not been described. The single *spire* or *capu* heterozygous mutants did not show any changes in morphology while the combination of the two heterozygous mutants reduced the number of branches comparable to the single homozygous mutants, indicating a genetic interaction between them (Fig. 3h). Such Capu/Spire interaction *in vivo* has only been shown in the development of an actin meshwork in the oocyte (Dahlgaard et al. 2007).

Single mutant c3da neuron clones (MARCM clones) of the previously characterised actin nucleator Arp2/3 complex component *arpc1*, of the anti-capping factor *ena*, of the actin severing factor *twinstar* and mutants of the actin bundler in c3da neurons *singed*, showed the previously reported reduced number of branches in c3da neurons (Fig. 3c,d,e,f,g) (Gao, Brenman et al. 1999, Nagel, Delandre et al. 2012, Nithianandam and Chien 2018, Sturner, Tatarnikova et al. 2019).

Remarkably, although all of these mutants showed a reduced number of branches in c3da neurons their dendritic phenotypes were clearly distinguishable from one another by eye. Thus, we analysed the dendritic trees further with a variety of features to characterise the differences observed in the mutants.

3 Comparative computation analysis of actin-binding proteins in vivo unravels the single elements of dendrite dynamics

Figure 3

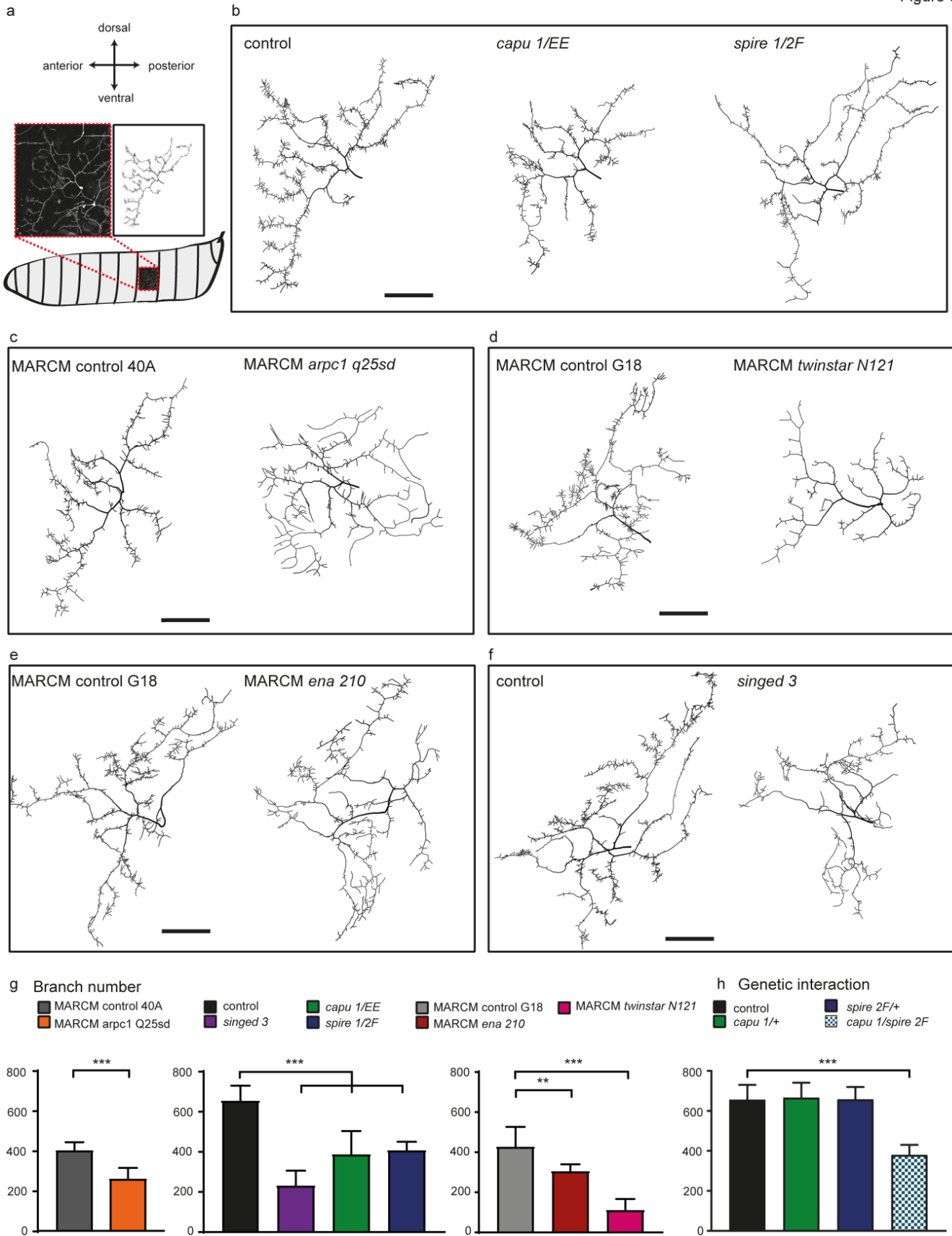


Fig. 3 Actin-binding proteins involved in terminal branch formation of c3da neurons. a) Illustration of the larval body wall with the lateral c3da neuron (ldaB) in segment A5 which was chosen consistently for all imaging. On the left the microscopy image and on the right the tracing. b) Representative tracing of *C161G4UASmCD8GFP/+*, *C161G4UASmCD8GFP/+;capu¹/capu^{EE}* or *C161G4UASmCD8GFP/+;spire¹/spire^{2F}*. c) Representative tracing of MARCM clones of control, *Gal4 5-40,UAS-Venus,sop-FLP;Gal80, FRT40A*, and *arpc1^{Q25sd}FRT40A* mutants. d) Representative tracing of *C161G4UASmCD8GFP/+* and *C161G4UASmCD8GFP/+;sn³*. e) Representative tracing of MARCM clones of control, *Gal4 5-40,UAS-Venus,sop-FLP; FRTG18,Gal80*, and *FRTG13 ena²¹⁰* mutants. f) Representative tracing of MARCM clones of control, *Gal4 5-40,UAS-Venus,sop-FLP; FRTG18,Gal80*, and *FRTG13tsr^{N121}* mutants. g) Quantification of total branch number of the different groups with controls. h) Quantification of total branch number in heterozygous mutants of *spire*, *capu*, or *spire capu* transheterozygous mutants. (* is $p < 0.05$, ** is $p < 0.01$ and *** is $p < 0.001$). Scale bar is 100 μm .

Dendritic tree features reveal the difference between actin-regulatory requirements

While the quantification of the number of branches as in the previous figure can be sufficient to state the requirement of a given protein, it is not adequate for understanding the morphological changes in the dendritic tree. Each neuronal type has typical dendrite morphology and we sought to identify a specific set of features than can describe the characteristic properties of c3da neurons. We defined a set of 28 features that are potentially relevant for the morphology of the c3da neurons from general dendritic branching features previously used to compare cell types (see Materials and Methods). Seven of these accurately described the differences between the ARP mutant morphologies, suggesting that they are key features (Fig. 4a).

Additionally to a reduced number of branches *spire* and *capu* mutants showed a reduced total length and reduced distances from the root (Fig. 4b, c). Indeed, *capu* and *spire* mutant trees had most of their branches closer to the cell soma (Fig. 3b). The *spire* mutants showed an additional increase in mean length of branches and decreased density of terminals (Fig.4c). These parameters, described the long main branches with very few TB seen in the dendritic trees of *spire* mutants trees (Fig. 3b). Suggesting that while both

spire and *capu* mutants lacked small TBs, only *spire* mutants seemed to have kept the main long branches.

The Arp2/3 complex is important for branch formation in all da neuron classes (Sturner, Tatarnikova et al. 2019). In the c3da neurons this loss of branches seemed to be compensated by an increase in mean length to such an extent that the total length of the dendritic tree was unchanged (Fig.4d). The reduced number of terminals and longer branches led to a decrease in the density of terminals and these terminals were more tortuous. Moreover the branches of *arpc1* mutants were more spread out resulting in larger distances between neighbouring terminal points (Fig.4d). Indicating that in comparison to the *arpc1* phenotype described for the c4da neurons, the c3da neurons maybe have a competing mechanism that is restricted by Arp2/3. A balance between a branching and an elongation mechanism, that when branching is reduced, by the loss of *arpc1*, leads to more elongation of the branches.

In da neurons *ena* has been proposed to play a role in the elongation of lateral branching in dendrites of all classes in the dorsal cluster (Gao, Brenman et al. 1999). C4da neurons display dendrite over-elongation and reduced branching in *ena* mutants as well as in loss of *robo* or *slit* potentially in a common mechanism (Dimitrova, Reissaus et al. 2008). Likewise in this work looking specifically at the c3da neurons *ena* mutants revealed a compensation for loss of branches by increasing mean branch length and spreading out more, measured as distance to nearest neighbour (Fig.4e).

The actin bundler *singed* localises to the characteristic actin enriched TBs of c3da neurons (Nagel, Delandre et al. 2012). *Singed* and *twinstar* mutants showed a reduced total length that could not be compensated by the increase in mean length (Fig. 4f, g). The branches were more spread out, quantified with the distance between neighbouring branches and density of terminal branches. The few branches that were left had an increased tortuosity, again suggesting proportionally more main branches. Additionally they both demonstrated an increase in branching angle that was not observed in any other mutant (Fig.4f, g).

A thorough parallel evaluation allowed us to pinpoint the seven morphometric features of c3da neurons that were necessary to describe the differences in dendrite morphology between these six ARPs. Thus, this analysis delineated how some of the proteins might be

3 Comparative computation analysis of actin-binding proteins in vivo unravels the single elements of dendrite dynamics

cooperating or competing to form the characteristic dendrite morphology of the c3da neurons.

3 Comparative computation analysis of actin-binding proteins in vivo unravels the single elements of dendrite dynamics

Figure 4

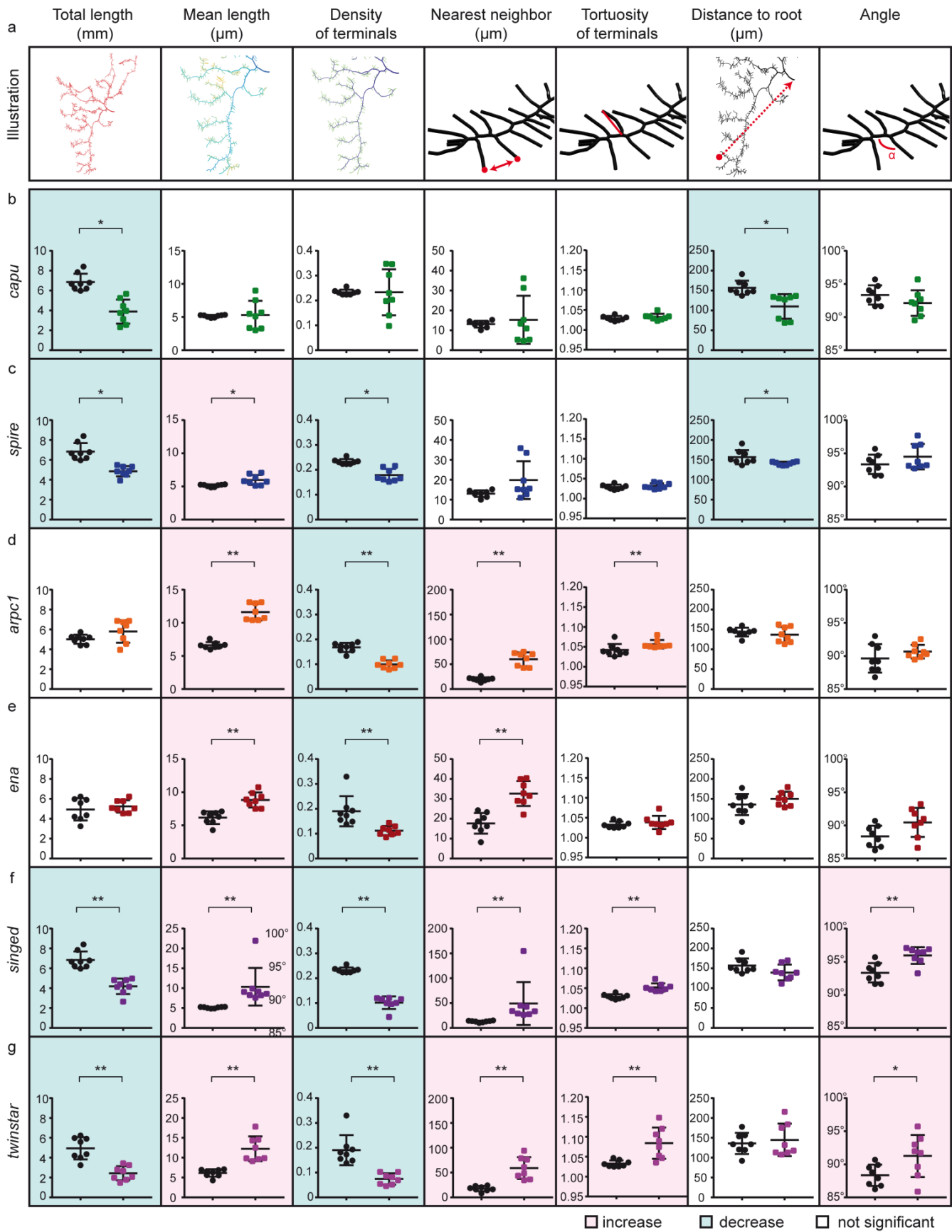


Fig. 4 Features of dendritic tree structure in c3da neurons. a) Illustration of the seven morphometric measures defining c3da neuronal morphologies: total length of the dendritic tree in mm (entire tree shown), the mean length of all branches defined in μm (different colours represent different lengths), the density of terminals along the length of main branches (purple = main branches, green = terminal branches), the distance of terminal points to the nearest neighbouring terminal point in μm , the mean Euclidean distance of terminal points to the soma in μm , the mean tortuosity of branches, the mean angle between branches. b-g) The seven measurements in lateral c3da neuron (lDaB) for each mutant versus corresponding control (black). The corrected p values are represented as stars (* is $p < 0.05$, ** is $p < 0.01$ and *** is $p < 0.001$). The background is highlighted in blue for a significant decrease and in red for a significant increase.

Branch dynamics pinpoint the functional role of each actin-binding protein

There are different ways in which the loss of dendritic branches, seen in the mutants, could arise. Defects in dendrite maintenance could have led to more dendrite retractions and disappearing of branches or dendrites could not be formed in the first place. To understand the reason behind the loss of branches in the different ARP mutants we performed a time-lapse analysis (see Supplementary Methods). Branches were categorised into one of the following five groups: stable, new, extending, retracting and disappearing branches. These numbers were divided by the total number of branches within the image frame (Fig. 5a, b). This allowed us to compare the different mutants and the branch dynamics independently of their discrepancy in loss of branches. We additionally tracked the terminal and branch points to measure the velocity of extension and retraction of branches quantified as the travelled distance of the branch over time ($\mu\text{m}/5\text{min}$).

The loss of *capu*, *spire* or *arpc1* led to a reduced number of newly forming branches (Fig. 5c, d, e), suggesting that these actin nucleation factors are important for this very first step of branch formation, as previously already demonstrated for *arpc1* (Sturner, Tatarnikova *et al.* 2019). Mutants of *spire*, showed an increase in stable branches that was linked to a decrease not only in the number of newly forming but also extending, retracting and disappearing branches (Fig. 5d). Thus, Spire displayed an additional role in branch dynamics, possibly linked to a function independent of Capu. The higher resolution of the time-lapse analysis in c3da neurons also allowed us to speculate over an additional role

for *arpc1* in preventing retraction and disappearing of a branch, as both were decreased in the mutant condition (Fig. 5e).

Enabled (*Ena*) encodes a substrate of the tyrosine kinase *Abl* and has been assigned several different functions, from facilitating actin polymerisation (Gertler, Niebuhr et al. 1996) to axon guidance (Wills, Bateman et al. 1999) and elongation (Gao, Brenman et al. 1999). *Ena* localizes to the barbed end of actin filaments and could respond to a variety of cues (Bashaw, Kidd et al. 2000, Forsthoefel, Liebl et al. 2005, Pasic, Kotova et al. 2008). The analysis of the morphology of the dendritic tree of *ena* mutants already made a role in elongation very unlikely as we observed an increase in average length and no change in total length of branches (Fig. 4e). The time-lapse analysis additionally showed an increase in branch extension and new formation of branches in absence of *ena*, which is again in contrast to a role in elongation (Fig. 5f). It might even suggest that *ena* hinders the small terminal branches from extending further. Additionally, there was a decrease in disappearing branches, indicating that a branchlet in presence of *ena* is unstable (Fig. 5f).

Fascin forms unipolar actin filaments bundles and is suggested to give filopodia the stiffness necessary for membrane protrusion (Vignjevic, Kojima et al. 2006). Loss of the bundling factor *singed* in the *c3da* neurons, however, led to an overall increase in dynamics, suggesting that the unipolar bundling of actin is restricting the dynamics of the branchlet (Fig. 5g).

The loss of *twinstar* showed almost no newly forming, extending, retracting or disappearing branches and almost all branches were unchanged in length when imaging the same distal region of the dendritic tree (Fig.5h), demonstrating that without actin remodelling through *twinstar* there are no branch dynamics. However, when specifically imaging areas of the dendritic tree closer to the cell body, that still displayed some TBs, there were no changes in overall dynamics of the TBs (see Supplementary Fig. 2). This suggested either that there was residual Twinstar protein present and sufficient in these areas, or that *twinstar* was not important for branch dynamics but for an initial prerequisite step.

Pairing a computation analysis of the dendritic tree morphology with a computational time-lapse analysis has empowered us to speculate on new and different functions of these six ARPs as previously described for *da* neurons. By examining the ARPs in the same dendritic branchlet in a comparative way we can make a first attempt at

3 Comparative computation analysis of actin-binding proteins in vivo unravels the single elements of dendrite dynamics

understanding how together they characterise the specific dynamics of small dendritic branchlets.

Figure 5

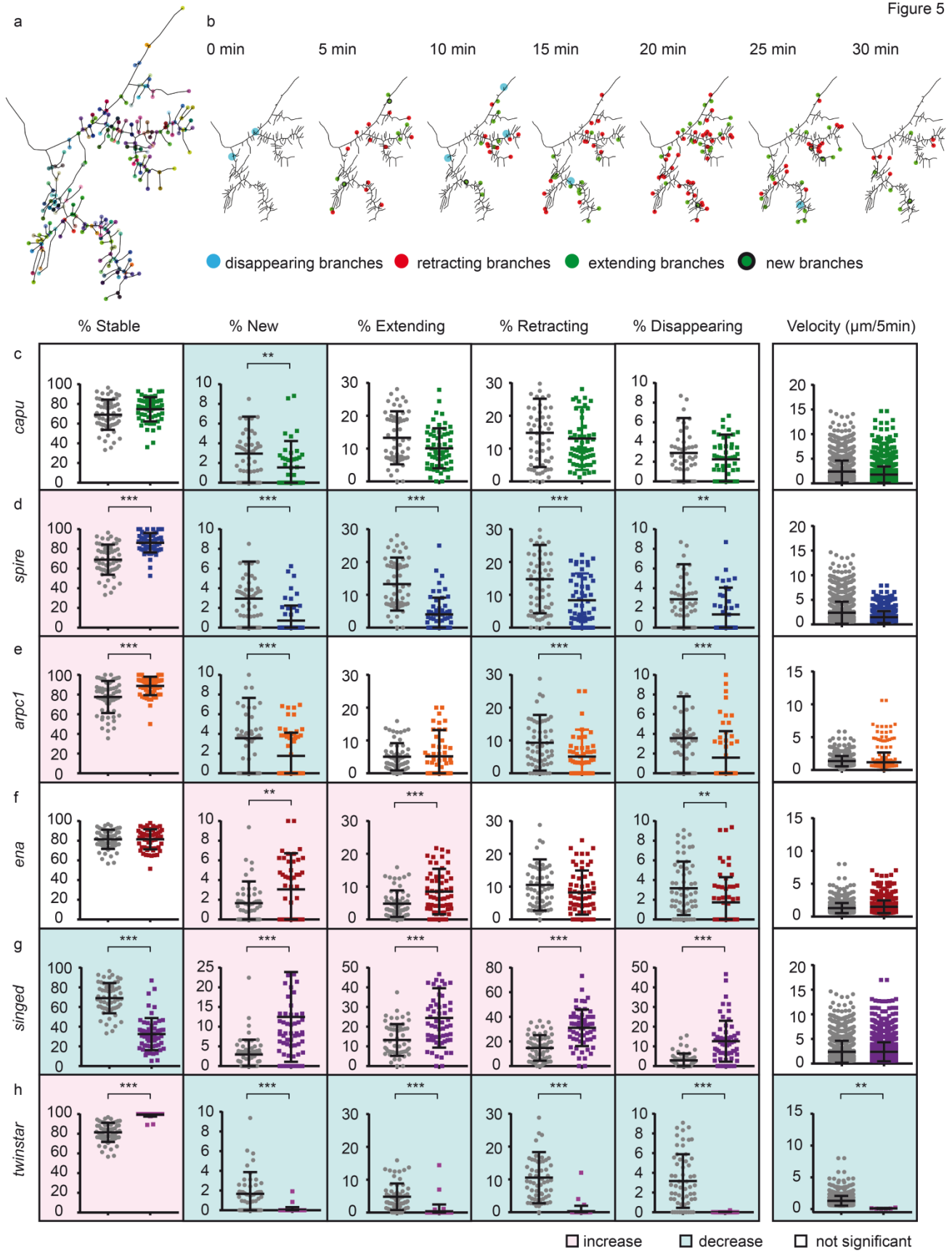


Fig. 5 Time-lapse analysis of terminal dendritic branches of c3da neurons. a) Tracing of a terminal region of a control c3da (ldaB) neuron. All branching points and terminal points are registered and illustrated as coloured points during the time-lapse analysis. b) Tracing of a terminal region of a control c3da (ldaB) neuron over 30 minutes in 7 steps of 5 minutes. Terminal branches that disappeared (blue), retracted (red,) extended (green), or newly formed (green with black ring) from one time point to the next are marked with a dot in the corresponding colour. c-e) The percentage of terminal branches that were stable, new, extending, retracting or disappearing within 30 minutes of time-lapse for each mutant versus corresponding control (grey/black). The average velocity of a terminal branch, quantified as the average change in length (extension + retraction) in μm per 5 minute. The corrected p values are represented as stars (* is $p < 0.05$, ** is $p < 0.01$ and *** is $p < 0.001$). The background is highlighted in blue for a significant decrease and in red for a significant increase.

A comparative computational analysis of actin-binding proteins reveals their independent functions in dendrite morphology and dynamics

The specific morphology and dynamics of dendritic branches relies on different assemblies of actin cytoskeleton regulatory and binding proteins (Konietzny, Bar et al. 2017). Here we characterised six ARPs in one specific type of dendritic branchlet, the terminal branches of c3da neurons, delineating the characteristic branch dynamics to generate a model for branchlet initiation, elongation and retraction (Fig.7). The data we obtained support a general model including these ARPs functions. Twinstar, an actin remodelling factor, is a prerequisite for any dynamics in the dendritic tree and from the FRAP analysis we suspect a role of Twinstar even after branch formation at the base of a branchlet resulting in the retrograde flow of actin (Fig.7a). The initiation of a branchlet is coordinated like in c4da neurons by the Arp2/3 complex, transiently localising at the base of a branchlet and building up branched actin. Two additional actin nucleation factors, Spire and Capu, nucleated straight actin filaments to push out the membrane for a new branchlet to arise (Fig.7b, c). The bundling factor Singed tightly bundles actin, restricting its dynamics and making it branch with a characteristic angle (Fig.7d). Together with Ena it gives the terminal branchlets their characteristic straight conformation. Ena, classically binding to the barbed end of actin, which from the FRAP data we know is localised at the

tip of the branchlet, is restricting the growth (Fig. 7e). Ena binding to the tip and Singed disappearing from the filament favours the retraction of the branchlet enhanced by Spire, that by itself acts as a severing or destabilising factor, maybe substituting or assisting Twinstar in this function (Fig.7f).

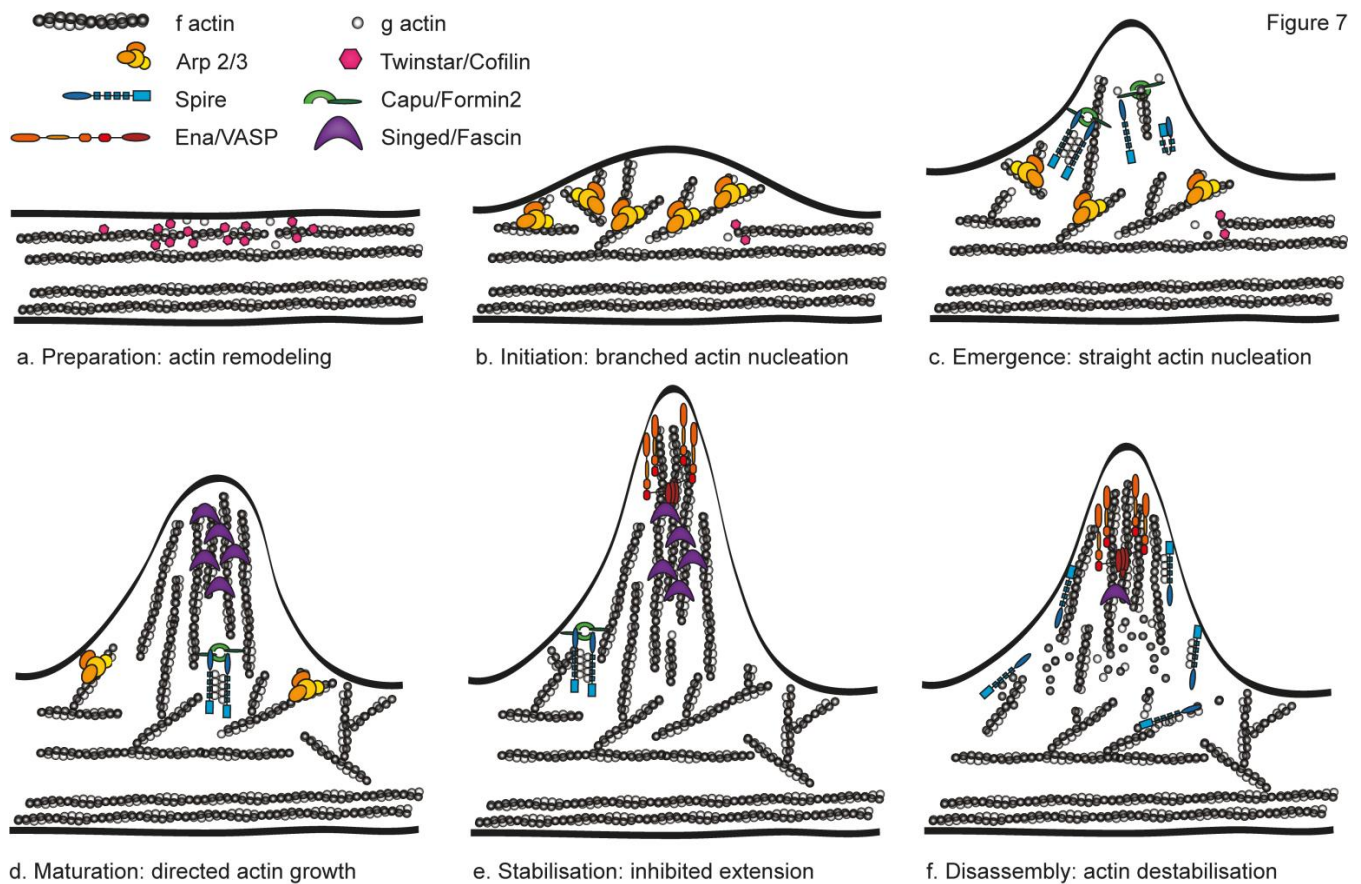


Fig. 7 Illustration of a model including six actin binding proteins in dendritic branch dynamics. 1) Actin remodelling and availability of a pool of monomeric actin (g actin), provided by Twinstar/Cofilin, is a prerequisite for the formation of new filamentous actin structures (f actin). 2) Membrane protrusion requires a branched actin network at the base, mediated by the actin nucleation complex Arp2/3. 3) Straight actin filaments, nucleated by Spire and Capu/Formin2 together, push out the membrane before 4) the actin filaments can be bundled by Singed/Fascin, to restrict their dynamics and give them their characteristic angle and shape. 5) Facilitated by the presence of Singed/Fascin, the mature terminal branchlet is limited in extending further by Ena/VASP. 6) Terminal

branches regularly retract and can disappear completely, facilitated by Ena/VASP and Spire that can destabilise the filaments.

C3da neuron model

The morphology and dynamics of the terminal branches of the c3da neurons is a characteristic feature of these neurons and a target for alternations in mutants of different ARPs. Computational modelling of these neurons require more restrictions than minimum wiring and space filling and needs to include the separation between main branches, here defined as branches of a length larger than 10 μ m, and terminal branches, shorter than 10 μ m.

The final growth model of the c3da neurons is currently being established by Prof. Dr. Hermann Cuntz and will then be included in this manuscript.

Discussion

In this project we wanted to address how different actin binding proteins work together to define dendritic branch properties and dynamics. We took a novel approach in which we probed already characterised ARPs in a very specific branchlet and class of neuron and performed an advanced computational analysis to understand how they might work together. For this we first had to understand the characteristic properties of these c3da neurons and the actin cytoskeleton underlying them. Secondly, we performed a targeted screen in which we selected ARPs with a defect in c3da neuron morphology and analysed their dendritic tree and dynamics of terminal branches. This allowed us to conclude on the functions of each ABP in dendrite dynamics and placing them inside a model. Finally we extracted the morphometric properties necessary to describe the similarities and differences between the mutants of different ARPs to put together a mathematical model that could describe the characteristic morphology of c3da neurons.

The actin cytoskeleton and actin dynamics in c3da neurons

Terminal branches of c3da neurons are highly actin enriched, which is the reason why we decided to concentrate our analysis of ARPs to the dynamics of these branchlets (Fig.2a). In da neurons FRAP analysis has been used to, for example, measure differences in cytoskeletal turnover in dendritic branchlets (Andersen, Li et al. 2005). In this case an immobile entire terminal branchlet was bleached and actin turnover was estimated to $t_{1/2} = 5$ minutes which is comparable to our data and bundled actin filaments in general (Andersen, Li et al. 2005). From the analysis in this project we can further conclude that actin retrograde flow in c3da neurons, first of all exists and that it is comparable to rates observed for neurons not containing the mammalian homologues of Twinstar, ADF/Cofilin (Flynn, Hellal et al. 2012). This suggests that extending TBs are resistant to Twinstar remodelling. Most importantly, however, the recovery of actin GFP signal at the tip of branchlets indicates that most barbed ends of f-actin are oriented towards the tip of the branchlet. This together with the previous EM data was the basis to hypothesise where ARPs might be placed according to their previously described biochemical function.

Comparative approach to dendrite dynamics

The three-dimensional structure and dynamics of actin within a dendritic branchlet are regulated by the coordinated action of specific subsets of ARPs. Here we were able to

demonstrate how a group of ARPs is responsible for the formation and characteristic dynamic steps of a specific type of branchlet, in the c3da neurons (Fig. 7).

Taking into account that previous work has demonstrated the arrest of actin blob propagation in *twinstar* RNAi, we place Twinstar at the prerequisite step of branch formation, sequestering actin filaments to boost the globular actin (g-actin) pool. Comparing our FRAP retrograde flow rates to the literature we suspect that *twinstar* is not required for the disassembly of actin within the small terminal branchlet of c3da neurons. We speculate that Spire might be the ARP that takes over the severing part in actin disassembly in a retracting branch. Keeping in mind that Spire by itself is a weak actin nucleator with WH2 nucleation activity attenuated by the FH2 domain (Quinlan, Hilgert et al. 2007), we deduce that all the properties independent of Capu should therefore be due to other properties of Spire. There have been suggestions that Spire could be sequestering four globular actin subunits with its four WASP-homology 2 (WH2) domains but this is the first time that *in vivo* data is supporting this hypothesis (Bosch, Le et al. 2007). Capu binds microtubules with high affinity, which in turn inhibits its actin nucleation activity (Rosales-Nieves, Johndrow et al. 2006, Roth-Johnson, Vizcarra et al. 2014). Microtubules are, however, never been seen protruding into small dendritic branches (Sturner, Tatarnikova et al. 2019). This would suggest that Capu and its interaction partner Spire would be sitting at the base of the dendritic branchlet for their nucleating function (Fig. 7c). Unfortunately, localisation of ARPs *in vivo* as demonstrated for the Arp2/3 complex or Singed in these neurons is not always feasible (Nagel, Delandre et al. 2012, Sturner, Tatarnikova et al. 2019). The additional effect of *arpc1* mutants on retracting and disappearing branches indicates that the branched actin meshwork at the base of a dendritic branch counteracts the depolymerisation of actin at the minus end (Fig. 7f). Whether this is due to a direct effect on actin treadmilling or an indirect effect by recruiting capping proteins or Twinstar we cannot assess with this data (Koestler, Steffen et al. 2013).

The loss of Singed leads to an overall increase in branch dynamics, suggesting that the conformational change of the filament is actually unfavourable for dynamics change. In the context of work demonstrating that Singed/Fascin can enhance Ena-mediated binding to barbed ends this gives a new hypothesis that could be probed in the c3da neurons (Bachmann, Fischer et al. 1999, Winkelmann, Bilancia et al. 2014). From our data we could imagine that, once Singed has bundled uni parallel f-actin, Ena binds in its tetramer

conformation bundling the barbed ends of f-actin. This could inhibit other factors from elongating the branchlet further but also inhibiting the branchlet from disappearing. How Ena could be regulating the dendritic branchlet in response to cues from for example Robo cannot be elucidated with this type of comparative approach. However, we could show that Ena is unlikely to be an elongation factor in the c3da neurons and that Ena seems to restrict branch formation and extension (Fig.4e, Fig. 5f). Singed share these defects in dynamics of the TBs (Fig. 4 increased newly forming and extending branches) and dendritic tree (Fig. 5 mean length, density of terminals, distance to nearest neighbour). If both are functioning as actin bundling factors this could be explained by stating that actin bundling not only restricts the dynamics of a branchlet but also hinders the formation of a TB.

The steps of branch dynamics (Formation, Extension, Stabilisation/Maturation, Retraction, and Disappearance) and the actin related functions of proteins have been well described in the past decade in different neurons and conditions and summarised to understand how they work together (Armijo-Weingart and Gallo 2017, Lanoue and Cooper 2019). The fact that every neuron class has characteristic dendrite morphologies however implicates that they also have different sets of ARPs that may differ in their function depending on one another. Here we compared and analysed a small set of ARPs and can already draw a first suggestion of how they might be causing the different characteristics of this neuron class.

The distinct morphology of c3da neurons model can be described with a combination of a minimum spanning tree and a growth model

How best to compare neuron structures is a fundamental question that requires computational tools to facilitate the analysis of large datasets (Li, Wang et al. 2017). Our data demonstrates that a thorough computational analysis can do more than just facilitate the quantification of a phenotype. It can help to trace back the function of a protein and elicit new insights into the contribution of several proteins together. General theories are getting close to understanding the dynamic growth process that forms classical space filling neurons, such as the dendrite morphology of c4da neurons (Nanda, Das et al. 2018, Baltruschat L. submitted 2018). Until now we were far from understanding the, at first sight, inefficient morphology of for example the c3da neurons.

The final results from the growth model of the c3da neurons will be discussed here.

Materials and Methods

Fly stains

Flies were reared on standard food in a 12 hr light-dark cycle at 25°C and 60% humidity unless otherwise indicated. The following strains were obtained from the Bloomington *Drosophila* Stock Centre: P(hsFLP)12, $y^1 w^*$; Arpc1^{Q25sd} P(neoFRT)40A/CyO (B#9137), P{UASp-Arpc1.GFP}1, w^* (B#26692), spir¹ cn¹ bw¹/CyO, l(2)DTS513¹ (B#5113), b¹ pr¹ spir^{2F} cn¹/CyO (B#8723), capu¹ cn¹ bw¹/CyO, l(2)DTS5131 (B#5094), capu^{EE} cn¹ bw¹/CyO (B#8788), sn³ (B#113), w^* ; P{FRT(w^{hs})}G13 ena²¹⁰/CyO (B#25404), w^* ; P{FRT(w^{hs})}G13 tsr^{N121}/CyO (B#9109), $y^1 w^*$; P{UAS-tsr.N}2.2.1/TM6B, P{Car20y}TPN1, Tb¹ (B#9235), $y^1 w^*$; P{w[+mC]=tubP-GAL80}LL10 P{ry[+t7.2]=neoFRT}40A/CyO (B#5192) and w^* ; the P{GawB}smid^{C161}/TM6B, Tb¹ (B#27893) (Shepherd and Smith 1996) was recombined with $y^1 w^*$; Pin^{Yt}/CyO; P{w^{+mC}=UAS-mCD8::GFP.L}LL6 (B#5130) on the third chromosome to make a stock expressing mCD8::GFP in c3da neurons. For the FRAP analyses w^* ; the P{GawB}smid^{C161}/TM6B, Tb¹ (B#27893) (Shepherd and Smith 1996) was recombined with UAS-mCD8-Cherry/ TM3 (kindly provided by Takashi Suzuki) and crossed to w^* ; P{UASp-GFP.Act5C}2-1 (B# 9258).

The M{UAS-spir. ORF.3xHA}ZH-86Fb (F001174) was obtained from FlyORF.

In addition, a pUAST (Brand and Perrimon 1993) containing a full-length capu construct with a mCherry fluorescent tag (Q24120, 1059 aa) was injected by BestGene (Chino Hills, CA, USA) to the 3rd Chromosome.

To generate MARCM clones the following line were obtained from the Kyoto Stock Centre: P{w[+m*]=GAL4}5-40 P{w[+mC]=UAS-Venus.pm}1 P{w[+mC]=SOP-FLP}42; P{w[+mC]=tubP-GAL80}LL10 P{ry[+t7.2]=neoFRT}40A / CyO (DGRC#109947), P{w[+m*]=GAL4}5-40 P{w[+mC]=UAS-Venus.pm}1 P{w[+mC]=SOP-FLP}42; P{w[+mW.hs]=FRT(w[hs])}G13 P{w[+mC]=tubP-GAL80}LL2 / CyO (DGRC#109948), w^* ; P{w[+mW.hs]=FRT(w[hs])}G13 (DGRC#106602).

Microscopy/Live imaging

The entire dendritic tree of *l*daB *c3da* neurons of the abdominal segment A5 of early third instar *Drosophila melanogaster* larvae were imaged with a LSM 780 Zeiss 40x oil objective, the software used was ZEN 2010. One neuron was imaged per animal, 8 animals per genotype. A time-lapse series over 30 minute every 30 seconds was taken of an anterior portion of the *l*daB neuron of early third instar larva with an Yokogawa Spinning-Disc on a Nikon stand (Andor, Oxford UK) with two back-illuminated EM-CCD cameras (Andor iXON DU-897) and a 60x oil objective. One neuron was imaged per animal, 10 animals per genotype.

FRAP experiments were performed with a LSM 800 Airyscan Microscope with a 63x/1.40 oil objective. A 488nm for GFP and 561nm for Cherry line of an Argon laser was used. The frame including the ROI (tip of a branchlet) was imaged three times before bleaching. The laser was set to 90% maximal power for bleaching and 2% maximal power for imaging. Photo-bleaching was achieved with 10 Iterations (scan speed at 3) of the region of interest. Imaging of the area was resumed immediately after photo-bleaching and continued every 30 s for at least ~300 s.

For all the above imaging the living larvae were covered in Halocarbon oil and immobilized between a coverslip and a glass slide. After imaging larvae were checked for vitality and set back on fly food, images taken from larvae that did not survive until hatching were excluded from the analysis.

FRAP analysis

A line analysis was conducted in the ImageJ software over time and space with a short macro that measures the intensity (I_{GFP} , I_{Cherry}) of each pixel of the two channels along the line over time. Moreover it tracks the extension of the branch along the line by comparing the intensity to an adjustable threshold (see Supplementary Script: Analysis_FRAP_macro). Background fluorescence intensities (I_{GFPbg} , I_{Cherrybg}) taken from a region outside the cell were subtracted from each individual region and frame. The values were normalized to the 3 pre-bleach values. Acquisition photo bleaching was determined by comparing the normalised mCherry signal (I_{nCherry}) in the bleached area over time, the area seems unaffected by experimental bleaching as there is even an increase in Cherry signal over time. In Figure 2 the normalised GFP Fluorescence ($I = (I_{\text{GFP}} - I_{\text{GFPbg}}) / I_{\text{N}}$) is visualised over time. Time point 0 (t_0) was defined at the first time point after photo bleaching (after 1:30 minutes) and the last time point as the t_{∞} . The average

halftime recovery was calculated $I_{1/2} = (I_{\infty} + I_0)/2$ and the time point closest was defined as $t_{1/2}$. The average retrograde movement of actin (M) was quantified by drawing a line at the distance the pixel below a 30% Intensity threshold had from the originally bleached area toward the main branch. There is a very slow retrograde movement of $M = 0,13 \mu\text{m}/\text{min}$ ($SD = 0.04$).

Dendritic arbour analysis

The image stacks were hand traced in 3D and analysed using the TREES toolbox (www.treestoolbox.org) (Cuntz, Forstner et al. 2010), an open source software package for MATLAB (Matworks, Natick, MA). Specifically for the c3da neurons we focussed on a set of 29 features that describe the morphological changes between groups.

Table of 28 features with description.

	Name	Description
1	Number of branches	Total number of terminal point indices in a tree. Equivalent to total number of branches.
2	Total length	Total cable length: sum of all length values of tree segments.
3	Mean branch length	Computes all the branch lengths of the tree and takes the mean.
4	Density 1	Number of terminal branches divided by the total length of main branches.
5	Mean distance to nearest neighbour	Computes the distance of a branch or terminal point to the closest branch or terminal point.
6	Mean tortuosity of terminals	Computes the tortuosity of the terminal segments of the tree. Tortuosity is defined as ration between path length and Euclidean length.
7	Mean Euclidean distance to root	The distance between all points of the tree and the root.
8	Mean branching angle	Returns the mean of the angle at each branching point in degree.
9	Total surface	Calculates the area of the tree from a 2D

3 Comparative computation analysis of actin-binding proteins in vivo unravels the single elements of dendrite dynamics

		Spanning field.
10	Total Volume	Returns the volume of all three segments in μm^3 .
11	Cable density	The total cable length divided by the surface area.
12	Number of branch points	Total number of branching point indices in a tree.
13	Maximal branch order	Calculate the maximum branch order value. Branch order values are applied to all nodes in a tree referring to the first node as the root of the tree. The values start at one and increase with each branch point.
14	Mean branch order	Calculate the mean branch order value.
15	Minimal branch order of terminals	Calculate the minimal branch order value for terminal branches.
16	Mean branch order of terminals	Calculate the mean branch order value for terminal branches.
17	Mean van pelt asymmetry index	Calculates the ratio of the sums of the daughter branches for each branching point and take the mean.
18	Density 2	Fraction of length of terminals/total length
19	Minimal branch length	Computes all the branch lengths of the tree and takes the minimum length.
20	Maximal branch length	Computes all the branch lengths of the tree and takes the maximal length.
21	Total length of terminals	The total cable length of all terminal points up to the first branching point.
22	Mean length of terminals	Computes all the cable length of all terminals up to the first branching point and takes the mean length.
23	Maximal length of terminals	Computes all the cable length of all terminals up to the first branching point and takes the maximum length.

3 Comparative computation analysis of actin-binding proteins in vivo unravels the single elements of dendrite dynamics

24	Maximal Euclidean distance to root	The maximum distance of a point on the tree and the root.
25	Mean Euclidean compactness	Euclidean distance to root/ (branch order+1)
26	Maximal path distance to root	Calculate the total path to the root of each node of a tree and takes the maximum.
27	Mean path distance to root	Calculate the total path to the root of each node of a tree and takes the mean.
28	Mean path compactness	Path distance to root/ (branch order+1)

Time-lapse analysis

The single images of the time series were traced every 5 minutes and registered using the `ui_tlbp_tree` script as described in (Baltruschat L. submitted 2018) tracking terminal and branch points. The `eval_timelapse` script categorizes the terminal branches into 5 groups: new branches that appear throughout the 30 minutes and disappearing branches, branches with are extending or retracting and branches that do not change in length within a certain threshold. Moreover it computes the velocity of branch movement, as the average distance covered by a terminal branch over time (see Supplementary Scripts: `Script_timelapse_analysis`).

Statistical analysis

Data were analysed using Prism 7.0 (GraphPad). Groups were compared using the Kruskal-Wallis test followed by Dunn's post hoc test accordingly. Single comparisons between two groups were analysed using the two tailed Wilcoxon Signed Rank Test. For multiple comparisons with several features for each group the p values were controlled for false discovery rate by the adaptive method of Benjamini, Krieger and Yekutieli with a Q% of 3 (Benjamini 2006) and controlled for statistical significance with the Holm-Sidak method (alpha of 0.05). The p values shown are all adjusted p values. (* is $p < 0.05$, ** is $p < 0.01$ and *** is $p < 0.001$).

Computational Model

Acknowledgements

We would like to acknowledge Prof. Dr. Eugen Kerkhoff for initial discussions on this project and for providing us the Capu full length rescue construct. We would like to thank the Bloomington Stock Centre and the Kyoto Stock Centre for fly stocks. We would like to acknowledge the microscope and image analysis facility at the DZNE in Bonn for the access to microscopes and support. Thank you especially to Manuel Schölling, from the Image and Data Analysis at DZNE, for helping with the FRAP Analysis. The Research was supported by the DFG (SPP1464).

Author contributions

T.S., H.C. and G.T. developed the project and designed the experiments. T.S. performed the experiments. H.C. developed the Trees Toolbox and the features. T.S., A.C. and H.C. developed the time-lapse analysis and the morphometric analysis for the c3da neurons. H.C. designed the growth model of the c4da and c3da neurons. T.S. wrote the manuscript.

Competing interests: The authors declare no competing financial interests.

References

- Abercrombie, M., J. E. Heaysman and S. M. Pegrum (1971). "The locomotion of fibroblasts in culture. IV. Electron microscopy of the leading lamella." *Exp Cell Res* **67**(2): 359-367.
- Andersen, R., Y. Li, M. Resseguie and J. E. Brenman (2005). "Calcium/calmodulin-dependent protein kinase II alters structural plasticity and cytoskeletal dynamics in *Drosophila*." *J Neurosci* **25**(39): 8878-8888.
- Armijo-Weingart, L. and G. Gallo (2017). "It takes a village to raise a branch: Cellular mechanisms of the initiation of axon collateral branches." *Mol Cell Neurosci* **84**: 36-47.
- Bachmann, C., L. Fischer, U. Walter and M. Reinhard (1999). "The EVH2 domain of the vasodilator-stimulated phosphoprotein mediates tetramerization, F-actin binding, and actin bundle formation." *J Biol Chem* **274**(33): 23549-23557.
- Baltruschat L., T. G., Cuntz H. (submitted 2018). "A developmental stretch-and-fill process that optimises dendritic wiring."
- Bashaw, G. J., T. Kidd, D. Murray, T. Pawson and C. S. Goodman (2000). "Repulsive axon guidance: Abelson and Enabled play opposing roles downstream of the roundabout receptor." *Cell* **101**(7): 703-715.
- Benjamini, Y., Krieger, A.M., & Yekutieli, D. (2006). "Adaptive linear step-up procedures that control the false discovery rate. 93." *Biometrika*. **(3)**: 491-507.
- Bird, A. D. and H. Cuntz (2019). "Dissecting Sholl Analysis into Its Functional Components." *Cell Rep* **27**(10): 3081-3096 e3085.
- Bosch, M., K. H. Le, B. Bugyi, J. J. Correia, L. Renault and M. F. Carlier (2007). "Analysis of the function of Spire in actin assembly and its synergy with formin and profilin." *Mol Cell* **28**(4): 555-568.
- Brand, A. H. and N. Perrimon (1993). "Targeted gene expression as a means of altering cell fates and generating dominant phenotypes." *Development* **118**(2): 401-415.
- Breitsprecher, D., A. K. Kieseewetter, J. Linkner, C. Urbanke, G. P. Resch, J. V. Small and J. Faix (2008). "Clustering of VASP actively drives processive, WH2 domain-mediated actin filament elongation." *EMBO J* **27**(22): 2943-2954.
- Cuntz, H., F. Forstner, A. Borst and M. Hausser (2010). "One rule to grow them all: a general theory of neuronal branching and its practical application." *PLoS Comput Biol* **6**(8).
- Dimitrova, S., A. Reissaus and G. Tavosanis (2008). "Slit and Robo regulate dendrite branching and elongation of space-filling neurons in *Drosophila*." *Dev Biol* **324**(1): 18-30.
- Faix, J. and K. Rottner (2006). "The making of filopodia." *Curr Opin Cell Biol* **18**(1): 18-25.
- Ferreira, T., Y. Ou, S. Li, E. Giniger and D. J. van Meyel (2014). "Dendrite architecture organized by transcriptional control of the F-actin nucleator Spire." *Development* **141**(3): 650-660.
- Flynn, K. C., F. Hellal, D. Neukirchen, S. Jacob, S. Tahirovic, S. Dupraz, S. Stern, B. K. Garvalov, C. Gurniak, A. E. Shaw, L. Meyn, R. Wedlich-Soldner, J. R. Bamberg, J. V. Small, W. Witke and F. Bradke (2012). "ADF/cofilin-mediated actin retrograde flow directs neurite formation in the developing brain." *Neuron* **76**(6): 1091-1107.
- Forsthoefel, D. J., E. C. Liebl, P. A. Kolodziej and M. A. Seeger (2005). "The Abelson tyrosine kinase, the Trio GEF and Enabled interact with the Netrin receptor Frazzled in *Drosophila*." *Development* **132**(8): 1983-1994.
- Gao, F. B., J. E. Brenman, L. Y. Jan and Y. N. Jan (1999). "Genes regulating dendritic outgrowth, branching, and routing in *Drosophila*." *Genes Dev* **13**(19): 2549-2561.
- Gates, M. A., R. Kannan and E. Giniger (2011). "A genome-wide analysis reveals that the *Drosophila* transcription factor Lola promotes axon growth in part by suppressing expression of the actin nucleation factor Spire." *Neural Dev* **6**: 37.
- Gertler, F. B., K. Niebuhr, M. Reinhard, J. Wehland and P. Soriano (1996). "Mena, a relative of VASP and *Drosophila* Enabled, is implicated in the control of microfilament dynamics." *Cell* **87**(2): 227-239.

3 Comparative computation analysis of actin-binding proteins in vivo unravels the single elements of dendrite dynamics

- Gillette, T. A. and G. A. Ascoli (2015). "Topological characterization of neuronal arbor morphology via sequence representation: I--motif analysis." *BMC Bioinformatics* **16**: 216.
- Grueber, W. B., L. Y. Jan and Y. N. Jan (2002). "Tiling of the Drosophila epidermis by multidendritic sensory neurons." *Development* **129**(12): 2867-2878.
- Gupton, S. L. and F. B. Gertler (2007). "Filopodia: the fingers that do the walking." *Sci STKE* **2007**(400): re5.
- Haralalka, S., C. Shelton, H. N. Cartwright, F. Guo, R. Trimble, R. P. Kumar and S. M. Abmayr (2014). "Live imaging provides new insights on dynamic F-actin filopodia and differential endocytosis during myoblast fusion in Drosophila." *PLoS One* **9**(12): e114126.
- Hatan, M., V. Shinder, D. Israeli, F. Schnorrer and T. Volk (2011). "The Drosophila blood brain barrier is maintained by GPCR-dependent dynamic actin structures." *J Cell Biol* **192**(2): 307-319.
- Hotulainen, P. and P. Lappalainen (2006). "Stress fibers are generated by two distinct actin assembly mechanisms in motile cells." *J Cell Biol* **173**(3): 383-394.
- Jan, Y. N. and L. Y. Jan (2010). "Branching out: mechanisms of dendritic arborization." *Nat Rev Neurosci* **11**(5): 316-328.
- Kiehart, D. P., C. G. Galbraith, K. A. Edwards, W. L. Rickoll and R. A. Montague (2000). "Multiple forces contribute to cell sheet morphogenesis for dorsal closure in Drosophila." *J Cell Biol* **149**(2): 471-490.
- Koestler, S. A., A. Steffen, M. Nemethova, M. Winterhoff, N. Luo, J. M. Holleboom, J. Krupp, S. Jacob, M. Vinzenz, F. Schur, K. Schluter, P. W. Gunning, C. Winkler, C. Schmeiser, J. Faix, T. E. Stradal, J. V. Small and K. Rottner (2013). "Arp2/3 complex is essential for actin network treadmilling as well as for targeting of capping protein and cofilin." *Mol Biol Cell* **24**(18): 2861-2875.
- Konietzny, A., J. Bar and M. Mikhaylova (2017). "Dendritic Actin Cytoskeleton: Structure, Functions, and Regulations." *Front Cell Neurosci* **11**: 147.
- Kovar, D. R., E. S. Harris, R. Mahaffy, H. N. Higgs and T. D. Pollard (2006). "Control of the assembly of ATP- and ADP-actin by formins and profilin." *Cell* **124**(2): 423-435.
- Lai, F. P., M. Szczodrak, J. Block, J. Faix, D. Breitsprecher, H. G. Mannherz, T. E. Stradal, G. A. Dunn, J. V. Small and K. Rottner (2008). "Arp2/3 complex interactions and actin network turnover in lamellipodia." *EMBO J* **27**(7): 982-992.
- Lanoue, V. and H. M. Cooper (2019). "Branching mechanisms shaping dendrite architecture." *Dev Biol* **451**(1): 16-24.
- Mullins, R. D., J. A. Heuser and T. D. Pollard (1998). "The interaction of Arp2/3 complex with actin: nucleation, high affinity pointed end capping, and formation of branching networks of filaments." *Proc Natl Acad Sci U S A* **95**(11): 6181-6186.
- Nagel, J., C. Delandre, Y. Zhang, F. Forstner, A. W. Moore and G. Tavosanis (2012). "Fascin controls neuronal class-specific dendrite arbor morphology." *Development* **139**(16): 2999-3009.
- Nanda, S., R. Das, S. Bhattacharjee, D. N. Cox and G. A. Ascoli (2018). "Morphological determinants of dendritic arborization neurons in Drosophila larva." *Brain Struct Funct* **223**(3): 1107-1120.
- Nithianandam, V. and C. T. Chien (2018). "Actin blobs prefigure dendrite branching sites." *J Cell Biol* **217**(10): 3731-3746.
- Pasic, L., T. Kotova and D. A. Schafer (2008). "Ena/VASP proteins capture actin filament barbed ends." *J Biol Chem* **283**(15): 9814-9819.
- Pruyne, D., M. Evangelista, C. Yang, E. Bi, S. Zigmund, A. Bretscher and C. Boone (2002). "Role of formins in actin assembly: nucleation and barbed-end association." *Science* **297**(5581): 612-615.
- Quinlan, M. E., S. Hilgert, A. Bedrossian, R. D. Mullins and E. Kerkhoff (2007). "Regulatory interactions between two actin nucleators, Spire and Cappuccino." *J Cell Biol* **179**(1): 117-128.
- Rosales-Nieves, A. E., J. E. Johndrow, L. C. Keller, C. R. Magie, D. M. Pinto-Santini and S. M. Parkhurst (2006). "Coordination of microtubule and microfilament dynamics by Drosophila Rho1, Spire and Cappuccino." *Nat Cell Biol* **8**(4): 367-376.

3 Comparative computation analysis of actin-binding proteins in vivo unravels the single elements of dendrite dynamics

Roth-Johnson, E. A., C. L. Vizcarra, J. S. Bois and M. E. Quinlan (2014). "Interaction between microtubules and the Drosophila formin Cappuccino and its effect on actin assembly." J Biol Chem **289**(7): 4395-4404.

Shepherd, D. and S. A. Smith (1996). "Central projections of persistent larval sensory neurons prefigure adult sensory pathways in the CNS of Drosophila." Development **122**(8): 2375-2384.

Smith, B. A., K. Daugherty-Clarke, B. L. Goode and J. Gelles (2013). "Pathway of actin filament branch formation by Arp2/3 complex revealed by single-molecule imaging." Proc Natl Acad Sci U S A **110**(4): 1285-1290.

Sturner, T., A. Tatarnikova, J. Mueller, B. Schaffran, H. Cuntz, Y. Zhang, M. Nemethova, S. Bogdan, V. Small and G. Tavosanis (2019). "Transient localization of the Arp2/3 complex initiates neuronal dendrite branching in vivo." Development **146**(7).

Vignjevic, D., S. Kojima, Y. Aratyn, O. Danciu, T. Svitkina and G. G. Borisy (2006). "Role of fascin in filopodial protrusion." J Cell Biol **174**(6): 863-875.

Vormberg, A., F. Effenberger, J. Muellerleile and H. Cuntz (2017). "Universal features of dendrites through centripetal branch ordering." PLoS Comput Biol **13**(7): e1005615.

Wang, Y. L. (1985). "Exchange of actin subunits at the leading edge of living fibroblasts: possible role of treadmilling." J Cell Biol **101**(2): 597-602.

Wills, Z., J. Bateman, C. A. Korey, A. Comer and D. Van Vactor (1999). "The tyrosine kinase Abl and its substrate enabled collaborate with the receptor phosphatase Dlar to control motor axon guidance." Neuron **22**(2): 301-312.

Winkelman, J. D., C. G. Bilancia, M. Peifer and D. R. Kovar (2014). "Ena/VASP Enabled is a highly processive actin polymerase tailored to self-assemble parallel-bundled F-actin networks with Fascin." Proc Natl Acad Sci U S A **111**(11): 4121-4126.

Yan, Z., W. Zhang, Y. He, D. Gorczyca, Y. Xiang, L. E. Cheng, S. Meltzer, L. Y. Jan and Y. N. Jan (2013). "Drosophila NOMPC is a mechanotransduction channel subunit for gentle-touch sensation." Nature **493**(7431): 221-225.

Zhang, M., X. Li, H. Zheng, X. Wen, S. Chen, J. Ye, S. Tang, F. Yao, Y. Li and Z. Yan (2018). "Brv1 Is Required for Drosophila Larvae to Sense Gentle Touch." Cell Rep **23**(1): 23-31.

Supplementary

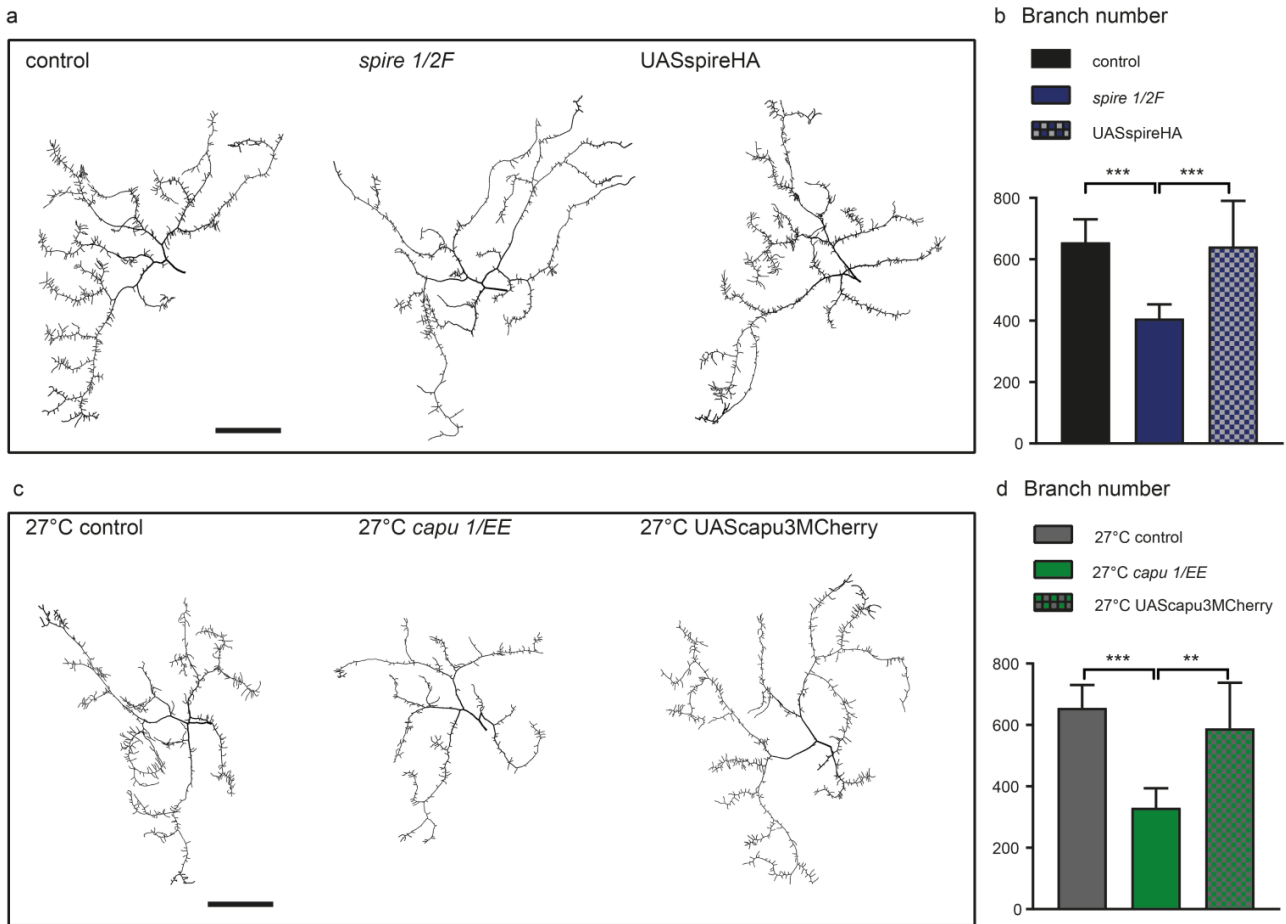
Supplementary Methods

Additional mutants or RNAi lines of actin regulatory proteins looked at in this study but not included as there was no phenotype seen in c3da neurons.

Mutant or RNAi target	Stock Number	Genotype
<i>dia</i> ⁵	B#9138	w*; <i>dia</i> ⁵ P{neoFRT}40A/CyO
<i>twf</i> ¹¹⁰	B#34540	w*; <i>twf</i> ¹¹⁰ /TM&B,Tb ¹
<i>chic</i> ⁰¹³²⁰	B#4892	<i>chic</i> ²²¹ <i>cn</i> ¹ /CyO; <i>ry</i> ⁵⁰⁶
Chic	VDRC#102759	Construct ID112358
Formin3	VDRC#107473	Construct ID110697
Formin3	VDRC#42302	Construct ID14823
dDAAM	VDRC#103921	Construct ID102786
dDAAM	VDRC#24885	Construct ID8382
Dia	VDRC#103941	Construct ID101745
Dia	VDRC#20518	Construct ID9442
Twinfilin	VDRC#25817	Construct ID10342
Twinfilin	VDRC#25817	Construct ID10342
Cheerio	VDRC#107451	Construct ID107518

Supplementary Figures

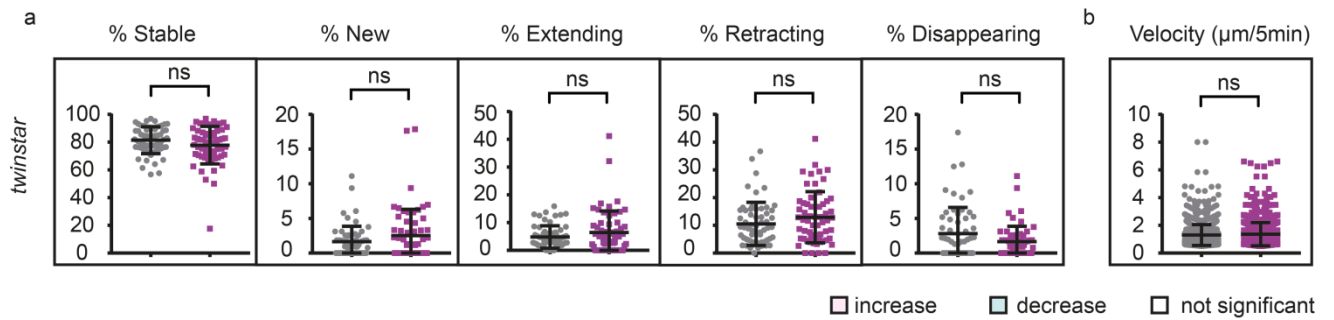
Supplementary Figure 1



Supplementary Fig. 1 Spire and Capu Rescue. a) Representative tracing of *C161G4UASmCD8GFP/+*, *C161G4UASmCD8GFP/+;spir¹/spir^{2F}* and *C161G4UASmCD8GFP/UASspireHA;spir¹/spir^{2F}*. b) Quantification of total branch number of the different groups with controls. c) Representative tracing of *C161G4UASmCD8GFP/+*, *C161G4UASmCD8GFP/+;capu¹/capu^{EE}*; *C161G4UASmCD8GFP/UAScapu3MCherry;capu¹/capu^{EE}* raised at 27°C. d) Quantification of total branch number of the different groups with controls. (* is $p < 0.05$, ** is $p < 0.01$ and *** is $p < 0.001$). Scale bar is 100 μm .

3 Comparative computation analysis of actin-binding proteins in vivo unravels the single elements of dendrite dynamics

Supplementary Figure 2



Supplementary Fig. 2 Branch dynamics of *twinstar* mutants close to the soma.

Branch dynamics measured in an area of the *twinstar* mutant dendritic tree that had the most TBs. a) The percentage of terminal branches that is stable, new, extending, retracting or disappearing within 30 minutes of time-lapse for each mutant versus corresponding control (grey/black). The average velocity of a terminal branch, quantified as the average change in length (extension + retraction) in µm per 5 minute. The corrected p values are represented as stars (ns is $p > 0.05$, * is $p < 0.05$, ** is $p < 0.01$ and *** is $p < 0.001$). All the branch dynamics measure are not significant compared to control.

3 Comparative computation analysis of actin-binding proteins in vivo unravels the single elements of dendrite dynamics

Supplementary Scripts

Analysis_FRAP_macro

```
INTENSITY_THRESHOLD = 10020;
FRAP_CHANNEL = 2;
j = 0;
run("Clear Results");

end = 0;

getDimensions(width, height, channels, slices, frames);
for(t = 0; t < frames; t++) {
    Stack.setFrame(t + 1);
    for(c = 0; c < channels; c++) {
        Stack.setChannel(c + 1);
        profile = getProfile();

        if (c+1 != FRAP_CHANNEL) {
            old_end = end;
            for (end = profile.length - 1; end > old_end; end--) {
                if (profile[end] > INTENSITY_THRESHOLD) {
                    break;
                }
            }
        }

        grewed_intensity = 0;
        for (i = old_end; i < end; i++) {
            grewed_intensity += profile[i] / (end - old_end);
        }

        for (i = 0; i < profile.length; i++) {
            setResult("Time", j, t + 1);
            setResult("Channel", j, c + 1);
            setResult("Distance", j, i);
            setResult("Value", j, profile[i]);
            setResult("Growth", j, end - old_end);
            setResult("GrowthIntensity", j, grewed_intensity);
            j + = 1;
        }
    }
}
updateResults();
```


3 Comparative computation analysis of actin-binding proteins in vivo unravels the single elements of dendrite dynamics

Scripts_static_features

```
% FEATURES_TREE Computes a feature vector for a tree.
% (trees package)
%
% feat = features_tree (intree, options)
% -----
%
% Computes a vector of features of a given tree.
%
% Input
% -----
% - intree    ::integer: index of tree in trees or structured tree
% - options   ::string:
%             {DEFAULT: ''}
%
% Output
% -----
% - feat     :: vector of computed tree features
%
% Example
% -----
% sample     = sample_tree;
% features_tree(sample)
%
% See also cluster_tree
% Uses ver_tree
%
% the TREES toolbox: edit, generate, visualise and analyse neuronal trees
% Copyright (C) 2009 - 2016 Hermann Cuntz

function [feat, varargout] = features_tree (intree, options)

% trees : contains the tree structures in the trees package
global trees

ver_tree (intree); % verify that input tree is a tree structure

% use full tree for this function
if ~isstruct (intree)
    tree = trees{intree};
else
    tree = intree;
end

if (nargin < 2) || isempty (options)
    % {DEFAULT: ''}
    options = '';
end

feature_names = {};
feature_names_short = {};
feature_values = {};

function add_feature(type, short, name, value)
    if numel(strfind(options, strcat('-x', type))) > 0
        return;
    end
    feature_names_short(end + 1) = short;
    feature_names{end + 1} = name;
    feature_values{end + 1} = value;
end

%% topological measures

% branch and terminal point indices
bidx = find(B_tree(tree));
tidx = find(T_tree(tree));
btidx = find(T_tree(tree) | B_tree(tree));

% number of branch points (size of tree)
add_feature('tot', 'nB', 'number of branch points', numel(bidx));
% number of terminal points (number of branches)
add_feature('tot', 'nT', 'number of terminal points', numel(tidx));
```

3 Comparative computation analysis of actin-binding proteins in vivo unravels the single elements of dendrite dynamics

```

% branch order
bo = BO_tree(tree);
add_feature('max', 'maxBO', 'maximal branch order', nanmax(bo));
add_feature('mean', 'meanBO', 'mean branch order', nanmean(bo(btidx)));
add_feature('std', 'stdBO', 'std of branch order', nanstd(bo(btidx)));
add_feature('min', 'minBOT', 'min branch order of terminals', nanmin(bo(tidx)));
add_feature('mean', 'meanBOT', 'mean branch order of terminals', nanmean(bo(tidx)));
add_feature('std', 'stdBOT', 'std of branch order of terminals', nanstd(bo(tidx)));

% asymmetry
asym_vp = asym_tree(tree, [], '-vp');
add_feature('mean', 'mA', 'mean van Pelt asymmetry index', nanmean(asym_vp));
add_feature('std', 'stdA', 'std of van Pelt asymmetry index over subtrees',
nanstd(asym_vp));

%% geometrical measures

% total cable length
totl = sum(len_tree(tree));
add_feature('tot', 'totL', 'total length', totl);

% diameter
if numel(strfind(options, '-xD')) == 0
    if isfield(tree, 'D')
        add_feature('mean', 'meanD', 'mean diameter', nanmean(tree.D));
        add_feature('std', 'stdD', 'std of diameter', nanstd(tree.D));
        ratio = ratio_tree(tree, tree.D);
        bratio = ratio(find(B_tree(tree)));
        add_feature('mean', 'meanTap', 'mean tapering ratio at branch points',
nanmean(bratio));
        add_feature('std', 'stdTap', 'std of tapering ratio at branch points',
nanstd(bratio));
        surf = surf_tree(tree);
        add_feature('tot', 'totS', 'total surface', nansum(surf));
        add_feature('tot', 'totV', 'total volume', nansum(vol_tree(tree)));
        % TODO mean / std surface + volume per branch
    else
        add_feature('mean', 'meanD', 'mean diameter', nan);
        add_feature('std', 'stdD', 'std of diameter', nan);
        add_feature('mean', 'meanTap', 'mean tapering ratio at branch points', nan);
        add_feature('std', 'stdTap', 'std of tapering ratio at branch points', nan);
        add_feature('tot', 'totS', 'total surface', nan);
        add_feature('abs', 'totV', 'total volume', nan);
    end
end

% volume
[~, cvol] = convhull(tree.X, tree.Y, tree.Z);
% WHATS THIS?
[~, ~, ~, vol] = v hull_tree(tree, [], [], [], [], ' ');
%cvol = sum(vol);
%add_feature('tot', 'volConvH', 'volume of convex hull', cvol);

% density
%add_feature('tot', 'dens', 'density (volume of convex hull / total path length)', cvol /
totl);

% nearest neighbour
X = [tree.X(btidx) tree.Y(btidx) tree.Z(btidx)];
if strfind(options, '-NN3')
    maxnn = 3;
else
    maxnn = 1;
end
nndists = zeros(numel(btidx), maxnn);
for i=1:numel(btidx)
    Xp = repmat(X(i, :), [numel(btidx) 1]);
    [ldists, perm] = sort(sum((X - Xp) .^ 2, 2));
    if numel(ldists) < 2
        continue;
    end
    nndists(i, :) = ldists(2:min(numel(ldists), maxnn + 1));
end

% density
add_feature('mean', 'meanNNdist', 'mean distance to nearest neighbor', nanmean(nndists(:,
1)));

```

3 Comparative computation analysis of actin-binding proteins in vivo unravels the single elements of dendrite dynamics

```

add_feature('std', 'stdNNDist', 'std distance to nearest neighbor', nanstd(nndists(:,
1)));

if strfind(options, '-NN3')
    add_feature('mean', 'mean3NNDist', 'mean distance to 3 nearest neighbors',
nanmean(nndists(:, 3)));
    add_feature('std', 'std3NNDist', 'std distance to 3 nearest neighbors',
nanstd(nndists(:, 3)));
end

% branch lengths
blens = blen_tree(tree);
add_feature('min', 'minBL', 'minimal branch length', nanmin(blens));
add_feature('mean', 'meanBL', 'mean branch length', nanmean(blens));
add_feature('std', 'stdBL', 'std of branch length', nanstd(blens));
add_feature('max', 'maxBL', 'max branch length', nanmax(blens));

terminals = T_tree(tree);
sect = dissect_tree(tree);
terminalb = [];
for i=1:size(blens, 1)
    if terminals(sect(i, 2))
        terminalb = [terminalb i];
    end
end
lts = blens(terminalb);
totlt = nansum(lts);
add_feature('tot', 'totLt', 'total length of terminals', totlt);
add_feature('mean', 'meanLt', 'mean length of terminals', nanmean(lts));
add_feature('std', 'stdLt', 'std of length of terminals', nanstd(lts));
add_feature('max', 'maxLt', 'maximal length of terminals', nanmax(lts));
add_feature('tot', 'fracLt', 'fraction of length of terminals / total length', totlt /
totl);
add_feature('tot', 'totTerm', 'total number of terminals', sum(terminals));
add_feature('denst', 'densTerm', 'density of terminals', sum(terminals)/(totl-totlt));

% euclidean distance
etree = eucl_tree(tree);

add_feature('max', 'maxDistEuc', 'maximal euclidean distance to root', nanmax(etree));
add_feature('mean', 'meanDistEuc', 'mean euclidean distance to root',
nanmean(etree(btidx)));
add_feature('std', 'stdDistEuc', 'std of euclidean distance to root',
nanstd(etree(btidx)));

compeuc = etree(btidx) ./ (bo(btidx) + 1);
add_feature('mean', 'meanCompactEuc', 'mean euclidean compactness (euclidean distance to
root / (branch order + 1))', nanmean(compeuc))
add_feature('std', 'stdCompactEuc', 'std of euclidean compactness', nanstd(compeuc))

ptree = Pvec_tree(tree);
add_feature('max', 'maxDistPatrh', 'maximal path distance to root', nanmax(ptree));
add_feature('mean', 'meanDistPath', 'mean path distance to root', nanmean(ptree(btidx)));
add_feature('std', 'stdDistPath', 'std of path distance to root', nanstd(ptree(btidx)));

comppath = ptree(btidx) ./ (bo(btidx) + 1);
add_feature('mean', 'meanCompactPath', 'mean path compactness (path length to root /
(branch order + 1))', nanmean(comppath))
add_feature('std', 'stdCompactPath', 'std of path compactness', nanstd(comppath))

% turtuosity
if sum(T_tree(tree)) == 1
    turt = NaN;
else
    turt = turt_tp_tree(tree);
end
add_feature('mean', 'meanT', 'mean turtuosity', nanmean(turt));
add_feature('std', 'stdT', 'std of turtuosity', nanstd(turt));

% branching angles
angles = angleB_tree(tree);
angles = rad2deg(angles);
bangles = angles(bidx);
add_feature('mean', 'meanBA', 'mean branching angle', nanmean(bangles));
add_feature('std', 'stdBA', 'std of branching angle', nanstd(bangles));

```

3 Comparative computation analysis of actin-binding proteins in vivo unravels the single elements of dendrite dynamics

```
% surface
surface = bwarea(span_tree(tree));
add_feature('sur', 'surf', 'surface', surface);

%cable density
add_feature('den', 'dens', 'density', totl/surface);

%%

feat = cell2mat(feature_values);
if numel(strfind(options, '-n')) > 0 && numel(strfind(options, '-l')) > 0
    varargout{1} = feature_names_short;
    varargout{2} = feature_names;
else
    if strfind(options, '-n')
        varargout{1} = feature_names_short;
    end
    if strfind(options, '-l')
        varargout{1} = feature_names;
    end
end
end

%Static Images Features
clear;
C161_control_static_voxel = load_tree('./RAW/DA_C161_control_sep.mtr');
C161_capu_static_voxel = load_tree('./RAW/DA_C161_capu_sep.mtr');
C161_spire_static_voxel = load_tree('./RAW/DA_C161_spire_sep.mtr');
C161_singed_static_voxel = load_tree('./RAW/DA_C161_singed_sep.mtr');
MARCM_40A_control_static_voxel = load_tree('./RAW/DAMARCM_40A_control_sep.mtr');
MARCM_G18_control_static_voxel = load_tree('./RAW/DAMARCM_G18_control_sep.mtr');
MARCM_40A_Arpcl_static_voxel = load_tree('./RAW/DAMARCM_40A_arpcl_sep.mtr');
MARCM_G18_ena_static_voxel = load_tree('./RAW/DAMARCM_G18_ena_sep.mtr');
MARCM_G18_twinstar_static_voxel = load_tree('./RAW/DAMARCM_G18_twinstar_sep.mtr');

%%
%C161 Control
features_C161_control = [];

for i=1:size(C161_control_static_voxel,2)
    [f, names_long] = features_c3_tree_07_08_19(C161_control_static_voxel{i}, '-r -cell -long -2d');
    features_C161_control = [features_C161_control; f];
    display([i])
end
%%
%C161 capu
features_C161_capu = [];

for i=1:size(C161_capu_static_voxel,2)
    [f, names_long] = features_c3_tree_07_08_19(C161_capu_static_voxel{i}, '-r -cell -long -2d');
    features_C161_capu = [features_C161_capu; f];
    display([i])
end
%%
%C161 spire
features_C161_spire = [];

for i=1:size(C161_spire_static_voxel,2)
    [f, names_long] = features_c3_tree_07_08_19(C161_spire_static_voxel{i}, '-r -cell -long -2d');
    features_C161_spire = [features_C161_spire; f];
    display([i])
end
%%
%C161 singed
features_C161_singed = [];

for i=1:size(C161_singed_static_voxel,2)
    [f, names_long] = features_c3_tree_07_08_19(C161_singed_static_voxel{i}, '-r -cell -long -2d');
    features_C161_singed = [features_C161_singed; f];
    display([i])
end
```

3 Comparative computation analysis of actin-binding proteins in vivo unravels the single elements of dendrite dynamics

```
end
%%
%%MARCM 40A Control
features_MARCM_40A_control = [];

for i=1:size(MARCM_40A_control_static_voxel,2)
[f, names_long] = features_c3_tree_07_08_19(MARCM_40A_control_static_voxel{i}, '-r -cell -long -2d');
features_MARCM_40A_control = [features_MARCM_40A_control; f];
display([i])
end
%%
%%MARCM 40A Arpc1
features_MARCM_40A_Arpc1 = [];

for i=1:size(MARCM_40A_Arpc1_static_voxel,2)
[f, names_long] = features_c3_tree_07_08_19(MARCM_40A_Arpc1_static_voxel{i}, '-r -cell -long -2d');
features_MARCM_40A_Arpc1 = [features_MARCM_40A_Arpc1; f];
display([i])
end
%%
%%MARCM G18 Control
features_MARCM_G18_control = [];

for i=1:size(MARCM_G18_control_static_voxel,2)
[f, names_long] = features_c3_tree_07_08_19(MARCM_G18_control_static_voxel{i}, '-r -cell -long -2d');
features_MARCM_G18_control = [features_MARCM_G18_control; f];
display([i])
end
%%
%%MARCM G18 Ena
features_MARCM_G18_Ena = [];

for i=1:size(MARCM_G18_ena_static_voxel ,2)
[f, names_long] = features_c3_tree_07_08_19(MARCM_G18_ena_static_voxel {i}, '-r -cell -long -2d');
features_MARCM_G18_Ena = [features_MARCM_G18_Ena; f];
display([i])
end
%%
%%MARCM G18 Twinstar
features_MARCM_G18_Twinstar = [];

for i=1:size(MARCM_G18_twinstar_static_voxel ,2)
[f, names_long] = features_c3_tree_07_08_19(MARCM_G18_twinstar_static_voxel {i}, '-r -cell -long -2d');
features_MARCM_G18_Twinstar = [features_MARCM_G18_Twinstar; f];
display([i])
end

%% %% Remove Correlated variables
%%
%% %% Pair-wise Anova Control - Capu
%%
%% control_capu_stat = zeros(1,size(features_capu,2));
%%
%% for i = 1:length(features_capu)
%%
%%     h = ttest(features_control(:,i),features_capu(:,i));
%%     control_capu_stat(i) = h;
%%
%% end
%%
%% %% Pair-wise Anova Control - spire
%%
%% control_spire_stat = zeros(1,size(features_spire,2));
%%
%% for i = 1:length(features_spire)
%%
%%     h = ttest(features_control(:,i),features_spire(:,i));
%%     control_spire_stat(i) = h;
%%
%% end
%%
```

3 Comparative computation analysis of actin-binding proteins in vivo unravels the single elements of dendrite dynamics

```
%% Pair-wise Anova Control - singed
%
% control_singed_stat = zeros(1,size(features_singed,2));
%
% for i = 1:length(features_singed)
%
%     h = ttest(features_control(:,i),features_singed(:,i));
%     control_singed_stat(i) = h;
%
% end
%
% %%
%
```

3 Comparative computation analysis of actin-binding proteins in vivo unravels the single elements of dendrite dynamics

Script_timelapse_analysis

```
%time lapse analysis terminal branches
%Andre castro 19/10/2017
%Tomke - Actin Regulatory Proteins, example Capu

%%
folder_list = {'\\fileserver.dzne.de\stuernert\Images\Tracings\Time Lapse quantification
Tomke\timelapse_C161_control\1 traced good',...
 '\\fileserver.dzne.de\stuernert\Images\Tracings\Time Lapse quantification
Tomke\timelapse_C161_control\2 traced',...
 '\\fileserver.dzne.de\stuernert\Images\Tracings\Time Lapse quantification
Tomke\timelapse_C161_control\3 traced',...
 '\\fileserver.dzne.de\stuernert\Images\Tracings\Time Lapse quantification
Tomke\timelapse_C161_control\4 traced',...
 '\\fileserver.dzne.de\stuernert\Images\Tracings\Time Lapse quantification
Tomke\timelapse_C161_control\5 traced',...
 '\\fileserver.dzne.de\stuernert\Images\Tracings\Time Lapse quantification
Tomke\timelapse_C161_control\6 traced',...
 '\\fileserver.dzne.de\stuernert\Images\Tracings\Time Lapse quantification
Tomke\timelapse_C161_control\7 traced',...
 '\\fileserver.dzne.de\stuernert\Images\Tracings\Time Lapse quantification
Tomke\timelapse_C161_control\8 traced',...
 '\\fileserver.dzne.de\stuernert\Images\Tracings\Time Lapse quantification
Tomke\timelapse_C161_control\9 traced',...
 '\\fileserver.dzne.de\stuernert\Images\Tracings\Time Lapse quantification
Tomke\timelapse_C161_control\10 traced'};

%%
for ni = 1: length(folder_list)
    pathname = folder_list{ni};
    fprintf('Tree number') ; disp(ni);
    cd( pathname);

    clearvars -except folder_list ni

load dTL;
TL = load_tree ('TL.mtr');
TL = TL{1,1}{1,1};
pTL = pTL{1,1}{1,1};
tic

Ti = []; % all rows in pTL that are terminal nodes
iBi = []; % rows in pTL that are branch points nodes
T_length = []; % total length of the tree

%%
for counterTL=1:size(TL,2)

    len = [];
    len = sum(len_tree(TL{counterTL}));
    T_length = [T_length; len];
    T1 = T_tree (TL{counterTL}); % terminal nodes of the tree
    B1 = B_tree (TL{counterTL}); % branch points nodes of the tree
    pTL1 = [];
    pTL1 = pTL (:, counterTL);

    % flag for incomplete registrations
    display([counterTL])

    BTnodes = sum(T_tree(TL{counterTL})) + sum(B_tree(TL{counterTL}));
    BTvector = [find(T1); find(B1)];

    if B1(1,1)==1 || T1(1,1)==1

        if length(pTL1(~isnan(pTL1))) ~= BTnodes ;
            warning('Registration INCOMPLETE!');

            for counter1=1:BTnodes % print non registered nodes
```

3 Comparative computation analysis of actin-binding proteins in vivo unravels the single elements of dendrite dynamics

```

        if isempty(find(BTvector(counter1,1) == pTL1)) == 1
            display([counter1 BTvector(counter1)])
        end

    end

else
    sprintf('registration complete')
end

else %if the root is branch point or a terminal point

    if length(pTL1(~isnan(pTL1))) ~= BTnodes + 1 ;
        warning('Registration INCOMPLETE 1!');

        for counter1=1:BTnodes % print non registered nodes

            if isempty(find(BTvector(counter1,1) == pTL1(2:end,1))) == 1
                display([counter1 BTvector(counter1)])
            end

        end

    else
        sprintf('registration complete 1')
    end

end

T1 = [0 ; T1];
B1 = [0 ; B1];

pTL1 (isnan(pTL1)) = 0;
pTL1 = pTL1 + 1;
T1 = pTL (logical (T1 (pTL1)), :); % rows in pTL that are terminal nodes in time point
= counterTL
Br1 = pTL (logical (B1 (pTL1)), :); % rows in pTL that are branch points nodes in time
point = counterTL

ipar = ipar_tree (TL{counterTL});
ipar = ipar + 1;
iparT1 = ipar (T1 (:,counterTL), :); % paths to root from time point = TL
iparB = B1 (iparT1); % branching points in the paths
cB = cumsum (iparB, 2);
cB (cB>0) = 1;
iB = sum (~cB, 2) +1; % numero de nos antes to primeiro branching point a contar do
Terminal Branch
iB1 = iparT1 (sub2ind (size (iparT1), (1:size (iparT1, 1))', iB)) - 1; % branching point
before each terminal branch

Brows = []; % rows in pTL that are branch points nodes for each time point
dummy = [];

for i=1:length(iB1)
    for ii=1:length(Br1)

        if Br1(ii,counterTL)==iB1(i);
            dummy = Br1(ii,:);
            Brows = [Brows;dummy];
        else
            continue
        end
    end
end

Ti = [Ti;T1];
iBi = [iBi;Brows];

Ti(isnan(Ti)) = 0;
iBi(isnan(iBi)) = 0;

```


3 Comparative computation analysis of actin-binding proteins in vivo unravels the single elements of dendrite dynamics

```

end

%% Terminal nodes and branch points throughout all time points
[Ti,iold,inew] = unique(Ti,'rows','stable');

bp_row=[]; % non repeated rows in pTL that are branch points nodes

for i=1:length(iold)

    dummy = iBi(iold(i),:);
    bp_row = [bp_row; dummy];

end

%%%%%%%%%%%%%%%%%%%%%%%%%%%%%%%%%%%%%%%%%%%%%%%%%%%%%%%%%%%%%%%%%%%%%%%%
%%%%%%%%%%%%%%%%%%%%%%%%%%%%%%%%%%%%%%%%%%%%%%%%%%%%%%%%%%%%%%%%%%%%%%%%

%% Compute terminal branches lengths

TB1 = zeros(size(Ti,1),size(Ti,2)); %Terminal branches lengths
Bpl = zeros(size(Ti,1),size(Ti,2)); %Branch Points before TP
TBp = zeros(size(Ti,1),size(Ti,2)); %Terminal Points after TB

for counter1=1:size(Ti,2)
    for counter2=1:size(Ti,1)

        pvec = Pvec_tree(TL{counter1});
        if Ti(counter2,counter1) > 0 && bp_row(counter2,counter1)> 0

            tbl = Ti(counter2,counter1);close
            bpl = bp_row(counter2,counter1);

            TB1(counter2,counter1)= pvec(tbl) - pvec(bpl);
            Bpl(counter2,counter1)= bpl; % for plotting
            TBp(counter2,counter1)= tbl; % for plotting

        elseif Ti(counter2,counter1) > 0 && bp_row(counter2,counter1)== 0

            counter_previous = find(bp_row(1:counter2,counter1),1,'last'); % in case a
            TP disappears and it shared a BP

            % with another TP, the remaining TP gets attached
            tbl = Ti(counter2,counter1);
            % with the next BP in the path
            bpl = bp_row(counter_previous,counter1);

            TB1(counter2,counter1)= pvec(tbl) - pvec(bpl);
            Bpl(counter2,counter1)= bpl; % for plotting
            TBp(counter2,counter1)= tbl; % for plotting

        else
            continue
        end

    end
end

% flag for dupliclate registrations %inf values negative values or NaN

for counter1=1:size(TB1,2)
    for counter2=1:size(TB1,1)

        if TB1(counter2,counter1) < 0 || isnan(TB1(counter2,counter1))==1 ||
        isinf(TB1(counter2,counter1))==1

            warning('Registration Duplicates!');
            display([counter2 counter1])

        end

    end

end
end

```

3 Comparative computation analysis of actin-binding proteins in vivo unravels the single elements of dendrite dynamics

```

%% Plot Terminal Branches and Branch Points pairs on the Trees

figure; hold on;
for counterTL = 1: length(TL)

plot_tree (TL{counterTL}, [], [], [], [], '-3l');

for counter = 1 : length (TBp)

    R = rand (1, 3);

    if Bpl (counter,counterTL) == 0 || TBp(counter,counterTL) == 0 ;
        continue
    else
        hp = plot (TL{counterTL}.X (Bpl (counter,counterTL)), TL{counterTL}.Y
(Bpl(counter,counterTL)), 'k. ');
        set (hp, 'markersize', 12, 'color', R);
        hp = plot (TL{counterTL}.X (TBp (counter, counterTL)), TL{counterTL}.Y
(TBp(counter,counterTL)), 'k. ');
        set (hp, 'markersize', 12, 'color', R);

    end

end

end

%% Threshold Artifact (0.5 um)
for counter=1:size(TB1,1)
    for counter2=1:size(TB1,2)-1

        present=TB1(counter,counter2+1);
        past=TB1(counter,counter2);

        if -0.5 <= present - past && present - past<= 0.5 && present > 0 && past
> 0;

            TB1 (counter,counter2+1) = TB1 (counter,counter2);

        elseif -0.5 >= present - past && present > 0 && past > 0;

            TB1 (counter,counter2+1) = TB1 (counter,counter2+1);

        elseif -0.5 <= present - past && present - past<= 0.5 && present > 0 && past ==
0;

            TB1 (counter,counter2+1) = TB1 (counter,counter2+1);

        else
            continue
        end
    end
end

%% Calculate the mean branch length
mean_TB1 = nanmean(TB1);

%% Calculate the main stem length
stem_length = [];

for i = 1: size(TB1,2)
    stem = T_length(i) - sum(TB1(:,i));
    stem_length = [stem_length; stem];
end

%% Calculate Terminal branches growth rate

TBgr = zeros(size(TB1,1),size(TB1,2)-1);

for counter=1:size(TB1,1)
    for counter2=1:size(TB1,2)-1

```

3 Comparative computation analysis of actin-binding proteins in vivo unravels the single elements of dendrite dynamics

```

present=TB1(counter,counter2+1);
past=TB1(counter,counter2);

if present>0 && past>0;
    TBgr (counter,counter2) = (present-past)/past*100; % value for retracting
and
                                                % extending branches

elseif present>0 && past==0;
    TBgr (counter,counter2)= -101; % value for the newly forming branches

elseif present==0 && past>0;
    TBgr (counter,counter2)= -100; % value for the disappearing branches

else present==0 && past==0;
    TBgr (counter,counter2)= -102; % value for the non existing branches

end
end
end

%% Plot Retracting and Growing/New TB

nodes_retract = zeros(size(TB1));
nodes_ext      = zeros(size(TB1));
nodes_disap   = zeros(size(TB1));
nodes_new     = zeros(size(TB1));

for counter=1:size(TB1,1)
    for counter2=1:size(TB1,2)-1

        present = TB1(counter,counter2+1);
        past    = TB1(counter,counter2);

        if present - past > 0
            nodes_ext(counter,counter2+1) = Ti(counter,counter2+1);

        elseif present - past < 0 && present>0
            nodes_retract(counter,counter2+1) = Ti(counter,counter2+1);

        elseif past> 0 && present ==0
            nodes_disap(counter,counter2) = Ti(counter,counter2);

        elseif present == -101
            nodes_new(counter,counter2) = Ti(counter,counter2);

        else
            continue
        end

    end
end

figure; hold on;
for counterTL = 1: length(TL)

plot_tree (TL{counterTL}, [], [], [], [], '-3l');

Rec = [1 0 0];
Ext = [0 1 0];
Dis = [0 1 1];
New = [0 1 0];

% extending nodes
for counter = 1 : length (TBp)

```

3 Comparative computation analysis of actin-binding proteins in vivo unravels the single elements of dendrite dynamics

```

    if nodes_ext (counter,counterTL) == 0
        continue
    else
        hp = plot (TL{counterTL}.X (nodes_ext (counter, counterTL)),
TL{counterTL}.Y (nodes_ext(counter,counterTL)), 'k. ');
        set (hp, 'markersize', 14, 'color', Ext);
    end
end

% retracting nodes
for counter = 1 : length (TBp)

    if nodes_retract (counter,counterTL) == 0
        continue
    else
        hp = plot (TL{counterTL}.X (nodes_retract (counter,counterTL)),
TL{counterTL}.Y (nodes_retract (counter,counterTL)), 'k. ');
        set (hp, 'markersize', 14, 'color', Rec);
    end

end

% disappearing nodes
for counter = 1 : length (TBp)

    if nodes_disap (counter,counterTL) == 0
        continue
    else
        hp = plot (TL{counterTL}.X (nodes_disap (counter,counterTL)),
TL{counterTL}.Y (nodes_disap (counter,counterTL)), 'k. ');
        set (hp, 'markersize', 25, 'color', Dis);
    end

end

% new nodes
for counter = 1 : length (TBp)

    if nodes_new (counter,counterTL) == 0
        continue
    else
        hp = plot (TL{counterTL}.X (nodes_new (counter,counterTL)), TL{counterTL}.Y
(nodes_new (counter,counterTL)), 'k. ');
        set (hp, 'markersize', 25, 'color', New);
    end

end

end

%% Terminal Branches dynamics at each time point

RetractTB = zeros(size(TBgr));
ExtTB     = zeros(size(TBgr));
NewTB     = zeros(size(TBgr));
DisapTB   = zeros(size(TBgr));
StaticTB  = zeros(size(TBgr));

for counter=1:size(TBgr,2)
    for counter2=1:size(TBgr,1)

        if TBgr(counter2,counter) == -100
            DisapTB(counter2,counter) = TBgr(counter2,counter);
            continue
        end
    end
end

```

3 Comparative computation analysis of actin-binding proteins in vivo unravels the single elements of dendrite dynamics

```

elseif TBgr(counter2,counter) ==0;
    StaticTB(counter2,counter) = 1 ; % value for static branches
    continue

elseif TBgr(counter2,counter)< 0    &&    TBgr(counter2,counter)>-100 ;
    RetractTB(counter2,counter) = TBgr(counter2,counter) ;
    continue

elseif TBgr(counter2,counter)    ==    -101 ;
    NewTB(counter2,counter)    =    TBgr(counter2,counter) ;
    continue

elseif TBgr(counter2,counter)    >    0    ;
    ExtTB(counter2,counter)    =    TBgr(counter2,counter) ;

else    TBgr(counter2,counter) ==    -102 ;
    continue

end

end

end

%Absolute values

RetractTB    =    logical(RetractTB);
ExtTB        =    logical(ExtTB);
NewTB        =    logical(NewTB);
DisapTB      =    logical(DisapTB);
StaticTB     =    logical(StaticTB);

normRetractTB    =    zeros(1,size(TBgr,2));
normExtTB        =    zeros(1,size(TBgr,2));
normNewTB        =    zeros(1,size(TBgr,2));
normDisapTB      =    zeros(1,size(TBgr,2));
normStaticTB     =    zeros(1,size(TBgr,2));

for counter=1:size(TL,2)-1

    normRetractTB(1,counter)    =    sum(RetractTB(:,counter)) /sum(T_tree(TL{1,counter}));
    normExtTB(1,counter)        =    sum(ExtTB(:,counter))    /sum(T_tree(TL{1,counter}));
    normNewTB(1,counter)        =    sum(NewTB(:,counter))    /sum(T_tree(TL{1,counter}));
    normDisapTB(1,counter)      =    sum(DisapTB(:,counter))  /sum(T_tree(TL{1,counter}));
    normStaticTB(1,counter)     =    sum(StaticTB(:,counter)) /sum(T_tree(TL{1,counter}));

end

%% Traveled Distance

Traveldist = zeros(size(TBgr));

for counter=1:size(TB1,1)
    for counter2=1:size(TB1,2)-1

        present=TB1(counter,counter2+1);
        past=TB1(counter,counter2);

        Traveldist(counter,counter2) = abs(present- past);

    end
end

%% Traveled Distance Extension and Retraction Split

Traveldist_ext = zeros(size(TBgr));
Traveldist_ret = zeros(size(TBgr));

for counter=1:size(TB1,1)
    for counter2=1:size(TB1,2)-1

```

3 Comparative computation analysis of actin-binding proteins in vivo unravels the single elements of dendrite dynamics

```

present = TBl(counter,counter2+1);
past    = TBl(counter,counter2);

if      present - past > 0
    Traveledist_ext (counter,counter2) = abs(present- past);
elseif  present - past < 0 & present>0
    Traveledist_ret (counter,counter2) = abs(present- past);

else continue
end
end
end
end

%% Split terminal branches in Groups

static_TBl = []; % TB that never changes length
stable_TBl = []; % TB that never disappears and it is there since the first time point
new_TBl    = []; % TB that appears (it can disappear afterwards)
disap_TBl  = []; % TB that it is there from the initial time point but that later disappears
(it can later appear again)

for i=1:size(TBl,1)

    [row,col]=find(TBl(i, :));

    if      length(find(col))==size(TBl,2) && sum(abs(TBgr(i, :)))<=size(TBl,2);
        static_TBl=[static_TBl;TBl(i,:)];
        continue

    elseif length(find(col))==size(TBl,2);
        stable_TBl=[stable_TBl;TBl(i,:)];
        continue

    elseif TBl(i,1)==0 && length(find(col))<size(TBl,2);
        new_TBl=[new_TBl;TBl(i,:)];
        continue

    else TBl(row(1,1),col(1,1))>0 && length(find(col))<size(TBl,2);
        disap_TBl=[disap_TBl;TBl(i,:)];
        continue

    end

end

end

%% Removes "zeros", "100" and "-100" from TBgr and replace them with NaNs
TBgr(TBgr==102) = NaN;
TBgr(TBgr==100) = NaN;
TBgr(TBgr==101) = NaN;

%% Removes "zeros" from TBlLiL replace them with NaNs
TBl(TBl==0)= NaN;

%% Split dynamics for fitting

%New Branches
new_TBl_markov = [];

for i = 1:size(new_TBl,1)

    [row,col] = find(new_TBl(i,:),1);
    dummy = new_TBl (i,col);
    new_TBl_markov = [new_TBl_markov; dummy];
end

%Disappearing Branches
disap_TBl_markov = [];

```

3 Comparative computation analysis of actin-binding proteins in vivo unravels the single elements of dendrite dynamics

```

for i = 1:size(disap_TBl,1)

    [row,col] = find(disap_TBl(i,:),1,'last');
    dummy = disap_TBl (i,col);
    disap_TBl_markov = [disap_TBl_markov; dummy];
end

%Growing, Retracting and Static Dynamics

grow_TBl_markov      =[];
retract_TBl_markov  =[];
static_TBl_markov    =[];

for i = 1:size(TBl,2)-1
for ii = 1:size(TBl,2)

    if      isnan(TBgr (ii,i))
        continue

    elseif  TBgr (ii,i) < 0;
        dummy = [TBl(ii,i),TBgr(ii,i)];
        retract_TBl_markov    =[retract_TBl_markov; dummy];
        continue

    elseif  TBgr (ii,i) == 0 ;
        dummy = [TBl(ii,i),TBgr(ii,i)];
        static_TBl_markov     =[static_TBl_markov; dummy];
        continue

    else    TBgr (ii,i) > 0 ;
        dummy = [TBl(ii,i),TBgr(ii,i)];
        grow_TBl_markov      =[grow_TBl_markov; dummy];
        continue

    end

end
end
%% Save Workspace

filename = [ 'capu' num2str(ni) '.mat' ];
save(filename);
end

%%
%Append Different Time Points
clear all;
clear all;

folder_list = {'\\fileserv.dzne.de\stuernert\Images\Tracings\Time Lapse quantification
Tomke\timelapse_C161_control\1 traced good',...
'\\fileserv.dzne.de\stuernert\Images\Tracings\Time Lapse quantification
Tomke\timelapse_C161_control\2 traced',...
'\\fileserv.dzne.de\stuernert\Images\Tracings\Time Lapse quantification
Tomke\timelapse_C161_control\3 traced',...
'\\fileserv.dzne.de\stuernert\Images\Tracings\Time Lapse quantification
Tomke\timelapse_C161_control\4 traced',...
'\\fileserv.dzne.de\stuernert\Images\Tracings\Time Lapse quantification
Tomke\timelapse_C161_control\5 traced',...
'\\fileserv.dzne.de\stuernert\Images\Tracings\Time Lapse quantification
Tomke\timelapse_C161_control\6 traced',...
'\\fileserv.dzne.de\stuernert\Images\Tracings\Time Lapse quantification
Tomke\timelapse_C161_control\7 traced',...
'\\fileserv.dzne.de\stuernert\Images\Tracings\Time Lapse quantification
Tomke\timelapse_C161_control\8 traced',...
'\\fileserv.dzne.de\stuernert\Images\Tracings\Time Lapse quantification
Tomke\timelapse_C161_control\9 traced',...
'\\fileserv.dzne.de\stuernert\Images\Tracings\Time Lapse quantification
Tomke\timelapse_C161_control\10 traced'};

stem_length_control=[];
TBl_length_control= [];
TBl_control = [];
mean_TBl_control = [];
TBgr_control = [];
normRetractTB_control = [];
normExtTB_control = [];

```

3 Comparative computation analysis of actin-binding proteins in vivo unravels the single elements of dendrite dynamics

```
normNewTB_control = [];  
normDisapTB_control = [];  
normStaticTB_control = [];  
  
Traveldist_control = [];  
Traveldist_ext_control = [];  
Traveldist_ret_control = [];  
  
static_TB1_control = [];  
stable_TB1_control = [];  
stable_TB1_control = [];  
stable_TB1_control = [];  
new_TB1_control = [];  
disap_TB1_control = [];  
Traveldist_control = [];  
  
new_TB1_markov_control = [];  
disap_TB1_markov_control = [];  
grow_TB1_markov_control = [];  
retract_TB1_markov_control = [];  
static_TB1_markov_control = [];  
  
for ci = 1: length(folder_list)  
    pathname = folder_list{ci};  
    cd( pathname);  
  
    filename = [ 'control' num2str(ci) '.mat' ];  
    load(filename);  
  
    dummy = [];  
    dummy = stem_length;  
    stem_length_control = [ stem_length_control; dummy];  
  
    dummy = [];  
    dummy = size(TB1,1);  
    TB1_length_control = [TB1_length_control; dummy];  
  
    dummy = [];  
    dummy = TB1;  
    TB1_control = [TB1_control; dummy];  
  
    dummy = [];  
    dummy = mean_TB1;  
    mean_TB1_control = [mean_TB1_control; dummy];  
  
    dummy = [];  
    dummy = TBgr;  
    TBgr_control = [TBgr_control; dummy];  
  
    dummy = [];  
    dummy = normRetractTB;  
    normRetractTB_control = [normRetractTB_control; dummy];  
  
    dummy = [];  
    dummy = normExtTB;  
    normExtTB_control = [normExtTB_control; dummy];  
  
    dummy = [];  
    dummy = normDisapTB;  
    normDisapTB_control = [normDisapTB_control; dummy];  
  
    dummy = [];  
    dummy = normNewTB;  
    normNewTB_control = [normNewTB_control; dummy];  
  
    dummy = [];  
    dummy = normStaticTB;  
    normStaticTB_control = [normStaticTB_control; dummy];  
  
    dummy = [];  
    dummy = Traveldist;  
    Traveldist_control = [Traveldist_control; dummy];  
  
    dummy = [];
```


3 Comparative computation analysis of actin-binding proteins in vivo unravels the single elements of dendrite dynamics

```
dummy = Traveldist_ext;
Traveldist_control = [Traveldist_control; dummy];

dummy = [];
dummy = Traveldist_ret;
Traveldist_control = [Traveldist_control; dummy];

dummy = [];
dummy = static_TBl;
static_TBl_control = [static_TBl_control; dummy];

dummy = [];
dummy = stable_TBl;
stable_TBl_control = [stable_TBl_control; dummy];

dummy = [];
dummy = new_TBl;
new_TBl_control = [new_TBl_control; dummy];

dummy = [];
dummy = disap_TBl;
disap_TBl_control = [disap_TBl_control; dummy];

dummy = [];
dummy = Traveldist;
Traveldist_control = [Traveldist_control; dummy];

%%%%%%%%%%

dummy = [];
dummy = new_TBl_markov;
new_TBl_markov_control = [new_TBl_markov_control; dummy];

dummy = [];
dummy = disap_TBl_markov;
disap_TBl_markov_control = [disap_TBl_markov_control; dummy];

dummy = [];
dummy = grow_TBl_markov;
grow_TBl_markov_control = [grow_TBl_markov_control; dummy];

dummy = [];
dummy = retract_TBl_markov;
retract_TBl_markov_control = [retract_TBl_markov_control; dummy];

dummy = [];
dummy = static_TBl_markov;
static_TBl_markov_control = [static_TBl_markov_control; dummy];

end

cd('\fileserv.dzne.de\stuernert\Images\Tracings\Time Lapse quantification
Tomke\timelapse_C161_control');
filename = [ 'C161_control.mat'];
save(filename);
```

3 Comparative computation analysis of actin-binding proteins in vivo unravels the single elements of dendrite dynamics

3.3 Summary

Dendrite defects are a key feature of many neuropathological and neurodegenerative diseases and correlate with cognitive impairments such as mental retardation and autism (Baloyannis, 2009; Kulkarni & Firestein, 2012; Nakano & Hirano, 1987; Ramocki & Zoghbi, 2008; Villalba & Smith, 2010). Thus, understanding the mechanisms governing the establishment of cell-type specific neuronal dendrites is highly relevant.

The da neurons of *Drosophila* have been used extensively for understanding dendrite differentiation and cell-type specific dendritic tree elaboration. Specifically, evidence derived from these neurons, has revealed transcription factor cascades, secretory pathways, defined cytoskeletal proteins, activity dependent plasticity and recently first advances in computational modelling of the different classes of da neurons (Baltruschat L., submitted 2018; Y. N. Jan & Jan, 2010; Nanda, Das, Bhattacharjee, Cox, & Ascoli, 2018; Singhanian & Grueber, 2014). The cytoskeleton plays a critical role in specifying and modulating dendritic shape. In particular, many regulators of the actin cytoskeleton have been well characterised biochemically over the years and their cellular function deduced from *in vitro* studies. *In vivo* the individual actin regulatory pathways have been studied mostly in isolation as in the previous chapter. We worked on improving the computational analysis of dendrite tree morphology. Further, we improved time lapse imaging in these neurons. Together this allowed us to conduct comparative studies at a new level (Baltruschat L., submitted 2018; Nanda et al., 2018; Nithianandam & Chien, 2018; Sturner et al., 2019). We investigated the general organisation of actin and its dynamics in the c3da neurons and conducted a comparative computational analysis of the function of six different actin regulatory proteins in dendritic tree architecture and branch dynamics.

Taken together, this study sets the stage for future in-depth analyses of proteins distinct effects on cytoskeletal-mediated architecture of dendrites. We demonstrated that a combination of a genetic study, improved live imaging and computational analysis can help us to understand the single *in vivo* function of a series of ARPs and, moreover, how this repertoire of ARPs can achieve the cell-type specific dendritic architecture and dynamics of c3da neurons.

3 Comparative computation analysis of actin-binding proteins in vivo unravels the single elements of dendrite dynamics

4 Conclusion

In this thesis, I analysed the basic structure and dynamics of the actin cytoskeleton and the role of actin regulatory proteins in the dendritic branches of da neurons in *Drosophila* larvae. I demonstrated with *in vivo* imaging that actin accumulates at sites in the dendritic tree where a new branch will arise. The electron microscopy images in this work gave a first insight into the architecture of actin filaments within a dendritic branchlet, with branched actin filaments localised at the base and straight actin filaments, partially bundled, within the branchlet. I conducted a FRAP analysis specifically in the c3da neurons, which demonstrated that actin filaments within the branch are orientated with the barbed end towards the tip. Moreover, this analysis revealed that actin filaments in these branches have a relatively slow actin turnover and slow retrograde flow, revealing the actin dynamics underlying these branchlets for the first time.

In chapter 2 I showed that the Arp2/3 complex transiently accumulates at the base of newly forming branches and is required for new branch formation in all classes of da neurons. Moreover, I revealed that it is under the control of the activator WAVE and the small GTPase Rac1. Further investigation of *in vivo* branch dynamics led to a new comparative approach, in which I analysed six actin regulatory proteins in parallel using computational tools to investigate mutant dendritic tree morphology and time-lapse. Based on the experimental evidence that I produced, I propose the following model of dendrite branch dynamics specific to the branches of c3da neurons. Formation of a new branch cannot be achieved without the severing and depolymerising factor Twinstar/Cofilin that allows the remodelling of actin and freeing of G-actin. The actin nucleator complex Arp2/3 builds up branched actin at the base to push out the membrane for a new branch to be formed. Specifically, in branches of c3da neurons two actin nucleators, Spire and Capu/Formin2, are important for new branch formation and dynamics. The bundling of actin filaments through Singed leads to the characteristic straight and almost 90° Angle of the c3da terminal branches and restricts all aspects of branch dynamics. Ena, a general actin regulator in da neurons, inhibits the extension and favours retraction of the terminal branches in c3da neurons. Spire additionally enhances the retraction of these branches, possibly with a role in actin filament destabilisation. Together these six actin regulators describe the characteristic morphology and dynamics of the c3da neurons. A synthetic growth algorithm described the c3da neurons for the first time with their characteristic short terminal branches. Parameter alterations of the model

4 Conclusion

allowed me to validate the mutant dendritic phenotypes and identify the restraints in the dendritic tree of c3da neurons.

This work points to three directions for future research. Firstly, this new approach to mutant analysis allows new insight also into already characterised mutant phenotypes and can be used to understand dendritic branches of other types of da neurons. Moreover, this enables future work to concentrate on more than one protein or mutant at a time, in a comparative manner. Secondly, since I demonstrate that in this model system I can analyse the function of actin regulatory proteins *in vivo*, investigations in which an actin regulator is activated or deactivated at a given time point can help to understand the local action of an actin regulator in the dendrite. Thirdly, the mathematical model of the c3da neurons is the first one to fully describe the morphology of the dendritic tree and will be of essence to all future work in these neurons.

The dynamics and morphology of dendrites, shown here in the specific example of the da neurons in *Drosophila* larvae, are coordinated by the underlying cytoskeleton. Understanding the *in vivo* function of conserved actin regulatory proteins, six of which were described here, can help to understand basic principles of this biological process. Genetic tools available in *Drosophila*, improved optical imaging and combining it with computational analysis will further enhance our ability to understand the single elements regulating dendrite morphology and dynamics.

Acronyms

°C	degrees Celsius
A	Abdominal
ADF	actin-depolymerisation factor
ADP	adenosine diphosphate
APC	adenomatous polyposis coli
ARP	actin regulatory protein
Arp2/3	actin-regulated protein-2/3
ATP	adenosine triphosphate
c1da	class I dendritic arborization neuron
c2da	class II dendritic arborization neuron
c3da	class III dendritic arborization neuron
c4da	class IV dendritic arborization neuron
Capu	Cappuccino
CNS	central nervous system
Cobl	Cordon-Bleu
CP	Capping protein
da	dendritic arborization
<i>Drosophila</i>	<i>Drosophila melanogaster</i>
Dscam1	Down syndrome cell adhesion molecule 1
ECM	extracellular matrix
<i>ena</i>	enabled
EVH1	Ena/VASP homology 1
EVH2	Ena/VASP homology 2
F-actin	filamentous actin
FH1	Formin homology 1
FH2	Formin homology 2
FRAP	Fluorescence recovery after photobleaching
FRY	Furry

Acronyms

FYVE	Fab 1, YOTB, Vac 1, EEA1
G-actin	globular actin
Gal4	Galactose-responsive transcription factor
GTP	guanosine triphosphate
JMY	Junction-mediating and regulatory protein
kDa	kilo dalton
KIND	kinase non-catalytic C-lobe domain
L3	third larval instar
LIM	Lin11, Isl-1 & Mec-3
Lola	Longitudinal lacking
MARCM	Mosaic analysis with a repressible cell marker
Mav	maverick
NPFs	nucleation-promoting factors
Pcdhs	Procadherins
Pdm1/2	POU domain proteins
Pi	inorganic phosphate
PNS	peripheral nervous system
Ret	re-arranged during transfection
RNA	Ribonucleic acid
RNAi	RNA interference
Robo	Roundabout
SAV	Salvador
Sd	Scalloped
TBM	tandem actin binding domain
TF	transcription factor
TGF- β	Transforming growth factor β
TIRF	total internal reflection fluorescence microscopy
TRC	Tricornered
UAS	Upstream Activating Sequence

Acronyms

VASP	Vasodilator-stimulated phosphoprotein
Vg	Vestigial
VopL/VopF	Vibro parahaemolyticus and Vibrio cholera factors
WASH	Wiskott–Aldrich syndrome protein and SCAR homologue
WASP	Wiskott-Aldrich syndrome protein
WAVE	WASP-family verprolin homologous protein
WCA	WH2, Cofilin-homogy and acidic region
WH2	Wiskott-Aldrich homology 2
WRC	WAVE regulatory complex
WTS	Warts
<i>Xenopus</i>	<i>Xenopus laevis</i>

Copyright and Licensing

The presented research articles in this cumulative thesis underlie the following copyright:

Chapter 2: Stürner and Tatarnikova et al., 2019 (Development)

This article was published on the 4th of April 2019 by The Company of Biologists Ltd <http://www.biologists.com/user-licence-1-1>. Institutional reposition will be held back for 12 months to comply with the open access rights and permissions of the journal.

CONTACT

tomke.stuerner@dzne.de

Reuterstraße 53
53115 Bonn (Germany)

tomke.christin

PUBLICATIONS

Stürner T. and Tavosanis G.
Rotating for elongation: Fat2 whips for the race. *J Cell Biol.* 2016 Feb 29;212(5):487-9. doi: 10.1083/jcb.201601091. Epub 2016 Feb 22.

Stürner T.*, Tatarnikova A.*, Mueller J., Schaffran B., Cuntz H., Zhang Y, Nemethova M., Bogdan S., Small V and Tavosanis G.
Transient localization of the Arp2/3 complex initiates neuronal dendrite branching *in vivo*. *Development* 2019 : dev.171397 doi: 10.1242/dev.171397 Published 25 March 2019

Stürner T., Castro A., Philipps M., Cuntz H.* and Tavosanis G.*
Comparative computation analysis of actin-binding proteins *in vivo* unravel the single elements of dendrite dynamics. In preparation.

*equal contribution

MEETINGS

Mai 2019: Oral Presentation and Chair at EMBO Workshop on Cell biology of the neuron in Crete

March 2019: Oral Presentation at the Bonn Brain in Bonn

March 2019: Oral Presentation at Bonn Forum Biomedizin in Bonn

September 2018: Oral Presentation at the Neurofly in Krakow

November 2017: Poser Presentation at the SFN in Washington

September 2015: Poster Presentation at the EDRG in Heidelberg

September 2014: Oral Presentation at the Actin Summer School in Regensburg

Tomke Stürner

CURRICULUM VITAE

WORK EXPERIENCE**PhD Student**

01/08/2014–Present

DZNE-Deutschen Zentrum für Neurodegenerative Erkrankungen,
Prof. Dr. Gaia Tavosanis,
Bonn (Germany)

The aim of my thesis is to elucidate how regulators of the actin cytoskeleton define the diverse characteristic shapes and dynamics of dendritic arbors of dendritic arborisation neurons in *Drosophila*. In one project I was able to demonstrate that (WAVE) through recruitment of the Arp 2/3 complex promotes the formation of a branched actin patch at the base of a newly forming branchlet. To elucidate the mechanisms of actin organization following this initial step, we asked which additional actin cytoskeletal proteins are required for branching in these neurons. Through a computational approach to dendrite morphology and dendritic branch dynamics I not only analyse the function of the proteins but also describe the interplay between actin nucleation, bundling, severing and elongation.

Master Thesis

01/10/2013–01/08/2014

Collaboration between DZNE Bonn and University Clinic Regensburg,
Prof. Dr. Eugen Kerkhoff,
Regensburg (Germany)

The topic of the thesis was "Phenotypic characterisation of the actin nucleation factor Spire in da neurons of *Drosophila melanogaster*". After a two month internship in the laboratory of Eugen Kerkhoff in which I prepared constructs and reagents I started my seven month Master thesis at the DZNE in Bonn. My data showed that the genetic mutant of spire has a simplified dendritic tree, a reduction in the total number of branches specifically of Class III da neurons. Besides learning the basics about the handling of *Drosophila*, I optimised the following methods: RT PCR, Western Blot, in-vivo imaging of da neurons in *Drosophila* larva, immunohistochemistry.

Internship I

01/02/2013-01/04/2013

University of Regensburg,
Prof. Dr. Stephan Schneuwly,
Regensburg (Germany)

For eight weeks I worked with the *Drosophila* homologue of Park9, a lysosomal membrane protein responsible for the Kufor-Rakeb Syndrome. Dpark9 knockdown flies show a premature aging effect by accumulating ubiquitinated proteins. The aim was to analyse p62 accumulates in a Dpark9 knockdown background and its phenotype. Methods involved were immunohistochemistry, histology, western blots, RT PCR and climbing assays.

SKILLS

- **Managing projects:** effectively managed several projects in parallel, achieving goals and targets on time.
- **Teaching:** successfully supervised and taught several B.Sc and M.Sc. students.
- **Presentation skills:** presented data and projects to both large and small groups within Germany and abroad.
- **Drosophila care and husbandry.**
- **Molecular and biochemical skills:** Very good training in PCR techniques, Southern blot, Western blot, in-situ hybridisation, Cloning, CRISPR, immunostaining of tissues and histological sections.
- **Dissections:** adult and larval brain dissections, filet preparations, brain paraffin sections.
- **Microscopy:** competent in light and confocal microscopy (laser, spinning disk, airy scan) and in-vivo time-lapse imaging (incl. FRAP).
- **Bioinformatics:** Chimera, ClustalX, ImageJ, Adobe Photoshop & Illustrator, Matlab (Trees Toolbox)
- **Programming:** basic script writing in Fiji and Matlab. Completed C++ Course at the University Bonn and currently training in Python with an Udemy Course.

LANGUAGES

Mother tongue: German
 Foreign languages: English – C2
 Spanish – C1
 French – B1

WORK EXPERIENCE (continued)

Internship II *01/06/2013-01/08/2013*
 University of Cambridge,
 Dr. Cahir O'Kane,
 Cambridge (United Kingdom)

During an internship of eight weeks I characterised the role of spatacsin (SPG11) and spastizin (SPG15), two proteins involved in autosomal recessive hereditary spastic paraplegia with thin corpus callosum (ARHSP-TCC) in a Drosophila model. A GFP-tagged construct of the Drosophila spatacsin was used for localisation in various tissues including fat body cells, larval brain and adult fly brain. I was able to show that the spatacsin protein localises around lipid droplets in the Drosophila fat body. Additionally I looked into possible mutant phenotypes using spatacsin and spastizin mutants. Immunomicroscopy was optimized for analyses of epidermal cells, fat body cells, larval brains and fly brains. A reduction and abnormality in lysosomal compartments was observed, which was affirmed in further experiments.

EDUCATION

Master's Degree in Experimental and Clinical Neuroscience (Ø 1.4) *2012-2014*
 University of Regensburg (Germany)

Bachelor's Degree in Molecular Biology (Ø 1.9) *2009-2012*
 Johannes Gutenberg-University of Mainz (Germany)



School Education:
 Secondary School, Mainz (Germany) *2003-2009*
 Primary/Secondary School, Nottingham (UK) *2001-2003*
 Primary School, Granada (Spain) *1997-2001*

ACTIVITIES & INTERESTS

For two years I was PhD representative for DZNE Bonn, for all ten DZNE sites and part of the Helmholtz Junior's. The work included regular meetings with the administration, group leaders, students and work council to discuss PhD issues. The organisation of a PhD retreat (venue, transport, programme, speakers, budget, company visits), a PhD lunch (part of the DZNE Lecture Series) and hosting speakers invited by the PhDs.

Apart from keeping fit with swimming and dancing I enjoy a challenge, whether it is a tough mudder run or hiking the Camino de Santiago.

REFERENCES

 Prof. Dr. Gaia Tavosanis
 DZNE Bonn (Germany)  Dr. Hermann Cuntz
 ESI Frankfurt (Germany)



References

- Abe, H., Ohshima, S., & Obinata, T. (1989). A cofilin-like protein is involved in the regulation of actin assembly in developing skeletal muscle. *J Biochem*, 106(4), 696-702. doi:10.1093/oxfordjournals.jbchem.a122919
- Abercrombie, M., Heaysman, J. E., & Pegrum, S. M. (1970). The locomotion of fibroblasts in culture. 3. Movements of particles on the dorsal surface of the leading lamella. *Exp Cell Res*, 62(2), 389-398. doi:10.1016/0014-4827(70)90570-7
- Ahuja, R., Pinyol, R., Reichenbach, N., Custer, L., Klingensmith, J., Kessels, M. M., & Qualmann, B. (2007). Cordon-bleu is an actin nucleation factor and controls neuronal morphology. *Cell*, 131(2), 337-350. doi:10.1016/j.cell.2007.08.030
- Albeg, A., Smith, C. J., Chatzigeorgiou, M., Feitelson, D. G., Hall, D. H., Schafer, W. R., Treinin, M. (2011). *C. elegans* multi-dendritic sensory neurons: morphology and function. *Mol Cell Neurosci*, 46(1), 308-317. doi:10.1016/j.mcn.2010.10.001
- Andersen, R., Li, Y., Resseguie, M., & Brenman, J. E. (2005). Calcium/calmodulin-dependent protein kinase II alters structural plasticity and cytoskeletal dynamics in *Drosophila*. *J Neurosci*, 25(39), 8878-8888. doi:10.1523/JNEUROSCI.2005-05.2005
- Andrianantoandro, E., & Pollard, T. D. (2006). Mechanism of actin filament turnover by severing and nucleation at different concentrations of ADF/cofilin. *Mol Cell*, 24(1), 13-23. doi:10.1016/j.molcel.2006.08.006
- Applewhite, D. A., Barzik, M., Kojima, S., Svitkina, T. M., Gertler, F. B., & Borisy, G. G. (2007). Ena/VASP proteins have an anti-capping independent function in filopodia formation. *Mol Biol Cell*, 18(7), 2579-2591. doi:10.1091/mbc.e06-11-0990
- Ascoli, G. A. (1999). Progress and perspectives in computational neuroanatomy. *Anat Rec*, 257(6), 195-207. doi:10.1002/(SICI)1097-0185(19991215)257:6<195::AID-AR5>3.0.CO;2-H
- Ascoli, G. A. (2002). Neuroanatomical algorithms for dendritic modelling. *Network*, 13(3), 247-260.
- Ascoli, G. A. K., J. L. (2000). L-neuron: A modeling tool for the efficient generation and parsimonious description of dendritic morphology. *Neurocomputing*, Elsevier, Volumes 32–33, Pages 1003-1011.
- Avvaru, B. S., Pernier, J., & Carlier, M. F. (2015). Dimeric WH2 repeats of VopF sequester actin monomers into non-nucleating linear string conformations: An X-ray scattering study. *J Struct Biol*, 190(2), 192-199. doi:10.1016/j.jsb.2015.03.008
- Bachmann, C., Fischer, L., Walter, U., & Reinhard, M. (1999). The EVH2 domain of the vasodilator-stimulated phosphoprotein mediates tetramerization, F-actin binding, and actin bundle formation. *J Biol Chem*, 274(33), 23549-23557. doi:10.1074/jbc.274.33.23549
- Baloyannis, S. J. (2009). Dendritic pathology in Alzheimer's disease. *J Neurol Sci*, 283(1-2), 153-157. doi:10.1016/j.jns.2009.02.370
- Baltruschat L., T. G., Cuntz H. (submitted 2018). A developmental stretch-and-fill process that optimises dendritic wiring.
- Bamburg, J. R. (1999). Proteins of the ADF/cofilin family: essential regulators of actin dynamics. *Annu Rev Cell Dev Biol*, 15, 185-230. doi:10.1146/annurev.cellbio.15.1.185
- Bar, J., Kobler, O., van Bommel, B., & Mikhaylova, M. (2016). Periodic F-actin structures shape the neck of dendritic spines. *Sci Rep*, 6, 37136. doi:10.1038/srep37136
- Bashaw, G. J., Kidd, T., Murray, D., Pawson, T., & Goodman, C. S. (2000). Repulsive axon guidance: Abelson and Enabled play opposing roles downstream of the roundabout receptor. *Cell*, 101(7), 703-715. doi:10.1016/s0092-8674(00)80883-1
- Bear, J. E., Svitkina, T. M., Krause, M., Schafer, D. A., Loureiro, J. J., Strasser, G. A., . . . Gertler, F. B. (2002). Antagonism between Ena/VASP proteins and actin filament capping regulates fibroblast motility. *Cell*, 109(4), 509-521. doi:10.1016/s0092-8674(02)00731-6

References

- Bejan, A. (2001). Shape and Structure, from Engineering to Nature. *Molecules : A Journal of Synthetic Chemistry and Natural Product Chemistry*, 6,12, 1057–1058. doi:10.3390/61201057
- Bellenchi, G. C., Gurniak, C. B., Perlas, E., Middei, S., Ammassari-Teule, M., & Witke, W. (2007). N-cofilin is associated with neuronal migration disorders and cell cycle control in the cerebral cortex. *Genes Dev*, 21(18), 2347-2357. doi:10.1101/gad.434307
- Bird, A. D., & Cuntz, H. (2019). Dissecting Sholl Analysis into Its Functional Components. *Cell Rep*, 27(10), 3081-3096 e3085. doi:10.1016/j.celrep.2019.04.097
- Blanchoin, L., Boujemaa-Paterski, R., Sykes, C., & Plastino, J. (2014). Actin dynamics, architecture, and mechanics in cell motility. *Physiol Rev*, 94(1), 235-263. doi:10.1152/physrev.00018.2013
- Blanchoin, L., Pollard, T. D., & Hitchcock-DeGregori, S. E. (2001). Inhibition of the Arp2/3 complex-nucleated actin polymerization and branch formation by tropomyosin. *Curr Biol*, 11(16), 1300-1304. doi:10.1016/s0960-9822(01)00395-5
- Bodmer, R., & Jan, Y. N. (1987). Morphological differentiation of the embryonic peripheral neurons in *Drosophila*. *Roux Arch Dev Biol*, 196(2), 69-77. doi:10.1007/BF00402027
- Borisy, G. G., & Svitkina, T. M. (2000). Actin machinery: pushing the envelope. *Curr Opin Cell Biol*, 12(1), 104-112.
- Bosch, M., Le, K. H., Bugyi, B., Correia, J. J., Renault, L., & Carlier, M. F. (2007). Analysis of the function of Spire in actin assembly and its synergy with formin and profilin. *Mol Cell*, 28(4), 555-568. doi:10.1016/j.molcel.2007.09.018
- Brand, A. H., & Perrimon, N. (1993). Targeted gene expression as a means of altering cell fates and generating dominant phenotypes. *Development*, 118(2), 401-415.
- Breitsprecher, D., Jaiswal, R., Bombardier, J. P., Gould, C. J., Gelles, J., & Goode, B. L. (2012). Rocket launcher mechanism of collaborative actin assembly defined by single-molecule imaging. *Science*, 336(6085), 1164-1168. doi:10.1126/science.1218062
- Breitsprecher, D., Kiesewetter, A. K., Linkner, J., Urbanke, C., Resch, G. P., Small, J. V., & Faix, J. (2008). Clustering of VASP actively drives processive, WH2 domain-mediated actin filament elongation. *EMBO J*, 27(22), 2943-2954. doi:10.1038/emboj.2008.211
- Burke, R. E., Marks, W. B., & Ulfhake, B. (1992). A parsimonious description of motoneuron dendritic morphology using computer simulation. *J Neurosci*, 12(6), 2403-2416.
- Caldwell, J. E., Heiss, S. G., Mermall, V., & Cooper, J. A. (1989). Effects of CapZ, an actin capping protein of muscle, on the polymerization of actin. *Biochemistry*, 28(21), 8506-8514. doi:10.1021/bi00447a036
- Cant, K., Knowles, B. A., Mooseker, M. S., & Cooley, L. (1994). *Drosophila* singed, a fascin homolog, is required for actin bundle formation during oogenesis and bristle extension. *J Cell Biol*, 125(2), 369-380. doi:10.1083/jcb.125.2.369
- Carlier, M. F., Laurent, V., Santolini, J., Melki, R., Didry, D., Xia, G. X., . . . Pantaloni, D. (1997). Actin depolymerizing factor (ADF/cofilin) enhances the rate of filament turnover: implication in actin-based motility. *J Cell Biol*, 136(6), 1307-1322. doi:10.1083/jcb.136.6.1307
- Carlier, M. F., Pantaloni, D., & Korn, E. D. (1987). The mechanisms of ATP hydrolysis accompanying the polymerization of Mg-actin and Ca-actin. *J Biol Chem*, 262(7), 3052-3059.
- Castellano, F., Le Clainche, C., Patin, D., Carlier, M. F., & Chavrier, P. (2001). A WASp-VASP complex regulates actin polymerization at the plasma membrane. *EMBO J*, 20(20), 5603-5614. doi:10.1093/emboj/20.20.5603
- Chen, X. J., Squarr, A. J., Stephan, R., Chen, B., Higgins, T. E., Barry, D. J., . . . Way, M. (2014). Ena/VASP proteins cooperate with the WAVE complex to regulate the actin cytoskeleton. *Dev Cell*, 30(5), 569-584. doi:10.1016/j.devcel.2014.08.001
- Cheng, L. E., Song, W., Looger, L. L., Jan, L. Y., & Jan, Y. N. (2010). The role of the TRP channel NompC in *Drosophila* larval and adult locomotion. *Neuron*, 67(3), 373-380. doi:10.1016/j.neuron.2010.07.004

References

- Chereau, D., Kerff, F., Graceffa, P., Grabarek, Z., Langsetmo, K., & Dominguez, R. (2005). Actin-bound structures of Wiskott-Aldrich syndrome protein (WASP)-homology domain 2 and the implications for filament assembly. *Proc Natl Acad Sci U S A*, 102(46), 16644-16649. doi:10.1073/pnas.0507021102
- Chhabra, E. S., & Higgs, H. N. (2006). INF2 Is a WASP homology 2 motif-containing formin that severs actin filaments and accelerates both polymerization and depolymerization. *J Biol Chem*, 281(36), 26754-26767. doi:10.1074/jbc.M604666200
- Ciccarelli, F. D., Bork, P., & Kerkhoff, E. (2003). The KIND module: a putative signalling domain evolved from the C lobe of the protein kinase fold. *Trends Biochem Sci*, 28(7), 349-352. doi:10.1016/S0968-0004(03)00116-6
- Cline, H., & Haas, K. (2008). The regulation of dendritic arbor development and plasticity by glutamatergic synaptic input: a review of the synaptotrophic hypothesis. *J Physiol*, 586(6), 1509-1517. doi:10.1113/jphysiol.2007.150029
- Cline, H. T. (2001). Dendritic arbor development and synaptogenesis. *Curr Opin Neurobiol*, 11(1), 118-126.
- Coles, C. H., & Bradke, F. (2015). Coordinating neuronal actin-microtubule dynamics. *Curr Biol*, 25(15), R677-691. doi:10.1016/j.cub.2015.06.020
- Colombo, A., Palma, K., Armijo, L., Mione, M., Signore, I. A., Morales, C., . . . Concha, M. L. (2013). Daam1a mediates asymmetric habenular morphogenesis by regulating dendritic and axonal outgrowth. *Development*, 140(19), 3997-4007. doi:10.1242/dev.091934
- Cooper, J. A., Buhle, E. L., Jr., Walker, S. B., Tsong, T. Y., & Pollard, T. D. (1983). Kinetic evidence for a monomer activation step in actin polymerization. *Biochemistry*, 22(9), 2193-2202. doi:10.1021/bi00278a021
- Cooper, J. A., & Pollard, T. D. (1985). Effect of capping protein on the kinetics of actin polymerization. *Biochemistry*, 24(3), 793-799. doi:10.1021/bi00324a039
- Corty, M. M., Tam, J., & Grueber, W. B. (2016). Dendritic diversification through transcription factor-mediated suppression of alternative morphologies. *Development*, 143(8), 1351-1362. doi:10.1242/dev.130906
- Cuntz, H., Forstner, F., Borst, A., & Hausser, M. (2010). One rule to grow them all: a general theory of neuronal branching and its practical application. *PLoS Comput Biol*, 6(8). doi:10.1371/journal.pcbi.1000877
- D'Este, E., Kamin, D., Gottfert, F., El-Hady, A., & Hell, S. W. (2015). STED nanoscopy reveals the ubiquity of subcortical cytoskeleton periodicity in living neurons. *Cell Rep*, 10(8), 1246-1251. doi:10.1016/j.celrep.2015.02.007
- Dailey, M. E., & Smith, S. J. (1996). The dynamics of dendritic structure in developing hippocampal slices. *J Neurosci*, 16(9), 2983-2994.
- De La Cruz, E. M. (2009). How cofilin severs an actin filament. *Biophys Rev*, 1(2), 51-59. doi:10.1007/s12551-009-0008-5
- Dent, E. W., Gupton, S. L., & Gertler, F. B. (2011). The growth cone cytoskeleton in axon outgrowth and guidance. *Cold Spring Harb Perspect Biol*, 3(3). doi:10.1101/cshperspect.a001800
- Dickson, B. J., & Gilestro, G. F. (2006). Regulation of commissural axon pathfinding by slit and its Robo receptors. *Annu Rev Cell Dev Biol*, 22, 651-675. doi:10.1146/annurev.cellbio.21.090704.151234
- Dimitrova, S., Reissaus, A., & Tavosanis, G. (2008). Slit and Robo regulate dendrite branching and elongation of space-filling neurons in *Drosophila*. *Dev Biol*, 324(1), 18-30. doi:10.1016/j.ydbio.2008.08.028
- Dominguez, R., & Holmes, K. C. (2011). Actin structure and function. *Annu Rev Biophys*, 40, 169-186. doi:10.1146/annurev-biophys-042910-155359
- Dong, X., Shen, K., & Bulow, H. E. (2015). Intrinsic and extrinsic mechanisms of dendritic morphogenesis. *Annu Rev Physiol*, 77, 271-300. doi:10.1146/annurev-physiol-021014-071746
- Elson, E. L., Felder, S. F., Jay, P. Y., Kolodney, M. S., & Pasternak, C. (1999). Forces in cell locomotion. *Biochem Soc Symp*, 65, 299-314.

References

- Emoto, K., He, Y., Ye, B., Grueber, W. B., Adler, P. N., Jan, L. Y., & Jan, Y. N. (2004). Control of dendritic branching and tiling by the Tricornered-kinase/Furry signaling pathway in *Drosophila* sensory neurons. *Cell*, 119(2), 245-256. doi:10.1016/j.cell.2004.09.036
- Etienne-Manneville, S., & Hall, A. (2002). Rho GTPases in cell biology. *Nature*, 420(6916), 629-635. doi:10.1038/nature01148
- Faix, J., & Rottner, K. (2006). The making of filopodia. *Curr Opin Cell Biol*, 18(1), 18-25. doi:10.1016/j.ceb.2005.11.002
- Fan, Y., Tang, X., Vitriol, E., Chen, G., & Zheng, J. Q. (2011). Actin capping protein is required for dendritic spine development and synapse formation. *J Neurosci*, 31(28), 10228-10233. doi:10.1523/JNEUROSCI.0115-11.2011
- Ferreira, T., Ou, Y., Li, S., Giniger, E., & van Meyel, D. J. (2014). Dendrite architecture organized by transcriptional control of the F-actin nucleator Spire. *Development*, 141(3), 650-660. doi:10.1242/dev.099655
- Fiala, J. C., Feinberg, M., Popov, V., & Harris, K. M. (1998). Synaptogenesis via dendritic filopodia in developing hippocampal area CA1. *J Neurosci*, 18(21), 8900-8911.
- Fowler, V. M. (2013). The human erythrocyte plasma membrane: a Rosetta Stone for decoding membrane-cytoskeleton structure. *Curr Top Membr*, 72, 39-88. doi:10.1016/B978-0-12-417027-8.00002-7
- Frieden, C. (1983). Polymerization of actin: mechanism of the Mg²⁺-induced process at pH 8 and 20 degrees C. *Proc Natl Acad Sci U S A*, 80(21), 6513-6517. doi:10.1073/pnas.80.21.6513
- Frieden, C., & Patane, K. (1985). Differences in G-actin containing bound ATP or ADP: the Mg²⁺-induced conformational change requires ATP. *Biochemistry*, 24(15), 4192-4196. doi:10.1021/bi00336a056
- Fujii, T., Iwane, A. H., Yanagida, T., & Namba, K. (2010). Direct visualization of secondary structures of F-actin by electron cryomicroscopy. *Nature*, 467(7316), 724-728. doi:10.1038/nature09372
- Fujiwara, I., Vavylonis, D., & Pollard, T. D. (2007). Polymerization kinetics of ADP- and ADP-Pi-actin determined by fluorescence microscopy. *Proc Natl Acad Sci U S A*, 104(21), 8827-8832. doi:10.1073/pnas.0702510104
- Gaillard, J., Ramabhadran, V., Neumann, E., Gurel, P., Blanchoin, L., Vantard, M., & Higgs, H. N. (2011). Differential interactions of the formins INF2, mDia1, and mDia2 with microtubules. *Mol Biol Cell*, 22(23), 4575-4587. doi:10.1091/mbc.E11-07-0616
- Gao, F. B., Brenman, J. E., Jan, L. Y., & Jan, Y. N. (1999). Genes regulating dendritic outgrowth, branching, and routing in *Drosophila*. *Genes Dev*, 13(19), 2549-2561. doi:10.1101/gad.13.19.2549
- Gates, M. A., Kannan, R., & Giniger, E. (2011). A genome-wide analysis reveals that the *Drosophila* transcription factor Lola promotes axon growth in part by suppressing expression of the actin nucleation factor Spire. *Neural Dev*, 6, 37. doi:10.1186/1749-8104-6-37
- Georges, P. C., Hadzimichalis, N. M., Sweet, E. S., & Firestein, B. L. (2008). The yin-yang of dendrite morphology: unity of actin and microtubules. *Mol Neurobiol*, 38(3), 270-284. doi:10.1007/s12035-008-8046-8
- Gershman, L. C., Newman, J., Selden, L. A., & Estes, J. E. (1984). Bound-cation exchange affects the lag phase in actin polymerization. *Biochemistry*, 23(10), 2199-2203. doi:10.1021/bi00305a015
- Goley, E. D., Ohkawa, T., Mancuso, J., Woodruff, J. B., D'Alessio, J. A., Cande, W. Z., . . . Welch, M. D. (2006). Dynamic nuclear actin assembly by Arp2/3 complex and a baculovirus WASP-like protein. *Science*, 314(5798), 464-467. doi:10.1126/science.1133348
- Golgi, C. (1873). Sulla struttura della sostanza grigia del cervello (Comunicazione preventiva). *Gaz. Med. Ital. Lomb.*, 33, 244-246.
- Goodman, C. S., Bastiani, M. J., Doe, C. Q., du Lac, S., Helfand, S. L., Kuwada, J. Y., & Thomas, J. B. (1984). Cell recognition during neuronal development. *Science*, 225(4668), 1271-1279. doi:10.1126/science.6474176
- Gordon, D. J., Boyer, J. L., & Korn, E. D. (1977). Comparative biochemistry of non-muscle actins. *J Biol Chem*, 252(22), 8300-8309.

References

- Grueber, W. B., Jan, L. Y., & Jan, Y. N. (2002). Tiling of the *Drosophila* epidermis by multidendritic sensory neurons. *Development*, 129(12), 2867-2878.
- Grueber, W. B., Jan, L. Y., & Jan, Y. N. (2003). Different levels of the homeodomain protein cut regulate distinct dendrite branching patterns of *Drosophila* multidendritic neurons. *Cell*, 112(6), 805-818. doi:10.1016/s0092-8674(03)00160-0
- Grueber, W. B., Yang, C. H., Ye, B., & Jan, Y. N. (2005). The development of neuronal morphology in insects. *Curr Biol*, 15(17), R730-738. doi:10.1016/j.cub.2005.08.023
- Grueber, W. B., Ye, B., Moore, A. W., Jan, L. Y., & Jan, Y. N. (2003). Dendrites of distinct classes of *Drosophila* sensory neurons show different capacities for homotypic repulsion. *Curr Biol*, 13(8), 618-626. doi:10.1016/s0960-9822(03)00207-0
- Gunsalus, K. C., Bonaccorsi, S., Williams, E., Verni, F., Gatti, M., & Goldberg, M. L. (1995). Mutations in twinstar, a *Drosophila* gene encoding a cofilin/ADF homologue, result in defects in centrosome migration and cytokinesis. *J Cell Biol*, 131(5), 1243-1259. doi:10.1083/jcb.131.5.1243
- Gupton, S. L., & Gertler, F. B. (2007). Filopodia: the fingers that do the walking. *Sci STKE*, 2007(400), re5. doi:10.1126/stke.4002007re5
- Gurel, P. S., Ge, P., Grintsevich, E. E., Shu, R., Blanchoin, L., Zhou, Z. H., . . . Higgs, H. N. (2014). INF2-mediated severing through actin filament encirclement and disruption. *Curr Biol*, 24(2), 156-164. doi:10.1016/j.cub.2013.12.018
- Gurniak, C. B., Perlas, E., & Witke, W. (2005). The actin depolymerizing factor n-cofilin is essential for neural tube morphogenesis and neural crest cell migration. *Dev Biol*, 278(1), 231-241. doi:10.1016/j.ydbio.2004.11.010
- Haas, K., Li, J., & Cline, H. T. (2006). AMPA receptors regulate experience-dependent dendritic arbor growth *in vivo*. *Proc Natl Acad Sci U S A*, 103(32), 12127-12131. doi:10.1073/pnas.0602670103
- Han, C., Wang, D., Soba, P., Zhu, S., Lin, X., Jan, L. Y., & Jan, Y. N. (2012). Integrins regulate repulsion-mediated dendritic patterning of *drosophila* sensory neurons by restricting dendrites in a 2D space. *Neuron*, 73(1), 64-78. doi:10.1016/j.neuron.2011.10.036
- Hanein, D., Volkman, N., Goldsmith, S., Michon, A. M., Lehman, W., Craig, R., . . . Matsudaira, P. (1998). An atomic model of fimbrin binding to F-actin and its implications for filament crosslinking and regulation. *Nat Struct Biol*, 5(9), 787-792. doi:10.1038/1828
- Harker, A. J., Katkar, H. H., Bidone, T. C., Aydin, F., Voth, G. A., Applewhite, D. A., & Kovar, D. R. (2019). Ena/VASP processive elongation is modulated by avidity on actin filaments bundled by the filopodia cross-linker fascin. *Mol Biol Cell*, 30(7), 851-862. doi:10.1091/mbc.E18-08-0500
- Hattori, Y., Sugimura, K., & Uemura, T. (2007). Selective expression of Knot/Collier, a transcriptional regulator of the EBF/Olf-1 family, endows the *Drosophila* sensory system with neuronal class-specific elaborated dendritic patterns. *Genes Cells*, 12(9), 1011-1022. doi:10.1111/j.1365-2443.2007.01107.x
- He, J., Zhou, R., Wu, Z., Carrasco, M. A., Kurshan, P. T., Farley, J. E., . . . Zhuang, X. (2016). Prevalent presence of periodic actin-spectrin-based membrane skeleton in a broad range of neuronal cell types and animal species. *Proc Natl Acad Sci U S A*, 113(21), 6029-6034. doi:10.1073/pnas.1605707113
- Higgs, H. N. (2004). There goes the neighbourhood: Eps8 joins the barbed-end crowd. *Nat Cell Biol*, 6(12), 1147-1149. doi:10.1038/ncb1204-1147
- Higgs, H. N., & Peterson, K. J. (2005). Phylogenetic analysis of the formin homology 2 domain. *Mol Biol Cell*, 16(1), 1-13. doi:10.1091/mbc.e04-07-0565
- Hild, G., Kalmar, L., Kardos, R., Nyitrai, M., & Bugyi, B. (2014). The other side of the coin: functional and structural versatility of ADF/cofilins. *Eur J Cell Biol*, 93(5-6), 238-251. doi:10.1016/j.ejcb.2013.12.001
- Hillman, D. E. (1979). Neuronal shape parameters and substructures as a basis of neuronal form. In: Schmitt F, editor. *The Neurosciences, Fourth Study Program*. Cambridge: MIT Press., pp. 477-498.
- Hillman, D. E. (1988). Parameters of dendritic shape and substructures: Intrinsic and extrinsic determination? In M. M. B. edited by R.J.Lasek (Ed.), *Intrinsic Determinants of Neuronal Form and Function* (pp. pp. 83-113). New York: : A.R.Liss.

References

- His, W. (1889). Die Neuroblasten und deren Entstehung im embryonalen Marke. . Abhandlungen der Mathematisch-Physischen Classe der Königlich Sächsischen Gesellschaft der Wissenschaften, 15, 311–372.
- Holmes, K. C., Popp, D., Gebhard, W., & Kabsch, W. (1990). Atomic model of the actin filament. *Nature*, 347(6288), 44-49. doi:10.1038/347044a0
- Holtmaat, A., Wilbrecht, L., Knott, G. W., Welker, E., & Svoboda, K. (2006). Experience-dependent and cell-type-specific spine growth in the neocortex. *Nature*, 441(7096), 979-983. doi:10.1038/nature04783
- Hou, W., Izadi, M., Nemitz, S., Haag, N., Kessels, M. M., & Qualmann, B. (2015). The Actin Nucleator Cobl Is Controlled by Calcium and Calmodulin. *PLoS Biol*, 13(9), e1002233. doi:10.1371/journal.pbio.1002233
- Hoyer, N., Zielke, P., Hu, C., Petersen, M., Sauter, K., Scharrenberg, R., . . . Soba, P. (2018). Ret and Substrate-Derived TGF-beta Maverick Regulate Space-Filling Dendrite Growth in Drosophila Sensory Neurons. *Cell Rep*, 24(9), 2261-2272 e2265. doi:10.1016/j.celrep.2018.07.092
- Hughes, C. L., & Thomas, J. B. (2007). A sensory feedback circuit coordinates muscle activity in Drosophila. *Mol Cell Neurosci*, 35(2), 383-396. doi:10.1016/j.mcn.2007.04.001
- Huttelmaier, S., Harbeck, B., Steffens, O., Messerschmidt, T., Illenberger, S., & Jockusch, B. M. (1999). Characterization of the actin binding properties of the vasodilator-stimulated phosphoprotein VASP. *FEBS Lett*, 451(1), 68-74. doi:10.1016/s0014-5793(99)00546-3
- Hwang, R. Y., Zhong, L., Xu, Y., Johnson, T., Zhang, F., Deisseroth, K., & Tracey, W. D. (2007). Nociceptive neurons protect Drosophila larvae from parasitoid wasps. *Curr Biol*, 17(24), 2105-2116. doi:10.1016/j.cub.2007.11.029
- Izeddin, I., Specht, C. G., Lelek, M., Darzacq, X., Triller, A., Zimmer, C., & Dahan, M. (2011). Super-resolution dynamic imaging of dendritic spines using a low-affinity photoconvertible actin probe. *PLoS One*, 6(1), e15611. doi:10.1371/journal.pone.0015611
- Jan, L. Y., & Jan, Y. N. (1982). Antibodies to horseradish peroxidase as specific neuronal markers in Drosophila and in grasshopper embryos. *Proc Natl Acad Sci U S A*, 79(8), 2700-2704. doi:10.1073/pnas.79.8.2700
- Jan, Y. N., & Jan, L. Y. (1993). HLH proteins, fly neurogenesis, and vertebrate myogenesis. *Cell*, 75(5), 827-830. doi:10.1016/0092-8674(93)90525-u
- Jan, Y. N., & Jan, L. Y. (2010). Branching out: mechanisms of dendritic arborization. *Nat Rev Neurosci*, 11(5), 316-328. doi:10.1038/nrn2836
- Jinushi-Nakao, S., Arvind, R., Amikura, R., Kinameri, E., Liu, A. W., & Moore, A. W. (2007). Knot/Collier and cut control different aspects of dendrite cytoskeleton and synergize to define final arbor shape. *Neuron*, 56(6), 963-978. doi:10.1016/j.neuron.2007.10.031
- Jonsson, F., Gurniak, C. B., Fleischer, B., Kirfel, G., & Witke, W. (2012). Immunological responses and actin dynamics in macrophages are controlled by N-cofilin but are independent from ADF. *PLoS One*, 7(4), e36034. doi:10.1371/journal.pone.0036034
- Jontes, J. D., Buchanan, J., & Smith, S. J. (2000). Growth cone and dendrite dynamics in zebrafish embryos: early events in synaptogenesis imaged *in vivo*. *Nat Neurosci*, 3(3), 231-237. doi:10.1038/72936
- Kaethner, R. J., & Stuermer, C. A. (1997). Dynamics of process formation during differentiation of tectal neurons in embryonic zebrafish. *J Neurobiol*, 32(6), 627-639.
- Kaufmann, W. E., & Moser, H. W. (2000). Dendritic anomalies in disorders associated with mental retardation. *Cereb Cortex*, 10(10), 981-991. doi:10.1093/cercor/10.10.981
- Kim, H. T., Lee, K. I., Kim, D. W., & Hwang, D. Y. (2013). An ECM-based culture system for the generation and maintenance of xeno-free human iPS cells. *Biomaterials*, 34(4), 1041-1050. doi:10.1016/j.biomaterials.2012.10.064
- Kim, M. D., Jan, L. Y., & Jan, Y. N. (2006). The bHLH-PAS protein Spineless is necessary for the diversification of dendrite morphology of Drosophila dendritic arborization neurons. *Genes Dev*, 20(20), 2806-2819. doi:10.1101/gad.1459706

References

- Kim, M. E., Shrestha, B. R., Blazeski, R., Mason, C. A., & Grueber, W. B. (2012). Integrins establish dendrite-substrate relationships that promote dendritic self-avoidance and patterning in drosophila sensory neurons. *Neuron*, 73(1), 79-91. doi:10.1016/j.neuron.2011.10.033
- Kiuchi, T., Nagai, T., Ohashi, K., & Mizuno, K. (2011). Measurements of spatiotemporal changes in G-actin concentration reveal its effect on stimulus-induced actin assembly and lamellipodium extension. *J Cell Biol*, 193(2), 365-380. doi:10.1083/jcb.201101035
- Klyachko, V. A., & Stevens, C. F. (2003). Connectivity optimization and the positioning of cortical areas. *Proc Natl Acad Sci U S A*, 100(13), 7937-7941. doi:10.1073/pnas.0932745100
- Kohmura, N., Senzaki, K., Hamada, S., Kai, N., Yasuda, R., Watanabe, M., . . . Yagi, T. (1998). Diversity revealed by a novel family of cadherins expressed in neurons at a synaptic complex. *Neuron*, 20(6), 1137-1151.
- Koike-Kumagai, M., Yasunaga, K., Morikawa, R., Kanamori, T., & Emoto, K. (2009). The target of rapamycin complex 2 controls dendritic tiling of *Drosophila* sensory neurons through the Tricornered kinase signalling pathway. *EMBO J*, 28(24), 3879-3892. doi:10.1038/emboj.2009.312
- Korobova, F., & Svitkina, T. (2010). Molecular architecture of synaptic actin cytoskeleton in hippocampal neurons reveals a mechanism of dendritic spine morphogenesis. *Mol Biol Cell*, 21(1), 165-176. doi:10.1091/mbc.E09-07-0596
- Kovar, D. R. (2006). Cell polarity: formin on the move. *Curr Biol*, 16(14), R535-538. doi:10.1016/j.cub.2006.06.039
- Kovar, D. R., & Pollard, T. D. (2004). Insertional assembly of actin filament barbed ends in association with formins produces piconewton forces. *Proc Natl Acad Sci U S A*, 101(41), 14725-14730. doi:10.1073/pnas.0405902101
- Kramer, A. P., & Stent, G. S. (1985). Developmental arborization of sensory neurons in the leech *Haementeria ghilianii*. II. Experimentally induced variations in the branching pattern. *J Neurosci*, 5(3), 768-775.
- Kuhn, J. R., & Pollard, T. D. (2005). Real-time measurements of actin filament polymerization by total internal reflection fluorescence microscopy. *Biophys J*, 88(2), 1387-1402. doi:10.1529/biophysj.104.047399
- Kulkarni, V. A., & Firestein, B. L. (2012). The dendritic tree and brain disorders. *Mol Cell Neurosci*, 50(1), 10-20. doi:10.1016/j.mcn.2012.03.005
- Kupferman, J. V., Basu, J., Russo, M. J., Guevarra, J., Cheung, S. K., & Siegelbaum, S. A. (2014). Reelin signaling specifies the molecular identity of the pyramidal neuron distal dendritic compartment. *Cell*, 158(6), 1335-1347. doi:10.1016/j.cell.2014.07.035
- Lambrechts, A., Kwiatkowski, A. V., Lanier, L. M., Bear, J. E., Vandekerckhove, J., Ampe, C., & Gertler, F. B. (2000). cAMP-dependent protein kinase phosphorylation of EVL, a Mena/VASP relative, regulates its interaction with actin and SH3 domains. *J Biol Chem*, 275(46), 36143-36151. doi:10.1074/jbc.M006274200
- Lanier, L. M., Gates, M. A., Witke, W., Menzies, A. S., Wehman, A. M., Macklis, J. D., . . . Gertler, F. B. (1999). Mena is required for neurulation and commissure formation. *Neuron*, 22(2), 313-325.
- Lappalainen, P. (2016). Actin-binding proteins: the long road to understanding the dynamic landscape of cellular actin networks. *Mol Biol Cell*, 27(16), 2519-2522. doi:10.1091/mbc.E15-10-0728
- Lappalainen, P., & Drubin, D. G. (1997). Cofilin promotes rapid actin filament turnover *in vivo*. *Nature*, 388(6637), 78-82. doi:10.1038/40418
- Lee, T., & Luo, L. (1999). Mosaic analysis with a repressible cell marker for studies of gene function in neuronal morphogenesis. *Neuron*, 22(3), 451-461.
- Lee, T., Winter, C., Marticke, S. S., Lee, A., & Luo, L. (2000). Essential roles of *Drosophila* RhoA in the regulation of neuroblast proliferation and dendritic but not axonal morphogenesis. *Neuron*, 25(2), 307-316.
- Lefebvre, J. L., Sanes, J. R., & Kay, J. N. (2015). Development of dendritic form and function. *Annu Rev Cell Dev Biol*, 31, 741-777. doi:10.1146/annurev-cellbio-100913-013020
- Letourneau, P. C. (2009). Actin in axons: stable scaffolds and dynamic filaments. *Results Probl Cell Differ*, 48, 65-90. doi:10.1007/400_2009_15

References

- Li, W., Wang, F., Menut, L., & Gao, F. B. (2004). BTB/POZ-zinc finger protein abrupt suppresses dendritic branching in a neuronal subtype-specific and dosage-dependent manner. *Neuron*, 43(6), 823-834. doi:10.1016/j.neuron.2004.08.040
- Lom, B., & Cohen-Cory, S. (1999). Brain-derived neurotrophic factor differentially regulates retinal ganglion cell dendritic and axonal arborization *in vivo*. *J Neurosci*, 19(22), 9928-9938.
- Long, H., Ou, Y., Rao, Y., & van Meyel, D. J. (2009). Dendrite branching and self-avoidance are controlled by Turtle, a conserved IgSF protein in *Drosophila*. *Development*, 136(20), 3475-3484. doi:10.1242/dev.040220
- Ma, L., & Tessier-Lavigne, M. (2007). Dual branch-promoting and branch-repelling actions of Slit/Robo signaling on peripheral and central branches of developing sensory axons. *J Neurosci*, 27(25), 6843-6851. doi:10.1523/JNEUROSCI.1479-07.2007
- Majewska, A. K., Newton, J. R., & Sur, M. (2006). Remodeling of synaptic structure in sensory cortical areas *in vivo*. *J Neurosci*, 26(11), 3021-3029. doi:10.1523/JNEUROSCI.4454-05.2006
- Matthews, B. J., Kim, M. E., Flanagan, J. J., Hattori, D., Clemens, J. C., Zipursky, S. L., & Grueber, W. B. (2007). Dendrite self-avoidance is controlled by Dscam. *Cell*, 129(3), 593-604. doi:10.1016/j.cell.2007.04.013
- McGough, A., Pope, B., Chiu, W., & Weeds, A. (1997). Cofilin changes the twist of F-actin: implications for actin filament dynamics and cellular function. *J Cell Biol*, 138(4), 771-781. doi:10.1083/jcb.138.4.771
- Meltzer, S., Yadav, S., Lee, J., Soba, P., Younger, S. H., Jin, P., . . . Jan, Y. N. (2016). Epidermis-Derived Semaphorin Promotes Dendrite Self-Avoidance by Regulating Dendrite-Substrate Adhesion in *Drosophila* Sensory Neurons. *Neuron*, 89(4), 741-755. doi:10.1016/j.neuron.2016.01.020
- Mizuno, K. (2013). Signaling mechanisms and functional roles of cofilin phosphorylation and dephosphorylation. *Cell Signal*, 25(2), 457-469. doi:10.1016/j.cellsig.2012.11.001
- Morgan, T. E., Lockerbie, R. O., Minamide, L. S., Browning, M. D., & Bamburg, J. R. (1993). Isolation and characterization of a regulated form of actin depolymerizing factor. *J Cell Biol*, 122(3), 623-633. doi:10.1083/jcb.122.3.623
- Mullins, R. D., Heuser, J. A., & Pollard, T. D. (1998). The interaction of Arp2/3 complex with actin: nucleation, high affinity pointed end capping, and formation of branching networks of filaments. *Proc Natl Acad Sci U S A*, 95(11), 6181-6186. doi:10.1073/pnas.95.11.6181
- Nag, S., Larsson, M., Robinson, R. C., & Burtnick, L. D. (2013). Gelsolin: the tail of a molecular gymnast. *Cytoskeleton (Hoboken)*, 70(7), 360-384. doi:10.1002/cm.21117
- Nagel, J., Delandre, C., Zhang, Y., Forstner, F., Moore, A. W., & Tavosanis, G. (2012). Fascin controls neuronal class-specific dendrite arbor morphology. *Development*, 139(16), 2999-3009. doi:10.1242/dev.077800
- Nakamura, Y., Wood, C. L., Patton, A. P., Jaafari, N., Henley, J. M., Mellor, J. R., & Hanley, J. G. (2011). PICK1 inhibition of the Arp2/3 complex controls dendritic spine size and synaptic plasticity. *EMBO J*, 30(4), 719-730. doi:10.1038/emboj.2010.357
- Nakano, I., & Hirano, A. (1987). Atrophic cell processes of large motor neurons in the anterior horn in amyotrophic lateral sclerosis: observation with silver impregnation method. *J Neuropathol Exp Neurol*, 46(1), 40-49. doi:10.1097/00005072-198701000-00004
- Namgoong, S., Boczkowska, M., Glista, M. J., Winkelman, J. D., Rebowski, G., Kovar, D. R., & Dominguez, R. (2011). Mechanism of actin filament nucleation by *Vibrio* VopL and implications for tandem W domain nucleation. *Nat Struct Mol Biol*, 18(9), 1060-1067. doi:10.1038/nsmb.2109
- Nanda, S., Das, R., Bhattacharjee, S., Cox, D. N., & Ascoli, G. A. (2018). Morphological determinants of dendritic arborization neurons in *Drosophila* larva. *Brain Struct Funct*, 223(3), 1107-1120. doi:10.1007/s00429-017-1541-9
- Ng, J., Nardine, T., Harms, M., Tzu, J., Goldstein, A., Sun, Y., . . . Luo, L. (2002). Rac GTPases control axon growth, guidance and branching. *Nature*, 416(6879), 442-447. doi:10.1038/416442a
- Niell, C. M., Meyer, M. P., & Smith, S. J. (2004). *In vivo* imaging of synapse formation on a growing dendritic arbor. *Nat Neurosci*, 7(3), 254-260. doi:10.1038/nn1191

References

- Nishida, E., Maekawa, S., & Sakai, H. (1984). Cofilin, a protein in porcine brain that binds to actin filaments and inhibits their interactions with myosin and tropomyosin. *Biochemistry*, 23(22), 5307-5313. doi:10.1021/bi00317a032
- Nithianandam, V., & Chien, C. T. (2018). Actin blobs prefigure dendrite branching sites. *J Cell Biol*, 217(10), 3731-3746. doi:10.1083/jcb.201711136
- O'Connor, T. P., Duerr, J. S., & Bentley, D. (1990). Pioneer growth cone steering decisions mediated by single filopodial contacts in situ. *J Neurosci*, 10(12), 3935-3946.
- Oda, T., Aihara, T., & Wakabayashi, K. (2016). Early nucleation events in the polymerization of actin, probed by time-resolved small-angle x-ray scattering. *Sci Rep*, 6, 34539. doi:10.1038/srep34539
- Okada, K., Bartolini, F., Deaconescu, A. M., Moseley, J. B., Dogic, Z., Grigorieff, N., . . . Goode, B. L. (2010). Adenomatous polyposis coli protein nucleates actin assembly and synergizes with the formin mDia1. *J Cell Biol*, 189(7), 1087-1096. doi:10.1083/jcb.201001016
- Ono, S., & Ono, K. (2002). Tropomyosin inhibits ADF/cofilin-dependent actin filament dynamics. *J Cell Biol*, 156(6), 1065-1076. doi:10.1083/jcb.200110013
- Otomo, T., & Rosen, M. K. (2005). [Structure and function of Formin homology 2 domain]. *Tanpakushitsu Kakusan Koso*, 50(9), 1088-1093.
- Pantaloni, D., Boujemaa, R., Didry, D., Gounon, P., & Carlier, M. F. (2000). The Arp2/3 complex branches filament barbed ends: functional antagonism with capping proteins. *Nat Cell Biol*, 2(7), 385-391. doi:10.1038/35017011
- Pantaloni, D., & Carlier, M. F. (1993). How profilin promotes actin filament assembly in the presence of thymosin beta 4. *Cell*, 75(5), 1007-1014. doi:10.1016/0092-8674(93)90544-z
- Pappas, C. T., Bhattacharya, N., Cooper, J. A., & Gregorio, C. C. (2008). Nebulin interacts with CapZ and regulates thin filament architecture within the Z-disc. *Mol Biol Cell*, 19(5), 1837-1847. doi:10.1091/mbc.E07-07-0690
- Parrish, J. Z., Emoto, K., Jan, L. Y., & Jan, Y. N. (2007). Polycomb genes interact with the tumor suppressor genes hippo and warts in the maintenance of Drosophila sensory neuron dendrites. *Genes Dev*, 21(8), 956-972. doi:10.1101/gad.1514507
- Parrish, J. Z., Kim, M. D., Jan, L. Y., & Jan, Y. N. (2006). Genome-wide analyses identify transcription factors required for proper morphogenesis of Drosophila sensory neuron dendrites. *Genes Dev*, 20(7), 820-835. doi:10.1101/gad.1391006
- Parrish, J. Z., Xu, P., Kim, C. C., Jan, L. Y., & Jan, Y. N. (2009). The microRNA bantam functions in epithelial cells to regulate scaling growth of dendrite arbors in drosophila sensory neurons. *Neuron*, 63(6), 788-802. doi:10.1016/j.neuron.2009.08.006
- Pasic, L., Kotova, T., & Schafer, D. A. (2008). Ena/VASP proteins capture actin filament barbed ends. *J Biol Chem*, 283(15), 9814-9819. doi:10.1074/jbc.M710475200
- Paul, A. S., & Pollard, T. D. (2009). Review of the mechanism of processive actin filament elongation by formins. *Cell Motil Cytoskeleton*, 66(8), 606-617. doi:10.1002/cm.20379
- Perala, N., Sariola, H., & Immonen, T. (2012). More than nervous: the emerging roles of plexins. *Differentiation*, 83(1), 77-91. doi:10.1016/j.diff.2011.08.001
- Perrin, B. J., & Ervasti, J. M. (2010). The actin gene family: function follows isoform. *Cytoskeleton (Hoboken)*, 67(10), 630-634. doi:10.1002/cm.20475
- Perry, V. H., & Linden, R. (1982). Evidence for dendritic competition in the developing retina. *Nature*, 297(5868), 683-685. doi:10.1038/297683a0
- Pittet, M. J., & Weissleder, R. (2011). Intravital imaging. *Cell*, 147(5), 983-991. doi:10.1016/j.cell.2011.11.004
- Pollard, T. D. (1986). Rate constants for the reactions of ATP- and ADP-actin with the ends of actin filaments. *J Cell Biol*, 103(6 Pt 2), 2747-2754. doi:10.1083/jcb.103.6.2747
- Pollard, T. D. (2007). Regulation of actin filament assembly by Arp2/3 complex and formins. *Annu Rev Biophys Biomol Struct*, 36, 451-477. doi:10.1146/annurev.biophys.35.040405.101936

References

- Pollard, T. D., & Beltzner, C. C. (2002). Structure and function of the Arp2/3 complex. *Curr Opin Struct Biol*, 12(6), 768-774.
- Pollard, T. D., Blanchoin, L., & Mullins, R. D. (2000). Molecular mechanisms controlling actin filament dynamics in nonmuscle cells. *Annu Rev Biophys Biomol Struct*, 29, 545-576. doi:10.1146/annurev.biophys.29.1.545
- Pollard, T. D., & Borisy, G. G. (2003). Cellular motility driven by assembly and disassembly of actin filaments. *Cell*, 112(4), 453-465. doi:10.1016/s0092-8674(03)00120-x
- Pollard, T. D., & Cooper, J. A. (2009). Actin, a central player in cell shape and movement. *Science*, 326(5957), 1208-1212. doi:10.1126/science.1175862
- Portera-Cailliau, C., Pan, D. T., & Yuste, R. (2003). Activity-regulated dynamic behavior of early dendritic protrusions: evidence for different types of dendritic filopodia. *J Neurosci*, 23(18), 7129-7142.
- Pring, M., Evangelista, M., Boone, C., Yang, C., & Zigmond, S. H. (2003). Mechanism of formin-induced nucleation of actin filaments. *Biochemistry*, 42(2), 486-496. doi:10.1021/bi026520j
- Prochniewicz, E., Janson, N., Thomas, D. D., & De la Cruz, E. M. (2005). Cofilin increases the torsional flexibility and dynamics of actin filaments. *J Mol Biol*, 353(5), 990-1000. doi:10.1016/j.jmb.2005.09.021
- Pruyne, D., Evangelista, M., Yang, C., Bi, E., Zigmond, S., Bretscher, A., & Boone, C. (2002). Role of formins in actin assembly: nucleation and barbed-end association. *Science*, 297(5581), 612-615. doi:10.1126/science.1072309
- Puram, S. V., & Bonni, A. (2013). Cell-intrinsic drivers of dendrite morphogenesis. *Development*, 140(23), 4657-4671. doi:10.1242/dev.087676
- Quinlan, M. E., Heuser, J. E., Kerkhoff, E., & Mullins, R. D. (2005). *Drosophila* Spire is an actin nucleation factor. *Nature*, 433(7024), 382-388. doi:10.1038/nature03241
- Quinlan, M. E., Hilgert, S., Bedrossian, A., Mullins, R. D., & Kerkhoff, E. (2007). Regulatory interactions between two actin nucleators, Spire and Cappuccino. *J Cell Biol*, 179(1), 117-128. doi:10.1083/jcb.200706196
- Quinlan, M. E., & Kerkhoff, E. (2008). Actin nucleation: bacteria get in-Spired. *Nat Cell Biol*, 10(1), 13-15. doi:10.1038/ncb0108-13
- Rall, W. (1962). Electrophysiology of a dendritic neuron model. *Biophys J*, 2(2 Pt 2), 145-167. doi:10.1016/s0006-3495(62)86953-7
- Ramocki, M. B., & Zoghbi, H. Y. (2008). Failure of neuronal homeostasis results in common neuropsychiatric phenotypes. *Nature*, 455(7215), 912-918. doi:10.1038/nature07457
- Ramón y Cajal, S. (1899-1904). *Textura del Sistema Nervioso del Hombre y de Los Vertebrados*. Madrid: Imprenta y Librería de Nicolás Moya.
- Reisler, E. (1993). Actin molecular structure and function. *Curr Opin Cell Biol*, 5(1), 41-47.
- Robinson, R. C., Turbedsky, K., Kaiser, D. A., Marchand, J. B., Higgs, H. N., Choe, S., & Pollard, T. D. (2001). Crystal structure of Arp2/3 complex. *Science*, 294(5547), 1679-1684. doi:10.1126/science.1066333
- Robles, E., Huttenlocher, A., & Gomez, T. M. (2003). Filopodial calcium transients regulate growth cone motility and guidance through local activation of calpain. *Neuron*, 38(4), 597-609.
- Rosales-Nieves, A. E., Johndrow, J. E., Keller, L. C., Magie, C. R., Pinto-Santini, D. M., & Parkhurst, S. M. (2006). Coordination of microtubule and microfilament dynamics by *Drosophila* Rho1, Spire and Cappuccino. *Nat Cell Biol*, 8(4), 367-376. doi:10.1038/ncb1385
- Sanchez-Soriano, N., Bottenberg, W., Fiala, A., Haessler, U., Kerassoviti, A., Knust, E., . . . Prokop, A. (2005). Are dendrites in *Drosophila* homologous to vertebrate dendrites? *Dev Biol*, 288(1), 126-138. doi:10.1016/j.ydbio.2005.09.026
- Sanes, J. R., & Zipursky, S. L. (2010). Design principles of insect and vertebrate visual systems. *Neuron*, 66(1), 15-36. doi:10.1016/j.neuron.2010.01.018
- Schmucker, D., Clemens, J. C., Shu, H., Worby, C. A., Xiao, J., Muda, M., . . . Zipursky, S. L. (2000). *Drosophila* Dscam is an axon guidance receptor exhibiting extraordinary molecular diversity. *Cell*, 101(6), 671-684. doi:10.1016/s0092-8674(00)80878-8

References

- Scott, E. K., Reuter, J. E., & Luo, L. (2003). Small GTPase Cdc42 is required for multiple aspects of dendritic morphogenesis. *J Neurosci*, 23(8), 3118-3123.
- Sept, D., & McCammon, J. A. (2001). Thermodynamics and kinetics of actin filament nucleation. *Biophys J*, 81(2), 667-674. doi:10.1016/S0006-3495(01)75731-1
- Shepherd, G. M., Stepanyants, A., Bureau, I., Chklovskii, D., & Svoboda, K. (2005). Geometric and functional organization of cortical circuits. *Nat Neurosci*, 8(6), 782-790. doi:10.1038/nn1447
- Sholl, D. A. (1956). *The organization of the cerebral cortex*. London, UK: Methuen.
- Sin, W. C., Haas, K., Ruthazer, E. S., & Cline, H. T. (2002). Dendrite growth increased by visual activity requires NMDA receptor and Rho GTPases. *Nature*, 419(6906), 475-480. doi:10.1038/nature00987
- Singhania, A., & Grueber, W. B. (2014). Development of the embryonic and larval peripheral nervous system of *Drosophila*. *Wiley Interdiscip Rev Dev Biol*, 3(3), 193-210. doi:10.1002/wdev.135
- Sjoblom, B., Salmazo, A., & Djinovic-Carugo, K. (2008). Alpha-actinin structure and regulation. *Cell Mol Life Sci*, 65(17), 2688-2701. doi:10.1007/s00018-008-8080-8
- Skoble, J., Auerbuch, V., Goley, E. D., Welch, M. D., & Portnoy, D. A. (2001). Pivotal role of VASP in Arp2/3 complex-mediated actin nucleation, actin branch-formation, and *Listeria monocytogenes* motility. *J Cell Biol*, 155(1), 89-100. doi:10.1083/jcb.200106061
- Small, J. V., Isenberg, G., & Celis, J. E. (1978). Polarity of actin at the leading edge of cultured cells. *Nature*, 272(5654), 638-639. doi:10.1038/272638a0
- Soba, P., Zhu, S., Emoto, K., Younger, S., Yang, S. J., Yu, H. H., . . . Jan, Y. N. (2007). *Drosophila* sensory neurons require Dscam for dendritic self-avoidance and proper dendritic field organization. *Neuron*, 54(3), 403-416. doi:10.1016/j.neuron.2007.03.029
- Song, W., Onishi, M., Jan, L. Y., & Jan, Y. N. (2007). Peripheral multidendritic sensory neurons are necessary for rhythmic locomotion behavior in *Drosophila* larvae. *Proc Natl Acad Sci U S A*, 104(12), 5199-5204. doi:10.1073/pnas.0700895104
- Stiefel, K. M., & Sejnowski, T. J. (2007). Mapping function onto neuronal morphology. *J Neurophysiol*, 98(1), 513-526. doi:10.1152/jn.00865.2006
- Sturner, T., Tatarnikova, A., Mueller, J., Schaffran, B., Cuntz, H., Zhang, Y., . . . Tavosanis, G. (2019). Transient localization of the Arp2/3 complex initiates neuronal dendrite branching *in vivo*. *Development*, 146(7). doi:10.1242/dev.171397
- Sugimura, K., Satoh, D., Estes, P., Crews, S., & Uemura, T. (2004). Development of morphological diversity of dendrites in *Drosophila* by the BTB-zinc finger protein abrupt. *Neuron*, 43(6), 809-822. doi:10.1016/j.neuron.2004.08.016
- Sugimura, K., Yamamoto, M., Niwa, R., Satoh, D., Goto, S., Taniguchi, M., . . . Uemura, T. (2003). Distinct developmental modes and lesion-induced reactions of dendrites of two classes of *Drosophila* sensory neurons. *J Neurosci*, 23(9), 3752-3760.
- Svitkina, T. M., & Borisy, G. G. (1999). Arp2/3 complex and actin depolymerizing factor/cofilin in dendritic organization and treadmilling of actin filament array in lamellipodia. *J Cell Biol*, 145(5), 1009-1026. doi:10.1083/jcb.145.5.1009
- Svitkina, T. M., Bulanova, E. A., Chaga, O. Y., Vignjevic, D. M., Kojima, S., Vasiliev, J. M., & Borisy, G. G. (2003). Mechanism of filopodia initiation by reorganization of a dendritic network. *J Cell Biol*, 160(3), 409-421. doi:10.1083/jcb.200210174
- Tenenbaum, C. M., Misra, M., Alizzi, R. A., & Gavis, E. R. (2017). Enclosure of Dendrites by Epidermal Cells Restricts Branching and Permits Coordinated Development of Spatially Overlapping Sensory Neurons. *Cell Rep*, 20(13), 3043-3056. doi:10.1016/j.celrep.2017.09.001
- Tracey, W. D., Jr., Wilson, R. I., Laurent, G., & Benzer, S. (2003). *painless*, a *Drosophila* gene essential for nociception. *Cell*, 113(2), 261-273. doi:10.1016/s0092-8674(03)00272-1
- Tsubouchi, A., Caldwell, J. C., & Tracey, W. D. (2012). Dendritic filopodia, Ripped Pocket, NOMPC, and NMDARs contribute to the sense of touch in *Drosophila* larvae. *Curr Biol*, 22(22), 2124-2134. doi:10.1016/j.cub.2012.09.019

References

- Turner, H. N., Armengol, K., Patel, A. A., Himmel, N. J., Sullivan, L., Iyer, S. C., . . . Cox, D. N. (2016). The TRP Channels Pkd2, NompC, and Trpm Act in Cold-Sensing Neurons to Mediate Unique Aversive Behaviors to Noxious Cold in *Drosophila*. *Curr Biol*, 26(23), 3116-3128. doi:10.1016/j.cub.2016.09.038
- Uemura, E., Carriquiry, A., Kliemann, W., & Goodwin, J. (1995). Mathematical modeling of dendritic growth *in vitro*. *Brain Res*, 671(2), 187-194. doi:10.1016/0006-8993(94)01310-e
- Urban, N. T., Willig, K. I., Hell, S. W., & Nagerl, U. V. (2011). STED nanoscopy of actin dynamics in synapses deep inside living brain slices. *Biophys J*, 101(5), 1277-1284. doi:10.1016/j.bpj.2011.07.027
- Urano, T., Liu, J., Zhang, P., Fan, Y., Egile, C., Li, R., . . . Zhan, X. (2001). Activation of Arp2/3 complex-mediated actin polymerization by cortactin. *Nat Cell Biol*, 3(3), 259-266. doi:10.1038/35060051
- Vaillant, A. R., Zanassi, P., Walsh, G. S., Aumont, A., Alonso, A., & Miller, F. D. (2002). Signaling mechanisms underlying reversible, activity-dependent dendrite formation. *Neuron*, 34(6), 985-998.
- Valnegri, P., Puram, S. V., & Bonni, A. (2015). Regulation of dendrite morphogenesis by extrinsic cues. *Trends Neurosci*, 38(7), 439-447. doi:10.1016/j.tins.2015.05.003
- van Elburg, R. A., & van Ooyen, A. (2010). Impact of dendritic size and dendritic topology on burst firing in pyramidal cells. *PLoS Comput Biol*, 6(5), e1000781. doi:10.1371/journal.pcbi.1000781
- Van Troys, M., Huyck, L., Leyman, S., Dhaese, S., Vandekerckhove, J., & Ampe, C. (2008). Ins and outs of ADF/cofilin activity and regulation. *Eur J Cell Biol*, 87(8-9), 649-667. doi:10.1016/j.ejcb.2008.04.001
- Vaughn, J. E. (1989). Fine structure of synaptogenesis in the vertebrate central nervous system. *Synapse*, 3(3), 255-285. doi:10.1002/syn.890030312
- Vavylonis, D., Yang, Q., & O'Shaughnessy, B. (2005). Actin polymerization kinetics, cap structure, and fluctuations. *Proc Natl Acad Sci U S A*, 102(24), 8543-8548. doi:10.1073/pnas.0501435102
- Verkhovskiy, A. B., Svitkina, T. M., & Borisy, G. G. (1997). Polarity sorting of actin filaments in cytochalasin-treated fibroblasts. *J Cell Sci*, 110 (Pt 15), 1693-1704.
- Vignjevic, D., Kojima, S., Aratyn, Y., Danciu, O., Svitkina, T., & Borisy, G. G. (2006). Role of fascin in filopodial protrusion. *J Cell Biol*, 174(6), 863-875. doi:10.1083/jcb.200603013
- Villalba, R. M., & Smith, Y. (2010). Striatal spine plasticity in Parkinson's disease. *Front Neuroanat*, 4, 133. doi:10.3389/fnana.2010.00133
- Wagner, C. R., Mahowald, A. P., & Miller, K. G. (2002). One of the two cytoplasmic actin isoforms in *Drosophila* is essential. *Proc Natl Acad Sci U S A*, 99(12), 8037-8042. doi:10.1073/pnas.082235499
- Wang, J., Zugates, C. T., Liang, I. H., Lee, C. H., & Lee, T. (2002). *Drosophila* Dscam is required for divergent segregation of sister branches and suppresses ectopic bifurcation of axons. *Neuron*, 33(4), 559-571.
- Wang, K. H., Brose, K., Arnott, D., Kidd, T., Goodman, C. S., Henzel, W., & Tessier-Lavigne, M. (1999). Biochemical purification of a mammalian slit protein as a positive regulator of sensory axon elongation and branching. *Cell*, 96(6), 771-784. doi:10.1016/s0092-8674(00)80588-7
- Watanabe, N., & Mitchison, T. J. (2002). Single-molecule speckle analysis of actin filament turnover in lamellipodia. *Science*, 295(5557), 1083-1086. doi:10.1126/science.1067470
- Weaver, A. M., Karginov, A. V., Kinley, A. W., Weed, S. A., Li, Y., Parsons, J. T., & Cooper, J. A. (2001). Cortactin promotes and stabilizes Arp2/3-induced actin filament network formation. *Curr Biol*, 11(5), 370-374. doi:10.1016/s0960-9822(01)00098-7
- Welch, M. D., & Mullins, R. D. (2002). Cellular control of actin nucleation. *Annu Rev Cell Dev Biol*, 18, 247-288. doi:10.1146/annurev.cellbio.18.040202.112133
- Wen, Q., & Chklovskii, D. B. (2008). A cost-benefit analysis of neuronal morphology. *J Neurophysiol*, 99(5), 2320-2328. doi:10.1152/jn.00280.2007
- Wen, Q., Stepanyants, A., Elston, G. N., Grosberg, A. Y., & Chklovskii, D. B. (2009). Maximization of the connectivity repertoire as a statistical principle governing the shapes of dendritic arbors. *Proc Natl Acad Sci U S A*, 106(30), 12536-12541. doi:10.1073/pnas.0901530106

References

- Willig, K. I., Steffens, H., Gregor, C., Herholt, A., Rossner, M. J., & Hell, S. W. (2014). Nanoscopy of filamentous actin in cortical dendrites of a living mouse. *Biophys J*, 106(1), L01-03. doi:10.1016/j.bpj.2013.11.1119
- Wioland, H., Guichard, B., Senju, Y., Myram, S., Lappalainen, P., Jegou, A., & Romet-Lemonne, G. (2017). ADF/Cofilin Accelerates Actin Dynamics by Severing Filaments and Promoting Their Depolymerization at Both Ends. *Curr Biol*, 27(13), 1956-1967 e1957. doi:10.1016/j.cub.2017.05.048
- Wojtowicz, W. M., Flanagan, J. J., Millard, S. S., Zipursky, S. L., & Clemens, J. C. (2004). Alternative splicing of *Drosophila* Dscam generates axon guidance receptors that exhibit isoform-specific homophilic binding. *Cell*, 118(5), 619-633. doi:10.1016/j.cell.2004.08.021
- Woodrum, D. T., Rich, S. A., & Pollard, T. D. (1975). Evidence for biased bidirectional polymerization of actin filaments using heavy meromyosin prepared by an improved method. *J Cell Biol*, 67(1), 231-237. doi:10.1083/jcb.67.1.231
- Wu, G. Y., Zou, D. J., Rajan, I., & Cline, H. (1999). Dendritic dynamics *in vivo* change during neuronal maturation. *J Neurosci*, 19(11), 4472-4483.
- Wu, Q., & Maniatis, T. (1999). A striking organization of a large family of human neural cadherin-like cell adhesion genes. *Cell*, 97(6), 779-790. doi:10.1016/s0092-8674(00)80789-8
- Xiang, Y., Yuan, Q., Vogt, N., Looger, L. L., Jan, L. Y., & Jan, Y. N. (2010). Light-avoidance-mediating photoreceptors tile the *Drosophila* larval body wall. *Nature*, 468(7326), 921-926. doi:10.1038/nature09576
- Xu, K., Zhong, G., & Zhuang, X. (2013). Actin, spectrin, and associated proteins form a periodic cytoskeletal structure in axons. *Science*, 339(6118), 452-456. doi:10.1126/science.1232251
- Yan, Z., Zhang, W., He, Y., Gorczyca, D., Xiang, Y., Cheng, L. E., . . . Jan, Y. N. (2013). *Drosophila* NOMPC is a mechanotransduction channel subunit for gentle-touch sensation. *Nature*, 493(7431), 221-225. doi:10.1038/nature11685
- Yang, S., Huang, F. K., Huang, J., Chen, S., Jakoncic, J., Leo-Macias, A., . . . Huang, X. Y. (2013). Molecular mechanism of fascin function in filopodial formation. *J Biol Chem*, 288(1), 274-284. doi:10.1074/jbc.M112.427971
- Yang, W. K., & Chien, C. T. (2019). Beyond being innervated: the epidermis actively shapes sensory dendritic patterning. *Open Biol*, 9(3), 180257. doi:10.1098/rsob.180257
- Ydenberg, C. A., Johnston, A., Weinstein, J., Bellavance, D., Jansen, S., & Goode, B. L. (2015). Combinatorial genetic analysis of a network of actin disassembly-promoting factors. *Cytoskeleton (Hoboken)*, 72(7), 349-361. doi:10.1002/cm.21231
- Yuste, R., & Bonhoeffer, T. (2004). Genesis of dendritic spines: insights from ultrastructural and imaging studies. *Nat Rev Neurosci*, 5(1), 24-34. doi:10.1038/nrn1300
- Zeth, K., Pechlivanis, M., Samol, A., Pleiser, S., Vornrhein, C., & Kerkhoff, E. (2011). Molecular basis of actin nucleation factor cooperativity: crystal structure of the Spir-1 kinase non-catalytic C-lobe domain (KIND)*formin-2 formin SPIR interaction motif (FSI) complex. *J Biol Chem*, 286(35), 30732-30739. doi:10.1074/jbc.M111.257782
- Zhong, L., Hwang, R. Y., & Tracey, W. D. (2010). Pickpocket is a DEG/ENaC protein required for mechanical nociception in *Drosophila* larvae. *Curr Biol*, 20(5), 429-434. doi:10.1016/j.cub.2009.12.057
- Zhu, H., Hummel, T., Clemens, J. C., Berdnik, D., Zipursky, S. L., & Luo, L. (2006). Dendritic patterning by Dscam and synaptic partner matching in the *Drosophila* antennal lobe. *Nat Neurosci*, 9(3), 349-355. doi:10.1038/nn1652
- Zipursky, S. L., & Sanes, J. R. (2010). Chemoaffinity revisited: dscams, protocadherins, and neural circuit assembly. *Cell*, 143(3), 343-353. doi:10.1016/j.cell.2010.10.009
- Zipursky, S. L., Venkatesh, T. R., Teplow, D. B., & Benzer, S. (1984). Neuronal development in the *Drosophila* retina: monoclonal antibodies as molecular probes. *Cell*, 36(1), 15-26. doi:10.1016/0092-8674(84)90069-2
- Zou, W., Dong, X., Broederdorf, T. R., Shen, A., Kramer, D. A., Shi, R., . . . Shen, K. (2018). A Dendritic Guidance Receptor Complex Brings Together Distinct Actin Regulators to Drive Efficient F-Actin Assembly and Branching. *Dev Cell*, 45(3), 362-375 e363. doi:10.1016/j.devcel.2018.04.008

Acknowledgement

This work would not have been possible without the help and support of numerous people. First, I would like to thank Prof. Dr. Gaia Tavosanis for her constant support of my work and excellent scientific guidance and discussions. Thank you, most of all, for giving me the experimental freedom to develop the project and for sending me across the globe to interact with other scientists. And of course, thank you to the whole Tavosanis lab for your help and your friendship.

Secondly, thank you to our collaborator Dr. Hermann Cuntz and all his lab members. I enjoyed every meeting and visit to Frankfurt to the fullest and through you was able to discover a different field of research. Thank you for challenging and supporting me.

Thirdly, an enormous thank you goes to my family, for being my role models in every way. To my mum, for unconditional support and teaching me to fight for what makes me happy. To my dad, for showing me that you can make a living doing what you love and for all the scientific discussions beyond biology. To my brothers, for being my brothers in every sense of the word and constantly confronting me with different points of view, as they should.

The last big thank you goes to all the amazing friends that have supported me over the years of my PhD in Bonn. To Giovanni, for always finding a way to make me laugh, whether it is with you or about you, we know it doesn't matter as long as we laugh.

To Barbara, Maral, Claudia, Telma, Steffi, Moni and Andrea for being there for Zumba, Jogging, Coffee, Beer and more, depending on the situation. Thank you for being amazing roommates, for not being muggles, for visiting me, for challenging me, for travelling with me and for enjoying this time with me.

To Rita: Ich danke dir für jahrelange Hilfe und bedingungslose Bereitschaft jederzeit für mich da zu sein. Ohne dich wäre mein Alltag im Labor nicht denkbar gewesen.

To Jeshlee, Matt, Mariangela, Luigi, Artemis, Nur, Pedro, André, Hanna, Astrid, Gurkan, Ayca, little Deniz, Nora, and Maren for all the dinners, trips and little adventures we had together.